



Modeling the Environmental Risks Associated with Pressure-Treated Wood Used in Sensitive Environments

Kenneth M. Brooks

Models provide an opportunity to predict outcomes based on theory, empirical data describing relationships, and site and temporal specific inputs. Levels of sophistication can vary from simple to extremely complex. However, complexity does not necessarily mean that models do a better job of predicting outcomes. Weather forecasting is an excellent example of low, albeit improving, success using very complex models largely necessitated by the complexity of atmospheric dynamics. The Microsoft Excel® spreadsheet models described in this chapter are relatively simple. Some of that simplicity was achieved by making worst-case assumptions for driving the models. This leads to predictions of environmental levels of contaminants that are generally higher than those actually observed in model verification studies, making the models conservative from an environmental risk perspective. It is emphasized that the models are not designed to provide exact predictions of environmental responses on small spatial scales (meters). They are designed to conservatively predict specific sites where there is a reasonable probability that pressure-treated wood projects will create an unacceptable environmental risk and a range of projects and sites where there is little environmental risk. In that regard, the author believes that *models do not have to make precise predictions to be useful*. The creosote risk assessment model of Brooks (1993) was the first effort and creosote will be used as an example of model development in this chapter. The CREORISK model was tested in the 10-y-long Sooke Basin Study (Goyette and Brooks, 1998, 2000; Brooks et al. 2006). Figure 9.1 describes the predicted and observed sediment concentrations of 16 parental polycyclic aromatic hydrocarbons (PAH) observed at Sooke Basin after the first

year, when concentrations in aerobic sediments were approaching a steady-state condition. This state illustrates both the conservative nature of the prediction as well as the convergence between actual and predicted values.

The creosote model was followed by a CCA-C model (Brooks 1996), which was the first to predict environmental concentrations of metals lost from immersed lumber and piling treated with a waterborne preservative containing copper, chromium, and arsenic. These models made predictions only for the immersed portions of pressure-treated wood structures. In fact, the portions of these structures that are above water and exposed to rainfall also contribute contaminants to sensitive environments. In 2003, the USDA Forest Service supported development of the “Timber Bridge Model” (Brooks 2005a), which filled this need by making predictions of environmental response to both

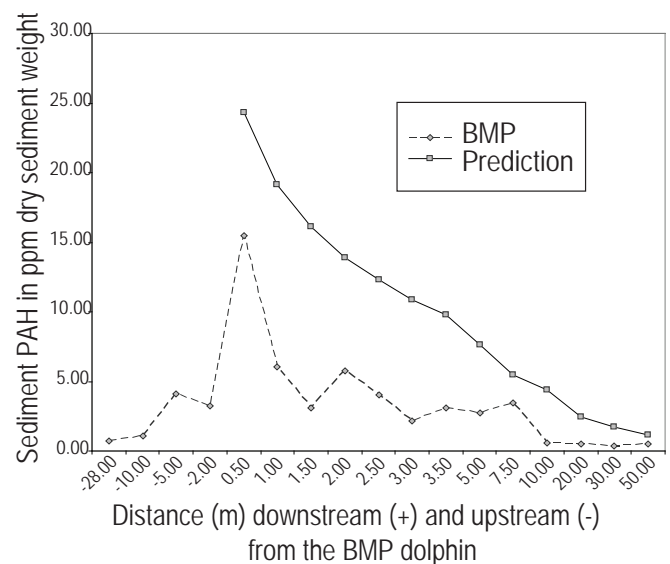


Figure 9.1 Comparison of predicted vs. observed sediment concentrations of total PAH adjacent to the BMP treated dolphin on day 384 of Environment Canada's Sooke Basin Creosote Risk Assessment study using a proximity model.

The author is Environmental Consultant with Aquatic Environmental Sciences, Port Townsend, WA 98368.

the above-water and in-water portions of treated-wood structures. The Timber Bridge Model has been expanded and diversified to evaluate structures built with wood treated with 11 preservatives: creosote, pentachlorophenol, copper naphthenate, ACZA, CCA-C, CA-B™, Wolman AG™, ACQ-B or C™, Wolman μ Cu Azole™, MicroPro Azole™, and MicroPro Quat™. Electronic versions of the model and the various spreadsheets (created with Microsoft Excel®) supporting the model can be downloaded from WWPinstitute.org.

9.1 ASSUMPTIONS USED IN MODELING THE ENVIRONMENTAL RESPONSE TO PRESSURE-TREATED WOOD

The predictions made by any model must be viewed with an understanding of the underlying assumptions. The metric system is used throughout this chapter:

Parameter	Units
Dimensional inputs	cm or cm ²
Density	g/cm ³
Speed	cm/s
Volume	cm ³
Water column concentrations	mg/L or μ g/L
Sediment concentrations	mg/kg or ppm

9.1.1 Benchmarks for assessing the suitability of specific projects

Predicted water column and sediment concentrations of contaminants from pressure-treated wood are added to measured or assumed background concentrations of the same contaminant and compared with the state and/or federal (U.S. Environmental Protection Agency) water and sediment quality criteria that were discussed in Chapter 5, including adopted benchmarks for those contaminants that do not have federal or state standards.

9.1.2 Preservative loss rates

The algorithms described in Chapter 7 were developed to predict preservative loss rates as a function of time or accumulated rainfall and the environmental factors that influence them (receiving water pH, salinity, temperature, preservative retention, wood species, etc.). Preservative loss rates must be predictable for modeling to be useful. Previous studies measuring loss rates indicate that the

production methods for treated wood products can have an important impact on the loss characteristics. To improve predictability, the industry has developed production "Best Management Practices" (BMPs) described in Chapter 11. Most of the algorithms described in Chapter 7 are based on leaching studies of products produced using these BMPs, and model predictions are only valid for projects specifying BMP treatments. For complex mixtures, such as creosote, information is not available describing the migration of all of the PAH species. In these cases, loss rates for the unmeasured PAH species are assumed to be proportional to their presence in the wood and the known loss rates of other PAH species.

9.1.3 Box models

In general, rainwater runoff from the overhead portions of structures represents a diffuse source of contaminants whose assessment is not amenable to the proximity model approach. Therefore, Brooks (2005a, 2006b) relied on box models for assessing timber bridges; this approach is recommended for all structures having large overhead (out of the water) leaching surface areas and/or numerous immersed treated wood members. The box model described herein is based on the following assumptions:

1. Current speeds are equal at all depths or can be adequately characterized using a mean current speed collected at the average water depth where treated wood is placed. This assumption greatly simplifies the model because both the preservative losses and the volume of the receiving water diluting the preservative are functions of water depth. Therefore, the model need only consider the amount of preservative lost to a unit depth of water and the volume of water in that unit depth that passes by the structure with some measurable speed.
2. Pressure-treated wood of known dimensions contributes contaminants to a box that is defined by the width of the structure orthogonal to the currents, the current speed, and the water's depth (see Figure 9.2).
3. The amount of preservative delivered into the box is determined by multiplying the loss rates developed in Chapter 7 by the total leaching surface area of the immersed treated wood and the predicted contaminant levels in rainwater runoff from the overhead structure by the anticipated volume of rainwater. Sediment concentrations accumulate over an extended period of time and the model assumes that rain falls at a steady rate for the life of the project (generally 35 y). The model includes

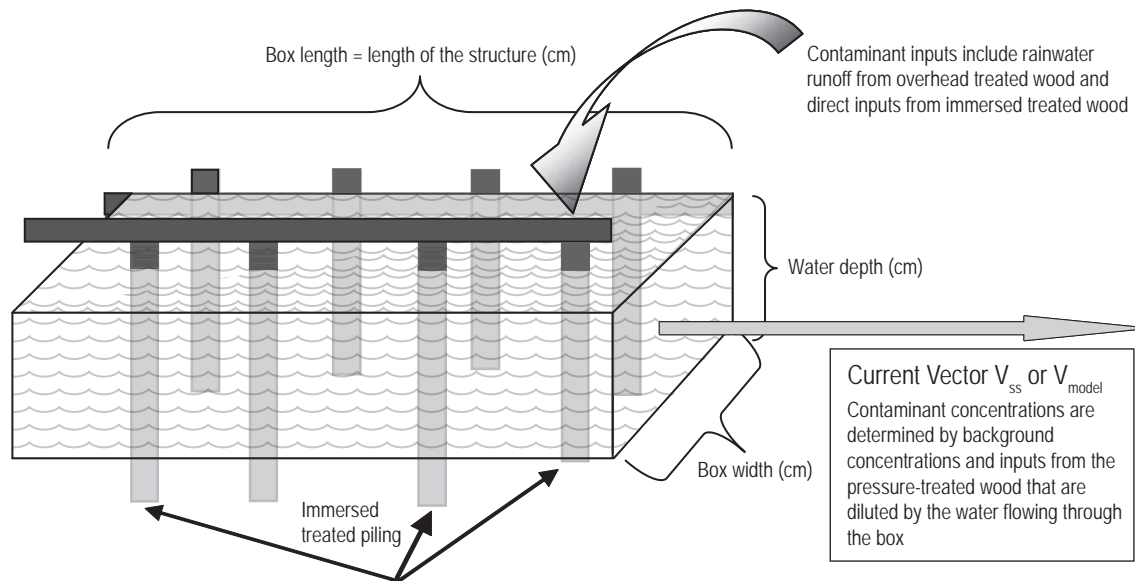


Figure 9.2 Conceptual drawing describing the box model methodology used to predict water column concentrations of contaminants migrating from structures into water.

provisions for estimating increased contaminant concentrations associated with short-term storm events that do not affect the flow of water under the structure.

4. The volume of dilution water is the width of the project measured orthogonal to the currents \times the current speed \times the period of time used in the loss algorithm \times the water's depth. For environments that are dominated by tidal currents, the worst case (minimum dilution) is assessed during the period within 0.5 h before or after slack tide.

9.1.4 Leaching surface areas for immersed treated wood

The leaching surface area of immersed piling (round stock) is $2\pi rl$ where $\pi = 3.14$ and r is the average radius of the immersed portion of the piling and l is the length of the immersed portion of the pile (i.e., the average water depth). For sawn timbers and lumber, the leaching surface area is $2twl$ where t is the lumber thickness; w is its width; and l is the length of immersed wood. The cross-sectional area of sawn lumber and timbers (end grain) is ignored because it is a very small proportion of the leaching surface area (2% of a piece of decking measuring 3.8 cm thick \times 14 cm wide \times 2.4 m long). For piling, one end grain is embedded in sediments and the other is above water, where it should be capped.

9.1.5 Leaching surface area of rainwater-exposed treated wood in overhead structures

Figure 9.3 is designed to assist planners in estimating the leaching surface area of overhead structures exposed to rainfall. The rainwater studies reported in Chapter 7 describe concentrations of active ingredients in runoff from treated decking ($\mu\text{g/L}$). Rainfall rates were not a significant determinant of contaminant concentrations in the runoff, suggesting that contact time was not a significant factor in determining the concentration of contaminants in runoff. Under any circumstances, determining contact time is problematic because of the variable orientation of treated wood surfaces with respect to gravity. All wetted surfaces are assumed to receive an amount of rainfall equal to a horizontal surface, and the concentration of contaminant in the runoff is equal to that observed in the deck studies (i.e., horizontal surfaces). This overestimates the loading of receiving waters because vertical surfaces do not receive the same amount of rainwater as do horizontal surfaces, except where wind is driving the rain at a 45° angle with respect to gravity. In that case, the down-wind vertical surfaces would not receive any rainfall, resulting in overestimating the leaching surface area. Although this assumption simplifies the model, predicted receiving water

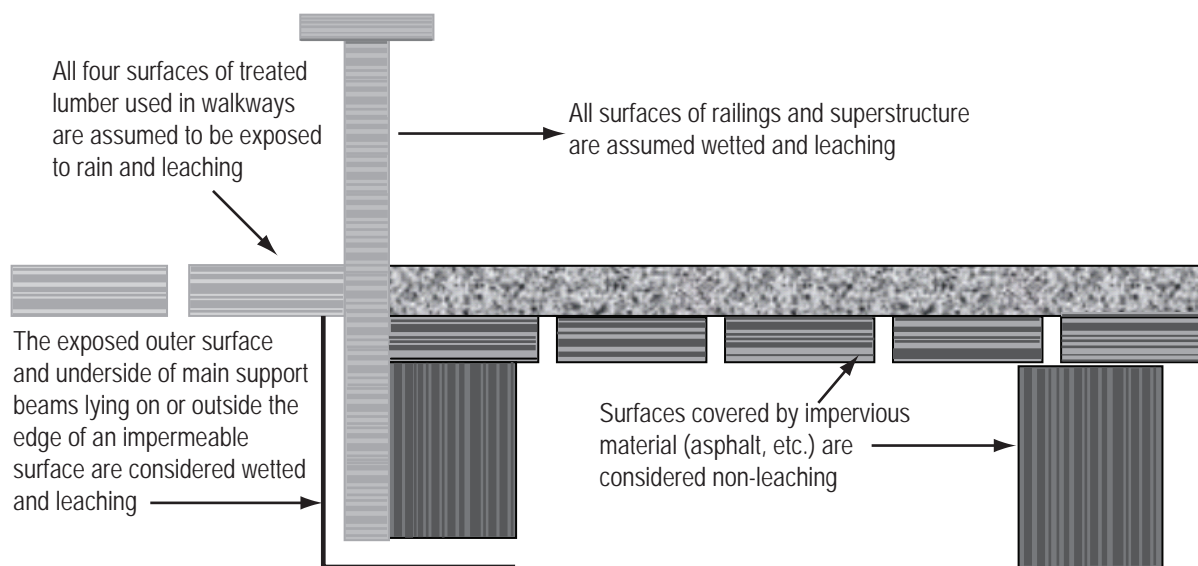


Figure 9.3 Guidelines for estimating the surface area of treated wood exposed to rainfall in association with timber bridges.

concentrations from rainwater runoff may be higher than observed.

9.1.6 Initial mixing depth of contaminants in rainwater falling on surface waters

The depth of water into which raindrops are diluted depends in part on turbulence (mechanical mixing) within the receiving water. However, in worst cases, the flow will be laminar, with little or no turbulent mixing. In these cases, the mixing depth will be determined by the penetration and mixing of rainwater into the receiving water and subsequently by diffusion. Diffusion is too slow in most currents to significantly affect these results, and turbulent mixing is site specific, chaotic, and difficult to model. Both of these factors, which would increase dilution and decrease predicted risk, are ignored in this model. Schlüssel et al. (1997) described a decrease in the proportional volume of rainwater falling into the upper layers of the ocean (V_r/V_o), where V_r is the volume of rainwater falling into a unit area of ocean, and V_o is the volume of ocean into which the rainwater is mixed. For moderately low rainfall rates of 0.1 to 5 mm/h, V_r/V_o was greater than 0.2 to depths of at least 4.0 cm, the highest value in his graph. However, assuming that the relationships are continuous, it appeared that typical rainfall rates of 5 to 10 mm/h would mix to depths >12 cm. Green and Houk (1979) empirically derived mixing depths of rain with freshwater through analysis of temperature, as a function of depth, of a cold

body of water subjected to a warm rain. For rainfall of mixed droplet sizes, falling at a rate of 2.1 cm/h, the mixing depth increased with time from about 20 cm depth at 15 min to 30 cm at 30 min and 35 cm at 1 h. For purposes of this model, rainfall will be assumed to mix in the upper 20 cm of the water column or to the full depth of the water when depths are <20 cm.

9.1.7 Receiving water current speeds

The model considers two types of currents. Steady-state currents (V_{ss}) are associated with lakes, rivers, streams, and some marine systems that are primarily influenced by major current systems. Currents are tidally driven in some estuarine and most marine systems. These systems are modeled as harmonics using the maximum observed current speed (V_{max}) and a cosine function to derive an estimate of the instantaneous current speed ($V_t = V_{max} * \text{Cos}(t)$). Assuming a semidiurnal tidal cycle, time is expressed in radians (one hour = $2\pi/12$ radians). Current speeds at slack tide are rarely zero (Brooks 2006a) and the model integrates the predicted tidal speed within 0.5 h on either side of slack tide to derive an average speed of $0.0645 * V_{max}$. This one hour at slack tide is the time during which worst case predictions of water column concentrations of contaminants are made in tidally driven systems. During this time, contaminants are assumed to accumulate in an area equal to the footprint of the structure plus a distance of $0.0645 * V_{max} * 3,600$ s. If the maximum current speed is 10 cm/s, this assumption increases the upstream,

downstream, and offshore dimensions of the box by 23 m. The inshore side of the box is fixed by the shoreline. User inputs are provided for V_{ss} and V_{max} . Where currents are a combination of harmonic and steady state vectors, a third speed is computed ($V_{model} = \text{Absoluted Value}(0.64 * V_{max} - V_{ss})$) where $0.64 * V_{max}$ is the average current speed during a 12-h exchange from low to high or high to low water. The model generally uses V_{model} for computations. However, for purposes of estimating the dilution of contaminants in water and sediments, the model uses the dominant current regime on the basis of whether $V_{ss} > V_{max}$.

9.1.8 Transport of metal and organic contaminants other than PAH to sediments

Metal contaminants are assumed to adsorb to clay particles suspended in the water column and to settle with a vertical velocity (V_v) that is determined by Stokes' equation (known as Stokes' law) [9.1] for the settling velocities of small particles:

$$V_v = g D^2(\rho_s - \rho_w)/18 \mu \quad [9.1]$$

where,

g = gravitational constant (980 cm/s²)

D = particle diameter (≤ 0.00039 cm for clay)

ρ_s = particle density (2.6 to 4.3 g/cm³)

ρ_w = density of water (0.998 @ 20°C)

μ = coefficient of molecular viscosity (10⁻² g/cm-s)

for freshwater at 20°C

Clay binding nuclei with $V_v = 0.0013$ to 0.005 were considered because they typically carry negative charges that bind divalent anions like copper or zinc. In the absence of site-specific information, a V_v of 0.005 cm/s will be assumed for bound metals and organic contaminants other than PAH. This velocity is specifically for $8 \mu\text{m}$ particles having a density of 2.6 g/cm³ in fresh water at 20°C. Settling velocities will be higher for higher density particles in warmer water and lower for smaller particles in colder fresh water or marine waters. The model allows substitutions for V_v .

9.1.9 Particulate transport model for creosote derived PAH

Based on the observation of small microsreens covering 1 to 2 cm² in the Sooke Basin studies and the results of

canister studies, Goyette and Brooks (1998) developed a particulate PAH transport hypothesis suggesting that hydrophobic PAH are released from creosote-treated wood as microliter-size particles that settle to the bottom. Unpublished laboratory observations by Brooks found that microliter quantities of creosote retained their integrity as they settled onto and eventually into quartz and ground oyster-shell sediments after being injected below the water surface. Creosote oil injected onto the surface of fresh water or 30 practical salinity units (PSU) seawater formed sheens. When disturbed, as by waves, these sheens were observed to break up into small angular particles that settled to the bottom and worked their way into sediments. These particles remained intact for several years when injected into sterile water. While these observations support this particulate PAH transport hypothesis, it has not been formally tested. The original creosote model (Brooks 2005) assumed a settling velocity of 0.050 cm/s, which would be associated with silt particles. This value has been found to result in reasonable predictions of the distribution of PAH contamination in sediments near structures and is retained in this model. Settling velocity has a significant effect on the spatial distribution of contaminants in sediments. Higher V_v values associated with larger, or denser particles result in higher concentrations of contaminants in a smaller area near the structure, and lower V_v values allow contaminants to be spread over larger areas, but at lower concentrations. The default V_v values are based on model verification studies described in Chapter 10 and at the end of this chapter. Changes by users are possible, but not recommended.

9.1.10 Dispersion of contaminants as they settle to sediments

Active ingredients migrating from treated wood are assumed to disperse horizontally within a cone defined as having the half angle described in Figure 9.4a as they settle to the sediments (Figure 9.4b). Highest concentrations are predicted in close proximity to the treated wood and the concentrations diminish with distance from the treated wood. Contaminants released from an incremental height of immersed wood (Δh) are dispersed over a larger incremental distance downstream (ΔD) by a factor equal to the current speed divided by the settling velocity (V_{model}/V_v). The increased area of deposition downstream due to the moving water is 20 times the current speed for settling speeds of 0.05 cm/s associated with PAH released from creosote-treated wood. In a moderate current of 10 cm/s,

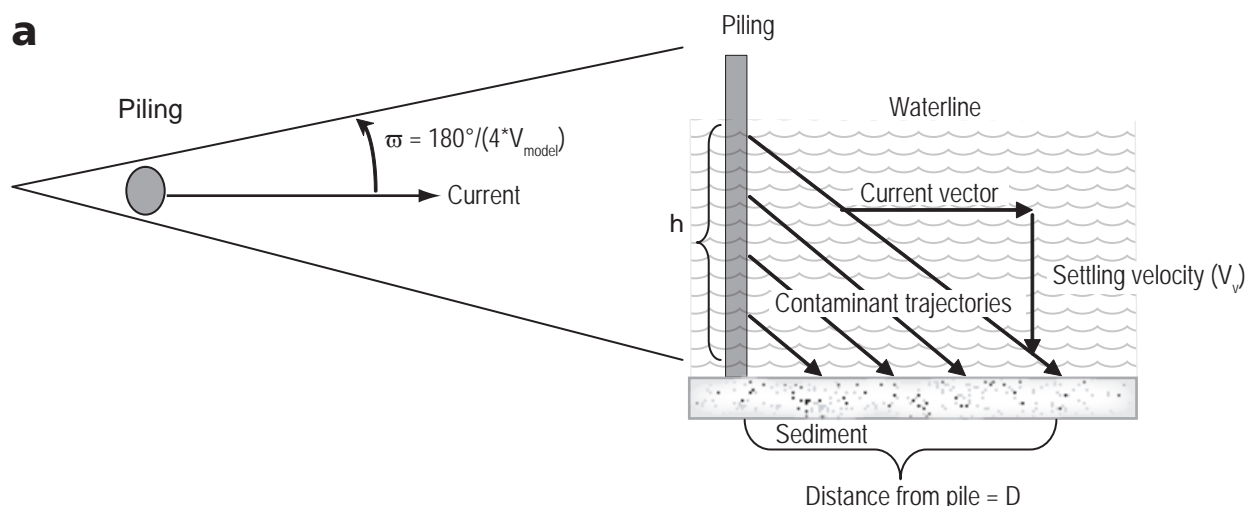


Figure 9.4 (a) Schematic showing assumed turbulent mixing of contaminants into a cone having a central angle equal to $180^\circ / (4 * V_{model})$, when V_{model} is > 0.5 cm/s downcurrent from a treated wood member or structure. (b) Schematic showing the settlement of contaminants down current from treated wood members or structures that describes the relationship between current vectors and settling velocity of a contaminant.

contaminants are spread downstream along a path that is 200 times longer than the incremental height of wood from which they were released.

9.1.11 Transport of contaminants in rainwater to sediments

In addition to the angular dispersion described above, the model assumes that contaminants derived from rainwater runoff will initially be mixed into the upper 20 cm of the water column and then dispersed along sediments in the manner described in Figure 9.5. The length of the sediment dilution zone downstream from the dripline is then given by $20 \text{ cm} * (V_{model} / V_v)$. The length of the sediment dilution zone is $400 * \text{current speed}$ for PAH. Contaminants from pressure-treated wood are assumed to be introduced on the upstream and downstream driplines of the structure.

9.1.12 Redistribution of sedimented contaminants

Contaminants are assumed to remain at the initial point of contact with sediments without further resuspension and redistribution downstream. This is considered a worst case because sediments that are resuspended and carried downstream are unlikely to resettle at concentrations equal to or higher than those found at the original site. In fact, storm waves and high river or stream flows during significant rainfall events will periodically resuspend fine-

grained sediments and organic matter with their adsorbed contaminants and distribute them over larger areas downcurrent from the treated wood structure.

9.1.13 Contaminant depth in sediments

Contaminants are assumed to be mixed into the top 2 cm of the sediment column by bioturbation and diffusion of porewater. Contaminant analyses in sectioned columns of sediment suggest that contaminants are more likely to be distributed to depths of 4-6 cm or greater. However, for purposes of predicting environmental concentrations, the 2-cm depth was chosen because it concentrates the predicted loss of contaminant in a small volume, resulting in higher concentrations and more conservative assessments.

9.1.14 Sediment density

The density of sediments generally varies between 2.6 g/cm^3 (quartz) and 4.3 g/cm^3 (garnet). Marine sediments may contain significant quantities of calcite (CaCO_3) associated with mollusk shell and shell fragments having a density of 2.7 g/cm^3 (Gilluly et al. 1968). To be conservative, a sediment density of $\rho = 2.6$ is recommended for both freshwater and marine sediments. However, users can vary this input when site-specific information suggests otherwise.

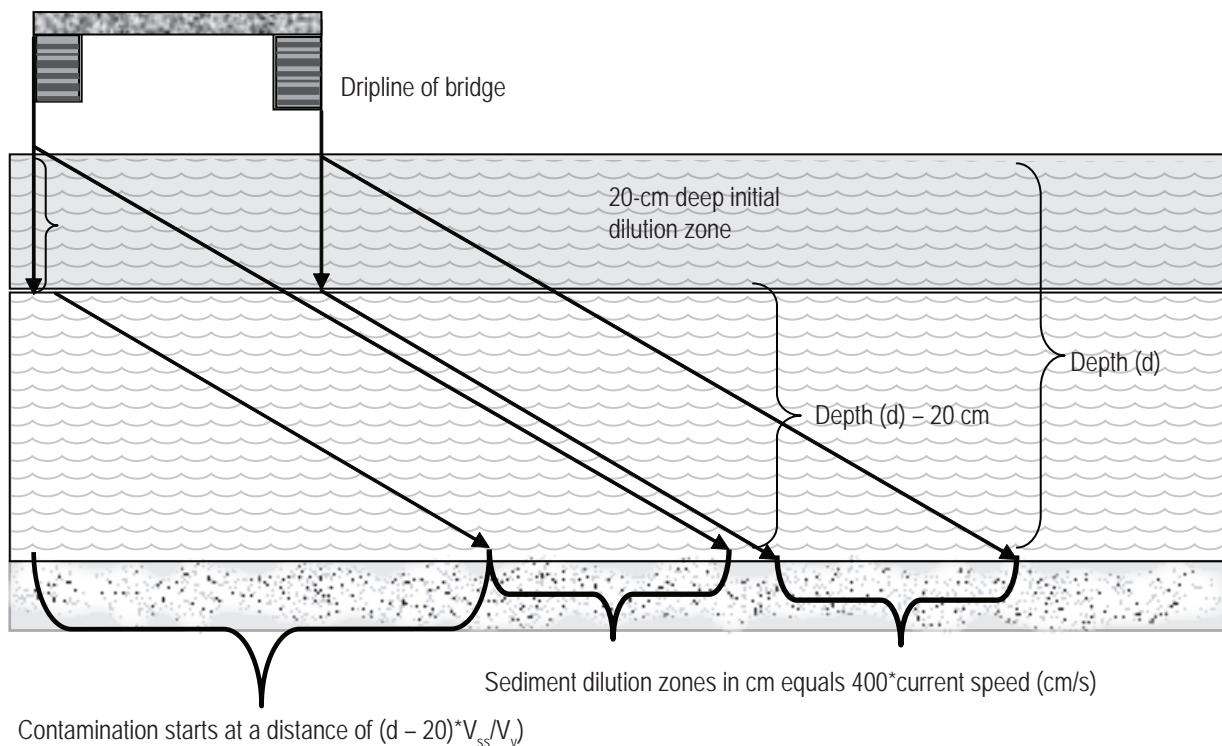


Figure 9.5 Schematic diagram describing the relationship between predicted sediment dilution zones, distance between the upstream and downstream bridge drip lines and receiving water current speed. Deposition occurs downstream at a minimum distance of $(d - 20) \cdot V_{ss} / V_v$ to $d \cdot V_{ss} / V_v$ and it extends to a maximum distance of $d \cdot V_{ss} / V_v$.

9.1.15 Accretion of new sediment

Sediments are accumulating in all aquatic environments—especially in depositional areas where silts, clays, and their adsorbed contaminants accumulate. Sediment accretion rates of 2 cm/y are common in Puget Sound. However, sedimentation rates, like rates of erosion, are difficult to predict. The model assumes no additional sedimentation that would dilute contaminants from pressure-treated wood structures.

9.2 FATE OF CONTAMINANTS RELEASED FROM PRESSURE-TREATED WOOD INTO AQUATIC ENVIRONMENTS

Contaminants are assumed to remain in the water column without degrading until they are sedimented. This is considered worst case because many contaminants, like the low molecular weight PAH, are quickly degraded in water by photooxidation, chemical oxidation and microbial metabolism (Sayler and Sherrill 1981, Colwell 1986, Cerniglia and Heitkamp 1989, Gardner et al. 1979, Borthwick

and Patrick 1982, MacGillivray and Shiaris 1993, Herbes 1981). However, due to their expected short resident time in the water column, organic contaminants released from creosote-treated wood are assumed to remain unchanged in the water column until they are sedimented. Metal contaminants like cupric ions (Cu^{2+}) quickly bind to anions, such as clay or dissolved inorganic matter like CaCO_3 , hydroxyl ions (OH^-) or HS^- , reducing their bioavailability, and, therefore their environmental risk.

The availability of these binding sites and detoxification of dissolved metals depend on a number of factors that are described in the Biotic Ligand Model (BLM) developed by Hydroqual (2007). However, due to the difficulty in measuring the many chemical inputs necessary to run the BLM and the seasonal variability of some of these parameters, the models described herein rely on hardness-dependent (CaCO_3) EPA water-quality criteria (WQC) for assessing the biological response to metals in the water column. In addition to creosote and pentachlorophenol, new preservatives rely on several organic biocides to either replace or compliment copper. The following paragraphs describe a methodology for predicting the accumulation

Table 9.1 Sediment PAH half lives in moderately contaminated sediments (>1.0 mg PAH/kg dry sediment), assuming aerobic conditions in the top 4 cm of sediment. Half-life values are based on data from Cerniglia and Heitkamp (1992) and normalized to 20°C.

LPAH (13% of sedimented TPAH). Half life (T = 20°C) = 30.5 days.				
Compound	Half-life (d)	% in creosote	% in sediment	LPAH half-life contribution (d)
Naphthalene	18	15.45	2.00	8.7
2-methyl naphthalene	101	2.15	0.28	6.8
Phenanthrene	29	12.85	1.67	11.7
Anthracene	72	1.45	0.19	3.3
Sums		31.90	4.14	30.5 days

HPAH (87% of sedimented TPAH). Half life (T = 20°C) = 242.3 d				
Compound	Half-life (days)	% in creosote	% in sediment	HPAH half-life contribution (d)
Pyrene	246	5.30	4.61	160.6
Benzo[α]anthracene	20	0.85	0.74	2.1
Chrysene	100	1.63	1.42	20.1
Benzo[α]pyrene	>1448	0.32	0.29	59.5
Sums		8.10	7.06	242.3 days

of these organic active ingredients. The process requires knowledge of the sedimented half-lives of the compounds and their release rates from pressure-treated wood as a function of the environmental variables that affect these endpoints. The more detailed our understanding is of these responses, the more accurate the predictions will be.

9.2.1 Degradation of sedimented metal contaminants

Metals are immutable and are assumed to accumulate and remain unchanged in sediments for the life of a treated-wood project. In these models, a project lifespan of 35 y is assumed for predicting total metal accumulation. All of the leaching studies reviewed and/or conducted to date (Brooks, 1996, 2002a, 1997, 1998, 2003a, 2003b, 2005b, 2005c, 2005d, 2007, 2009a, 2009b) have reported exponential declines in metal loss rates from pressure-treated wood with variable long-term loss rates. Models for metal-based preservatives allow users to specify longer project lifespans when warranted. The additional accumulation of metal is determined by multiplying the long-term loss rate in the metal loss algorithm by the number of years specified by the user.

9.2.2 Degradation of sedimented PAH

Failure to predict degradation rates can result in significant errors in predicting long-term contaminant accumulations. Rates are dependent on a number of factors including pH, temperature, concentrations of organic carbon, and redox

potential. Cerniglia and Heitkamp (1989) presented a summary of PAH half-lives (Table 9.1) that form the basis of this analysis after normalizing to rates at 20°C. The half-life contributions for each compound are summed to estimate the half-life of creosote in sediments. Individual PAH contributions are the percent of each compound divided by the sum of the percentages of the represented compounds (LPAH = low molecular weight; HPAH = high molecular weight; and TPAH = LPAH + HPAH) times the half-life. The half-life contribution for naphthalene is $18 \text{ d} * (0.1545 / 0.3190) = 8.7 \text{ d}$.

Assuming that 87% of sedimented TPAH are HPAH and that 13% are LPAH, the TPAH half-life would be 214.8 d. Note that Equation [9.2] does not include corrections for temperature or redox potential, which will be discussed in a subsequent section of this chapter.

$$\begin{aligned} \text{TPAH half-life at } 20^\circ\text{C} = & \quad [9.2] \\ 0.13 * 30.5 \text{ days} + 0.87 * 242.3 \text{ days} = & \\ 214.8 \text{ days} & \end{aligned}$$

Of the compounds included in the analysis, it appears that phenanthrene, pyrene, chrysene, and benzo[α]pyrene would be the PAH species most likely found in sediments associated with creosote pilings. One study showed elevated levels of pyrene, phenanthrene, chrysene, and fluoranthene within one meter of recently installed creosoted pilings (EVS Consultants 1994). The EVS study also found that 83% of the sedimented PAH were high molecular weight and 17% were low molecular weight at the most

contaminated station. These findings are in agreement with Malins et al.'s (1985) values of 87% and 13% for high and low molecular weights, respectively.

9.2.2.1 Additional factors affecting PAH degradation

PAH degradation rates are a function of several physical and biotic factors:

Oxygen availability

Microbial metabolism of aromatic hydrocarbons requires molecular oxygen as a first step in breaking the ring by bacterial enzymes known as dioxygenases (Sayler and Sherrill 1981). Dissolved oxygen is seldom depressed in the water column of open aquatic systems. However, oxygen diffuses slowly into sediments and is rapidly used by macrofauna and microorganisms in the upper few centimeters of the substrate. Heavy organic loading, particularly in poorly flushed areas, can exacerbate oxygen deficits, creating anoxic conditions on the surface of sediments or at very shallow depths (1 to 2 cm). Hambrick et al. (1980) reported the effect of oxidation-reduction potential on the microbial degradation of naphthalene in aquatic sediments from a salt marsh stream near an oil field in Louisiana. The redox potential of submerged sediments ranged from -300 mV for anoxic sediments up to +700 mV for highly aerobic sediments. Hambrick et al. (1980) found that mineralization of naphthalene at pH values of 5.0, 6.5, and 8.0 increased as redox values increased from -250 to +510 mV and concluded that oxygen availability was an important factor for PAH mineralization. Degradation studies by Bauer and Capone (1985) suggest that PAH buried in anaerobic sediments may persist for many years. This model will evaluate sediment oxygen levels through measurement of the redox potential discontinuity (RPD), which is simply the distance below the sediment surface at which the sediment color changes to dark gray or black. The black color is evidence of iron sulfides associated with anaerobic conditions. RPD is measured by inserting a clear plastic or

glass cylinder vertically into the sediment and measuring the depth of the discontinuity in centimeters. For purposes of this analysis, Equation [9.3] is used to describe the response to decreasing depths of the RPD. Years of work at organically loaded aquaculture sites (see for instance Brooks et al. 2002, 2004) suggests the redox potentials associated with varying RPD depths shown in Table 9.2. Corrections are provided in the last column of the table.

$$\text{PAH degradation factor in response to decreasing RPD} = \exp^{[(4-\text{RPD})]^3} \quad [9.3]$$

Temperature

Temperature directly affects the rate at which PAH are degraded by microorganisms in natural ecosystems. Several investigators have reported seasonal fluxes in heterotrophic activity and PAH degradation rates. The highest activities are found in summer and the lowest in winter. The magnitude of temperature effects on PAH degradation was demonstrated in anthracene and naphthalene by Bauer and Capone (1985). Similarly, Sayler and Sherrill (1981) demonstrated increased phenanthrene degradation as a function of temperature between 5° and 37°C. For the current model, the preceding data were normalized to a temperature of 20°C. Linear regression on the transformed data gave the results presented in Table 9.3. Further normalizing each of the component coefficients to their relative proportions in creosote oil provided

Table 9.2 PAH half-life corrections associated with depth of the RPD or redox potential measured in the upper 2.0 cm of the sediment column.

Depth of RPD (cm)	Associated redox (mV)	Half-life correction
≥ 4	+100	1.00
3	0 to +50	1.04
2	-50 to 0	1.34
1	-100 to -50	2.72
0 cm	<-100	10.70

Table 9.3 Relationship between phenanthrene, anthracene, and naphthalene mineralization and incubation temperature.

Compound	Regression	R _a ²	Probability that Coef = 0.0
Phenanthrene	Degradation (D) _i = 2.033 T (°C)	0.937	P = 0.002
Anthracene	Degradation (D) _i = 0.568 T (°C)	0.979	P = 0.011
Naphthalene	Degradation (D) _i = 1.249 T (°C)	0.971	P = 0.014
Total PAH	Degradation (D) _i = 1.555 T (°C)		

Note: Data between 5 and 37°C were used in the analysis. For purposes of this analysis, the degradation coefficients were normalized to their proportional presence in creosote oil to obtain an estimate of the effect of temperature on total PAH degradation and accumulation in sediment. Coefficients of determination (R_a²) are ≥0.94 for each of the regressions.

an estimate for total PAH degradation response to temperature.

To accommodate the needs of this model, the data used to develop Table 9.3 were normalized to 20°C, giving Equation [9.4]. At 8°C, the model predicts degradation rates that are 37.6% of those observed at 20°C, while rates at 30°C are 141% of those observed at 20°C.

$$\text{PAH Thermal Accumulation Factor} = \frac{1}{0.047T(^{\circ}\text{C})} \quad [9.4]$$

Bacterial population density and species

Bacterial populations (species) within a microbial community do not all have the same spectrum of enzymatic capability. Relatively few bacterial species are known to contain the necessary genetic material to code for the production of PAH-degrading enzymes. It is generally accepted that bacterial enzymes have co-evolved with the presence of growth-supporting substrates or as a response to the destruction of potentially toxic substrates. Complete mineralization of a growth-supporting substrate results from multiple enzymes acting sequentially under complex systems of product and substrate regulation. Consequently, novel PAH substrates or PAH substrates reaching high concentrations due to anthropogenic sources may resist complete mineralization due to a lack of specific enzymes or enzyme complexes. Lack of a complete enzyme system may result in a phenomenon known as co-oxidation or co-metabolism, in which a PAH substrate may be partially oxidized by a non-specific enzyme while the bacterial cell grows at the expense of another substrate.

Bacterial enzymes involved in the metabolism of PAH are induced, meaning that they are synthesized when an unknown, but finite, quantity of PAH interacts with DNA in the bacterial cell. There are no known active transport systems that facilitate the accumulation of PAH in bacterial cells. The passive diffusion rate of PAH onto and into the bacterial cell is concentration dependent and potentially rate limited if the bacterial cell is competing with inorganic and organic particle surfaces as sites for PAH adsorption. Therefore, the solubility of PAH, which ranges from 12.5 mg/L for naphthalene to 10 ng-L⁻¹ for benzo[*a*]pyrene, is a major determinant affecting PAH availability to microbes. It is generally thought that microbes metabolize low molecular weight PAH (2 and 3 rings) much more readily than high molecular weight PAH (4 or more rings). In part, this is due to the reduced solubility of HPAH. Those PAH

with more than three condensed benzene rings do not serve as sole substrates for microbial growth, though they may be subject to co-metabolism when other substrates are available. For the purposes of this analysis, we will assume that sufficient PAH are released over an extended period of time, such that microbial communities with PAH-metabolizing enzyme systems are stimulated and that there are sufficient quantities of LPAH and other primary substrates allowing for the co-metabolism of HPAH. No corrections for microbial community adaptation will be included in this model.

9.2.2.2 Polycyclic Aromatic Hydrocarbon Degradation Model

Combining the results of the above arguments provides a dimensionless half-life based on temperature and dissolved oxygen availability in the sediments (Equation [9.5]), which is applied to the half-life factor.

$$\text{PAH}_{\text{half-life}} = (214.8 \text{ days} * \exp^{[(4 - \text{RPD})/3]^3}) / 0.047T(^{\circ}\text{C}) \quad [9.5]$$

9.2.3 Degradation of pentachlorophenol in aquatic environments

Pentachlorophenol (penta) may be dissolved in water or sorbed to suspended matter or bottom sediments. In addition, penta is taken up by fauna and flora that metabolize the compound at varying rates. Penta readily degrades in the environment by chemical, microbiological, and photochemical processes (USDA 1980, Eisler 1989). Half-life in sediments can range from days to years, depending on environmental conditions. The ultimate fate of penta appears to be burial in anaerobic sediments under infrequently encountered conditions or mineralization to carbon dioxide and water. Penta that is dissolved in water may be removed by volatilization, photodegradation, absorption, or biodegradation. Photochemical degradation is a function of the spectrum and intensity of incident light and appears to proceed rapidly in natural environments, with half-lives of 0.15 to 15 d (Smith et al. 1987). Boyle et al. (1980) examined the degradation of pentachlorophenol in a two-by-two array of microcosms with and without natural lake sediments held under aerobic and anaerobic conditions. At the end of the 131-d experiment, the authors determined the pentachlorophenol half-life under each of the four conditions (Table 9.4). Boyle et al. (1980) also partitioned ¹⁴C at the end of the experi-

Table 9.4 Pentachlorophenol remaining in water and sediments at the end of 131 d in each of four aquaria (Boyle et al. 1980).

Test conditions	Total penta in water (mg)	Water half-life (d)	Penta in sediments (mg)	Total penta (mg)
Aerobic without mud (lighted)	0.95	18.6		0.950
Aerobic with mud (lighted)	0.21	13.9	0.03	0.240
Anaerobic without mud (dark)	16.00	79.8		16.000
Anaerobic with mud (dark)	0.005	12.8	0.04	0.045

Note: Residues are in milligrams of pentachlorophenol for each compartment at the end of 131 days. One hundred milligrams of pentachlorophenol were originally added to the aquaria. The water column half-life is given for penta as determined in this experiment.

ment. The bulk (99%) of the sedimented ^{14}C was observed in the non-biogenic clay fraction. They also found ^{14}C in algae, floating flocculent material, and other biogenic material in the water column. Minimal ^{14}C was observed elsewhere in the microcosms (including the aquarium sides and cover). The authors concluded that pentachlorophenol degradation was positively correlated with incident light levels, pH, oxygen, and the presence of sediment. They concluded that pentachlorophenol is likely most persistent in the deoxygenated hypolimnion water of lakes.

Fisher (1990) concluded that the half-life of dissolved and sedimented pentachlorophenol would be on the order of one week in aerobic and organically rich environments. Middaugh et al. (1993) determined that the gram-negative bacterium, *Pseudomonas* sp. (strain SR3) was able to degrade penta, which provided an adequate sole carbon source to sustain growth. Nearly complete degradation of 39,000 to 40,000 μg penta/L was accomplished by acclimated *Pseudomonas* sp. Pentachlorophenol half-lives in freshwater streams reported in McAllister et al. (1996) varied between 40 and 120 h. A number of environmental factors affect the rate at which pentachlorophenol is degraded in natural aquatic environments.

9.2.3.1 Effects of pH and water temperature on the degradation of dissolved pentachlorophenol

Valo et al. (1985) found that metabolism of pentachlorophenol was inhibited at temperatures less than 8°C or greater than 50°C with optimum degradation at 28°C. Jarvinen and Puhakka (1994) and Jarvinen et al. (1994) found that 99% of the penta present in contaminated groundwater was degraded at temperatures of 5° to 10°C, while no penta degradation was observed with acclimated *Pseudomonas* at 0°C (Trevors 1982). Pentachlorophenol degradation rates at 4°C were dependent on the specific *Pseudomonas* strain used. However, an average of 28.2% of the initial 50,000 μg penta/L substrate was metabolized

in 80 d at 4°C, while 50.2% of the same concentration was metabolized in 8 d at 20°C. Valo et al. (1985) observed pentachlorophenol degradation at pH values between 5.6 and 8.0. A neutral or slightly acidic pH was found to be optimum. Wong and Crosby (1981) observed pentachlorophenol half-lives of approximately 100 h at pH 3.3 and 3.5 h at pH 7.3 in sterile solutions containing 100,000 μg penta/L. No pentachlorophenol degradation was observed in flasks maintained in the dark. It appears that pentachlorophenol degradation is optimum at pH values between about 6.5 and 8.0, and at temperatures between 10 and 30°C. These are conditions expected in much of North America during all seasons except winter, when low temperatures at northern latitudes can be expected to decrease pentachlorophenol degradation rates. In addition, pentachlorophenol is expected to degrade more slowly in areas with exceptionally low pH.

9.2.3.2 Adaptation to pentachlorophenol by microbial communities

Larsson et al. (1988) and Larsson and Lemkemeier (1989) observed significantly higher pentachlorophenol degradation by unacclimated microbial communities inhabiting brown water lakes containing high levels of humic acid when compared with clear water lakes. These authors concluded that the microbial communities inhabiting brown water lakes had adapted to the higher phenol levels naturally present in the water and therefore were pre-acclimated to metabolize pentachlorophenol. McAllister et al. (1996) reviewed the literature pertaining to the microbial degradation of pentachlorophenol and confirmed that sediment pentachlorophenol levels exceeding 300 $\mu\text{g}/\text{kg}$ inhibit microbial degradation until a period of acclimation had passed. Once acclimation had begun, it appeared that the higher the initial concentration of PCP, the longer the maximum number of viable cells capable of degrading PCP was maintained. Gonzalez and Hu (1991) observed that lag phases of 10 h occurred at 10 mg/L, 30 h at 20 mg/L, 55 h at 44 mg/L, 80 h at 80 mg/L and 200 h

at 200 mg/L. In summary, it appeared that microbial communities were not generally pre-adapted to metabolize pentachlorophenol. Initial exposure of naïve bacterial communities to penta concentrations as low as 300 µg penta/L reduced their growth. An adaptation period of several hours to perhaps two weeks is necessary for community adaptation to pentachlorophenol. Following this time, however, adapted communities can tolerate much higher concentrations of pentachlorophenol, which they rapidly metabolize.

9.2.3.3 Effects of additional sources of carbon on pentachlorophenol metabolism

Topp et al. (1988) studied the response of penta-degrading *Flavobacterium* sp. to high levels of penta with and without the addition of sodium glutamate as a co-metabolite. They found that specific activity of penta-degrading cells in the absence of supplementary carbon was 1.51×10^{-13} g penta/cell-h. They showed that the form and amount of alternate substrates was important in determining the metabolism of pentachlorophenol. For instance, optimal stimulation of pentachlorophenol removal required the addition of 3.0 g sodium glutamate/L. However, glutamate in combination with glucose or cellobiose partially repressed penta metabolism. *Flavobacterium* removed 2.5% of the penta from a 25,000 µg/L initial concentration. The addition of 4 g sodium glutamate/L increased metabolism, resulting in the removal of 61.9% of the penta in 3 h. However, when the mixture was amended with 4 g sodium glutamate and 5 g/L glucose, penta metabolism was reduced to 15.5% in 3 h. The combination of the two substrates reduced penta metabolism because, in a separate experiment, the authors found that the addition of 0.5 g of glucose to the medium in the absence of sodium glutamate resulted in the complete degradation of an initial 61,000 µg penta/L solution by *Flavobacterium* sp. The amount of penta removal decreased when incremental amounts of sodium glutamate were added to the glucose. Topp et al. (1988) did not discuss the possibility that *Flavobacterium* sp. acclimated to and degraded pentachlorophenol as a sole carbon source—but preferentially shifted to alternate substrates when available. Perhaps rather than acting antagonistically, the combination of sodium glutamate and glucose acted synergistically, reducing the dependence of the bacteria on pentachlorophenol. Yu and Ward (1995) observed maximum pentachlorophenol degradation in medium supplemented with glucose and peptone.

Topp et al. (1988) found that amendment with a supplementary source of carbon reduced the lag time required before significant penta metabolism commenced. These authors noted that penta concentrations greater than 20,000 µg/L and 500,000 µg/L inhibited *Escherichia coli* and *Pseudomonas* spp., respectively. They also reported that 50,000 µg penta/L was degraded as a sole carbon source after a lag phase of 90 h.

Pentachlorophenol half-lives in freshwater streams reported in McAllister et al. (1996) varied between 40 and 120 h. Consistent with Liu et al. (1981), McAllister et al. (1996) reported that additional substrates tended to reduce penta degradation rates and hypothesized that adsorbed penta was less bioavailable. McAllister et al. (1996) also noted that the most widely studied pentachlorophenol degrading microorganisms are the pure-culture bacterial strains, *Flavobacterium* sp. and *Rhodococcus chlorophenolicus*. The enzymes responsible for initiating the catabolism of pentachlorophenol by *Flavobacterium* sp. have been isolated and characterized. Furthermore, the genes encoding these enzymes have been characterized and cloned into *E. coli*, which then demonstrated the ability to degrade pentachlorophenol. These reports suggest that pentachlorophenol will be degraded more rapidly in organically rich environments. However, some caution is necessary because there is evidence that some combinations of co-metabolites can slow degradation rates.

9.2.3.4 Effects of water hardness on the fate of dissolved pentachlorophenol

Brockway et al. (1984) observed no significant effect of water hardness on fate or bioactivity of penta in their mesocosm study.

9.2.3.5 Sedimentation of pentachlorophenol

Fisher (1990) constructed microcosms with water at pH 4, 6, and 8 and sediments with 0.0 and 3.0% total organic carbon. She found that more penta was partitioned to the sediments at lower pH than at higher pH. In addition, she reported a positive correlation between sediment TOC and penta concentration. Organisms in the high TOC microcosms accumulated significantly less penta than did those in the 0.0% TOC systems. This work is consistent with Eisler's (1989) observation that pentachlorophenol is fully protonated and lipophilic at low pH, whereas it is ionized at high pH and unlikely to adsorb to organic ligands. Shimizu et al. (1992) determined the adsorption coefficients of pentachlorophenol in aquatic environments with

varying organic carbon content (0.72 to 2.38%) and varying clay content (10.1 to 60.8%). They concluded that the adsorption coefficient at pH values between 6 and 8 was not influenced significantly by organic carbon content (correlation coefficient = 0.12), but was positively correlated with clay content (correlation coefficient = 0.94). This work suggests that clay particles (which frequently carry an electrical charge), rather than particulate or dissolved organic carbon, form a more likely adsorption nucleus in aquatic environments. In summary, it appears that the potential for sedimentation of pentachlorophenol is a complex problem driven by at least the following parameters:

- Water column pH. At reduced pH values, penta tends to be fully protonated and more lipophilic. It would therefore, be expected to adsorb to dissolved or particulate organic matter. On the other hand, more of the penta is expected to be ionized at higher pH, with a higher potential for binding to polar adsorption nuclei represented by particulate inorganic matter (silt and clay).
- It appears that more pentachlorophenol will be partitioned from the water column to sediments having increased clay content. This can have a significant effect on penta removal from the water column.

9.2.3.6 Degradation of sedimented pentachlorophenol

Bryand and Rogers (1990) describe the degradation of pentachlorophenol in anaerobic sediments from diverse locations around the world. They observed that dechlorination did not occur for at least the first 15 d of exposure in unadapted sediments. However, following that adaptation period, pentachlorophenol was completely degraded by 33 d. A second addition of 70 mg pentachlorophenol/kg sediment on d 33 was rapidly dechlorinated to about 25 mg/kg in 2 d. In contrast, they observed no biotransformation within a 40-d period of penta added to unadapted Cherokee Pond sediments. The point made in this study was that not all microbes have the ability to dechlorinate penta as a first degradative step. Their study is consistent with other reports indicating that unacclimated, but biologically rich, sediments require a period of approximately 2 wk before the emergence of a microbial community that is capable of aerobic or anaerobic degradation of pentachlorophenol. However, once established, these communities rapidly catabolize penta. Interestingly,

these authors found no degradation of pentachlorophenol in autoclaved sediments—further emphasizing the microbial nature of the observed degradation. Van Gestel and Ma (1988) determined pentachlorophenol half-lives in low pH and organically rich Holten (pH = 5.6; 6.1% organic matter) and Kooyenburg (pH ~ 5.0; 3.7% organic matter) soils of 23.2 to 47.9 d respectively. There was no significant difference in the half-lives of pentachlorophenol in these two sediments. Smith and Novak (1987) found that pentachlorophenol concentrations as high as 25,000 µg/L in saturated soils were degraded to non-detectable levels in less than 3 mo. They found that chlorophenol degradation rates were linearly related to the initial concentration and varied between 100 µg/L-d at an initial concentration of 200 µg/L to >10,000 µg/L-d at an initial concentration of ca. 800,000 µg/L.

9.2.3.7 Effects of sediment oxidation-reduction potential

Delaune et al. (1983) examined the degradation of pentachlorophenol in estuarine sediments following a major accidental spill in a Louisiana Gulf Coast estuary. They completed a series of laboratory experiments in which pH was manipulated between 5.0 and 9.0 and sediment redox between -250 mV and +500 mV. The authors found maximum degradation at pH = 8.0 with declines at either lower or higher values. Pentachlorophenol was observed to degrade at all values of redox. However, significantly higher degradation rates were observed under aerobic (+250 and +500 mV) than with reducing (0.0 and -250 mV) conditions. A half-life of ca. 24 d was apparent at pH 6.5 and a redox potential of +500 mV. However, at this pH, minimal degradation was observed at any other value of redox. At a pH of 8.0, significant degradation was observed at +250 and +500 mV redox potentials and a half-life of 26.5 d was apparent at +500 mV. The authors found that pentachlorophenol was more tightly bound to oxidized sediment solids than to reduced sediments. Therefore, they concluded that there was a tendency for pentachlorophenol to become preferentially associated with the thin oxidized surface sediment horizon, as well as with suspended colloidal particulates, which would also tend to be oxidized. Under either condition, the penta would be retained in the photic zone of shallow estuaries where the potential for photodegradation would be enhanced. The authors concluded that although tidal transport and photodegradation in the water column could play a role in the removal of residual pentachlorophenol from a spill area, their laboratory studies suggested that degradation under

either aerobic or anaerobic conditions could account for the disappearance of residual penta left in the immediate vicinity of the spill or that which was transported from the spill site and deposited onto the bottom in adjacent waterbodies.

9.2.3.8 Anaerobic degradation of pentachlorophenol

Guthrie et al. (1984) studied anaerobic degradation of pentachlorophenol as a component of sewage sludge during treatment and found that methanogenic bacteria were unaffected by pentachlorophenol concentrations <200 µg/L. Acclimation of the bacterial flora to penta raised the inhibition threshold to about 600 µg/L. They found that pentachlorophenol was biodegradable in anaerobic environments and that removal was so complete that the soluble concentrations in the Phase II reactors were below detection limits (5 µg/L). Sorption appeared a minor mechanism of penta removal and volatilization was considered insignificant. The authors concluded that pentachlorophenol undergoes extensive anaerobic biodegradation—especially in acclimated microbial communities. Anaerobic degradation of pentachlorophenol has been confirmed by Kudo (1989). Liu et al. (1981) observed similar results in their comparison of aerobic and anaerobic degradation of sedimented pentachlorophenol at pH = 7.0. They observed an increase in the aerobic half-life of 0.36 d to 190 d under anaerobic conditions. They also found that the inclusion of either sodium chlorophenolate or glucose as a second substrate inhibited, rather than enhanced the anaerobic degradation of pentachlorophenol. In contrast, Valo et al. (1985) found that pentachlorophenol degradation was enhanced by the addition of 40 mM NH₄Cl. Bryant and Rogers (1990) examined the degradation of pentachlorophenol in anaerobic sediments from Georgia, Florida, New York, and the Soviet Union. They observed an adaptation period of ca. 15 to 20 d during which little penta degradation occurred. Degradation in adapted anaerobic sediments was rapid with an unstated half-life of 2 to 7 d. Pentachlorophenol half-lives in plants (Benner and Tjeerdema 1993); and rainbow trout (Glickman et al. 1977) are shorter on the order of a few hours to several days. The data reviewed in this section is summarized in Table 9.5.

Data from a number of studies (Baker et al. 1980, DeLaune et al. 1983, Boyle et al. 1980) were interpreted to produce half-lives as a function of initial penta concentration, reduction oxidation potential, pH, and

temperature (Table 9.6). Sedimented half-life was estimated assuming that microbes required 15 d to adapt to penta and that degradation rates remained linear at all times. Although the database is small and the methodology is not precise, the results are consistent with the remainder of the literature. These penta half-lives are important for predicting sediment accumulation. These data were analyzed using linear and non-linear regression analysis. Within the ranges of the data at hand, sedimented pentachlorophenol half-life was not a function of the initial concentration ($p = 0.10$) or temperature ($p = 0.40$). In addition, the constant term was not significant ($p = 0.42$). Redox potential and pH were significant factors ($p = 0.001$ and $p < 0.000$, respectively). The final regression (Equation [9.6]) was significant ($P < 0.00015$) and explained 76% of the variation in the database ($R^2_a = 0.76$). The underlying assumptions requiring normally distributed residuals and homoscedasticity were met.

$$\text{Sedimented penta half-life} = 18.194 * \text{pH} - 0.293 * \text{Redox (mV)} \quad [9.6]$$

The data were also used to construct a series of curves using a quadratic smoothing routine in Statistica™ software (Figure 9.6). Under normal environmental conditions, the redox potential in surface sediments will vary between -100 and +400 mV and the pH is expected to vary between 6 and 8.5. Figure 9.6 suggests that under these conditions, sedimented pentachlorophenol half-lives will vary significantly between 12.7 d and 176.4 d. The linear equation used to make predictions in this model predicts a half-life of 24.8 d at pH = 7.8 and a redox potential of +400 mV and 156.6 d at pH = 7.0 and -100 mV.

9.2.3.9 Pentachlorophenol case studies

Seidler et al. (1986) examined the transport and fate of pentachlorophenol-contaminated wastewater as it passed through two estuarine ponds being used to grow shrimp in Florida. Pentachlorophenol was added to the test ponds by broadcasting 500 mg of sodium-pentachlorophenolate in acetone on day zero, followed by the addition of 250 mg on alternate days thereafter to provide a theoretical concentration of 10 µg penta/L. Pentachlorophenol concentrations of 3 to 5 µg/L were observed in the treatment ponds during the first 22 d of the study. The authors predicted that 99.9% of the added penta would be dissolved in the phenolate form at a pH of 8.0, suggesting that photolysis would be the most significant degradation

Table 9.5 Summary of pentachlorophenol half-lives, principle reasons for degradation, and the effects of various environmental parameters on degradation rates.

a. Reported pentachlorophenol half-life in water			
Author		Half-life (days)	Conditions
Boyle et al. (1980)		18.6	Aerobic in the laboratory
Boyle et al. (1980)		79.8	Anaerobic in the laboratory
Crossland and Wolff (1985)		2.0 to 4.7	Outdoor mesocosms
Liu et al. (1981)		0.36	Aerobic in the laboratory
Liu et al. (1981)		190.0	Anaerobic in laboratory
Wong and Crosby (1981)		2.0	pH 7.3 (natural sun-light)
Yu and Ward (1995)		~1.5	Mixed bacterial cultures
b. Effects of pH on pentachlorophenol half-life			
Author	pH	Half-life (hours)	Conditions
Wong and Crosby (1981)	7.3	3.5	Laboratory F40BL lamps
Wong and Crosby (1981)	3.3	100.0	Laboratory F40 BL lamps
Wong and Crosby (1981)	7.3	48.0	Natural sunlight
c. Effects of ambient temperature on pentachlorophenol half-life			
Author	T°C	Half-life (days)	Conditions
Topp et al. (1988)	4	>80	<i>Pseudomonas</i> cultures
Topp et al. (1988)	20	<12	<i>Pseudomonas</i> cultures
d. Anticipated half-life of pentachlorophenol in soils or sediments			
Author		Half-life (days)	Conditions
DeLaune et al. (1983)		24 to 26	Natural estuarine sediments
McAllister et al. (1996)		10 to 70	Flooded soils
McAllister et al. (1996)		< 2 to >5	Freshwater streams
Neary et al. (1990)		Average 30	Southern ecosystems
Smith and Novak (1987)		<5	9 to 13 mg PCP/L unsaturated soil
Smith and Novak (1987)		~15	Average 3 mg PCP/L unsaturated soil
e. Effects of sediment reduction – oxidation potential			
Author		Half-life aerobic (days)	Half-life anaerobic (days)
Boyle et al. (1980)		13.9	12.8
Bryant and Rogers (1990)			2 to 5
McAllister et al. (1996)			144
f. Pentachlorophenol half-life in plants and animals.			
Author	Species	Penta half-life (hours)	
Benner and Tjeerdema (1993)	<i>Atherinops affinis</i>	52.7 hours	
Glickman et al. (1977)	<i>Onchorhynchus mykiss</i>	6.2 to 6.9 hours	

process. They calculated a penta half-life of 2 d for the ponds being treated. Seidler et al. (1986) claimed that sediments contained 54 times more pentachlorophenol than was found in the water column. However, the data presented in their paper suggest that sediment levels mimicked water column levels with a concentration factor of one to perhaps ten. Sediment concentrations of pentachlorophenol averaged about 5 µg/kg with a maximum of about 18 µg/kg. The authors suggested that a chronic influx of pentachlorophenol at a concentration of 10 µg/L

to an estuarine environment resulted in elevated concentrations in the water, sediment, and shrimp. Penta concentrations in the shrimp (maximum of about 18 µg/g on d 20) were positively correlated with water column concentrations rather than with sediment concentrations. This suggests direct uptake from the water rather than bio-magnification from macrofaunal prey. Once the source of pentachlorophenol was removed, the compound rapidly disappeared from the water, shrimp, and sediments—apparently in a matter of hours or days.

Table 9.6 Estimated sedimented pentachlorophenol half-lives as a function of the initial pentachlorophenol concentration, reduction-oxidation potential, pH and temperature. Sedimented penta half-lives were estimated from data in Baker et al. (1980), DeLaune et al. (1983), and Boyle et al. (1980).

Source	Initial penta concentration(µg/kg)	Redox potential (mV)	pH	Temp (°C)	Half-life (days)
Baker	100.0	250	7.1	0.0	47.5
Baker	100.0	250	6.9	20.0	36.7
Boyle	1400.0	0	4.5	15.0	13.0
Boyle	1400.0	250	6.8	15.0	7.5
DeLaune	20.0	500	6.5	33.1	6.0
DeLaune	20.0	250	6.5	33.1	103.5
DeLaune	20.0	0	6.5	33.1	178.8
DeLaune	20.0	500	8.0	33.1	12.0
DeLaune	20.0	250	8.0	33.1	32.5
DeLaune	20.0	0	8.0	33.1	81.0
DeLaune	20.0	-250.0	8.0	33.1	290.0
DeLaune	20.0	500.0	9.0	33.1	50.0
DeLaune	20.0	250.0	9.0	33.1	50.0

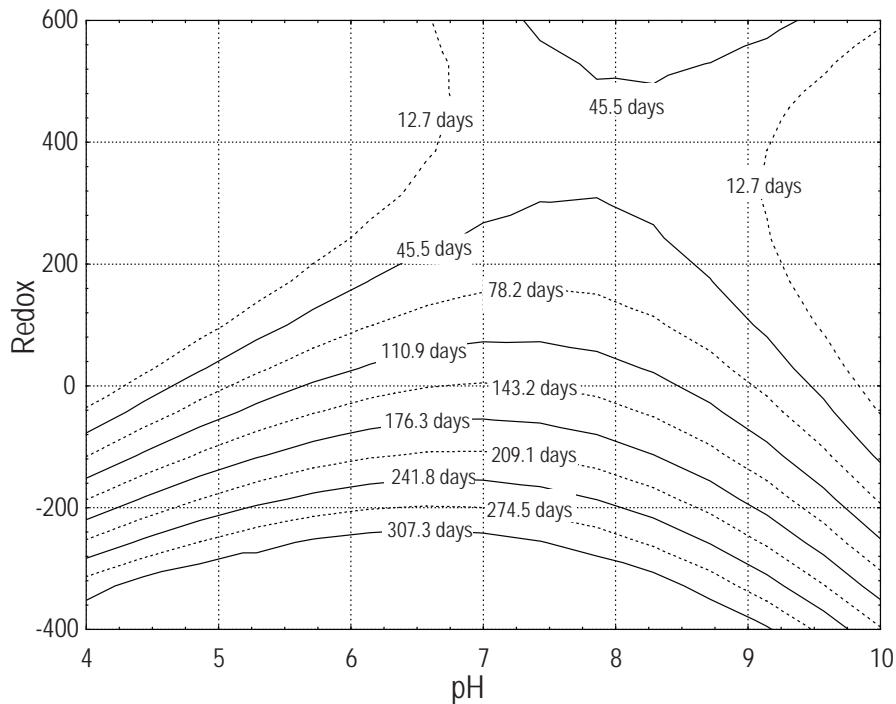


Figure 9.6 Contour plot showing the effects of pH and redox potential on penta half-lives as determined using a quadratic solution of data in Table 9.6 with sediment reduction-oxidation potential (mV) and pH as independent factors. 3-D contour plot $z = -715.685 + 243.79x - 1.042y - 17.252x^2 + 0.073xy + 0.001y^2$.

Crossland and Wolff (1985) determined the half-life of pentachlorophenol in outdoor ponds repeatedly dosed to maintain a concentration of 50 to 100 μg penta/L. The authors hypothesized that evaporation, sorption, hydrolysis, biodegradation, and indirect phototransformation of penta would be of minor importance under the environmental conditions. The partition coefficient for penta between water and sediments was predicted to be near unity. The authors used the SOLAR mathematical model to calculate a direct photodegradation rate constant for the transformation of penta in the ponds whose pH varied between 7.3 and 10.3, with a mean of 8.3. A series of bioassays were conducted and pond invertebrates were enumerated at levels of taxonomy exceeding Order. The results appeared consistent with the general body of literature describing the toxicity of pentachlorophenol. The observed half-lives of pentachlorophenol in the three treatment ponds varied between 2.0 and 4.7 d and were in good agreement with the predicted half-lives based on results of the SOLAR analysis. The authors concluded that direct phototransformation was responsible for nearly all of the pentachlorophenol degradation observed in this study. In addition, sediment concentrations of pentachlorophenol at the end of the study were very similar to water column concentrations. They hypothesized that an insufficient period of time had elapsed for development of a microbial community capable of efficiently metabolizing penta in the sediments.

Robinson et al. (1983) examined the degradation of pentachlorophenol in a series of experimental ponds contaminated by a single high dose of pentachlorophenol (1,000 $\mu\text{g}/\text{L}$) followed by a series of small doses (0.2, 0.2, 0.4, and 0.4 mg/L) at monthly intervals. Two of the replicated sets of ponds held only phytoplankton, whereas the third set of ponds contained rooted macrophytes. The authors found higher metabolism of pentachlorophenol in the ponds containing rooted macrophytes. The increased degradation of penta in the macrophyte ponds resulted in lower body burdens in channel catfish, bluegill, and largemouth bass. These fish species survived the highest dose of penta (1,000 $\mu\text{g}/\text{L}$) in the pond containing macrophytes, but succumbed in the ponds containing only phytoplankton. The authors suggested three hypotheses as possible explanations for these results. However, only two of those hypotheses appear different from each other: (1) the presence of the macrophytes resulted in a different chemical or physical environment in the ponds that increased penta degradation; and (2) the macrophytes or

aufwuchs community associated with the macrophytes were incorporating penta as a conjugate or within the cell structure.

Fisher (1990) observed that the concentration of dissolved pentachlorophenol increased with increasing pH but that the uptake by both organisms and sediments was decreased. She also observed that increasing sediment organic carbon was associated with higher sediment levels of penta and reduced concentrations in the water column. Delaune et al. (1983) studied the fate of pentachlorophenol following a major spill in a Louisiana Gulf coast estuary and found that pentachlorophenol degradation was strongly influenced by sediment pH and redox potential. Degradation rates decreased with decreasing sediment redox and were maximized at $\text{pH} = 8.0$, with reduced degradation at either higher or lower pH values. In addition, these authors found that penta was more tightly bound to oxidized sediment than to reduced sediment. They observed that essentially all of the pentachlorophenol had disappeared from the spill area within 18 mo and hypothesized that observed microbial degradation could account for the degradation. Sediments in the study area contained 3% to 5% carbon and the sediment pH was essentially neutral at 6.8.

It is apparent that a variety of microorganisms are able to degrade pentachlorophenol. In general, it appears that aerobic degradation is more efficient than anaerobic degradation and that increased degradation occurs at moderate temperatures (between 10°C and 35°C). In most instances, it appears that penta degradation by microbial communities is enhanced by the presence of alternate carbon substrates.

9.2.4 Degradation of other organic compounds used in pressure-treated wood

Over the last 5 y, several new preservative systems that incorporate organic compounds such as imidacloprid, tebuconazole, and/or propiconazole have been used as co-biocides with copper or have been used as purely organic wood preservatives. Concentrations of these organic compounds in rainwater runoff from pressure-treated wood have been determined for some of these systems and rainwater concentrations have been developed for micronized copper preservatives that include one or more of these biocides. Available data describing the half-lives of these compounds in sediments are summarized in Table 9.7.

9.2.4.1 Imidacloprid

Imidacloprid is a nicotinimide insecticide with a water solubility of 610 mg/L, a low vapor pressure (1.5×10^{-9} mm Hg) and a low $\log K_{ow}$ of 0.57. It is not expected to bioaccumulate nor is it expected to adsorb to suspended particulates. This compound readily absorbs UV radiation in the spectrum of sunlight and a high rate of photolysis has been observed with a half-life of 4 h. Imidacloprid is also degraded by bacteria in sediments containing elevated concentrations of organic carbon and has a half-life of less than 14 d, as opposed to 27.1 d in sediments containing low concentrations of organic carbon. Bacterial catabolism is slowed in oligotrophic sediments but a specific half-life was not provided (Bayer 2001). These results suggest that in water, imidacloprid will remain in the water column where it will be quickly degraded by photolysis. However, consistent with the approach taken in the other risk assessments, it will be assumed that all of the compound will be sedimented with vertical velocities associated with clay particles where it will be degraded in sediments with a half-life of 14 d.

9.2.4.2 Tebuconazole

This fungicide has a water solubility of 32 mg/L at 20°C, a low vapor pressure (1.3×10^{-8} mmHg) and a moderate $\log K_{ow}$ of 3.7. Based on these chemical characteristics, it is not expected to volatilize from water. The U.S. Environmental Protection Agency (EPA) reports that tebuconazole is resistant to hydrolysis and photolysis (Aqueous $DT_{50} = 590$) Tebuconazole will likely adsorb to suspended organic particulates (POM) and eventually be deposited in sediments. Tebuconazole has a relatively low-to-moderate bioconcentration factor (BCF) of 141. Detailed data describing tebuconazole degradation in sediment was not found; however, a half-life of 43 to 49 d for total tebuconazole degradation has been reported in mesocosm studies containing water and sediments (LANXESS 2004, 2005). For purposes of this risk assessment, an aquatic half-life of 49 d will be assumed and all of the tebuconazole released from pressure-treated wood will enter the sediment.

nazole degradation has been reported in mesocosm studies containing water and sediments (LANXESS 2004, 2005). For purposes of this risk assessment, an aquatic half-life of 49 d will be assumed and all of the tebuconazole released from pressure-treated wood will enter the sediment.

9.2.4.3 Propiconazole

This fungicide has a water solubility of 150 mg/L at 20°C, vapor pressure of 5.6×10^{-5} Pa at 25°C, and a $\log K_{ow}$ of 3.72 at 25°C. Propiconazole is relatively photostable ($DT_{50} = 47$ to 984 d at 30 to 50° N latitude) and is not subjected to significant hydrolysis ($DT_{50} = 25$ to 85 d). Degradation half-lives in sediments were not available; however, the DT_{50} in aerobic soils ranged from 20 to 103 d in the USA, 120 to 140 d in Switzerland, and 17 to 411 d in Germany. Anaerobic sediment half-life was not available. For purposes of this risk assessment, all of the propiconazole released from pressure-treated wood is assumed to adsorb to particulate organic matter and be sedimented with a half-life equal to the median value for soils of 111 d.

Excepting CA-B, all of the preservatives listed in Table 9.7 are intended for aboveground use where they will only be subjected to rainwater. Copper azoles (CA-B and CBA-A) are listed in the AWWA Book of Standards (Use Category 4C) for ground contact and/or for use in fresh water. Brooks (2005) determined copper and tebuconazole loss rates for immersed CA-B treated southern pine as a function of diluent temperature and pH. The results ($\mu\text{g TEB}/\text{cm}^2\text{-day}$) for tebuconazole are provided in Equation [9.7]. The exponential function was evaluated using Equation [9.8] to with a degradation half-life of 46 d to estimate the accumulation of tebuconazole in sediments associated with immersed CA-B treated southern pine. Equation [9.8] predicts the maximum accumulation of tebuconazole in sediments as a function of pH at values

Table 9.7 Temporal characteristics of organic compounds in rainwater runoff and the half-lives of imidacloprid, tebuconazole, and propiconazole in aquatic environments.

Compound (preservative)	Concentrations in rainwater ($\mu\text{g}/\text{L}$)	Half-life in water	Half-life (d)	
			In aerobic sediments	In anaerobic sediments
Log10 Imidacloprid (WAG)	$1.14 + 1.45 \times \text{Exp}^{-0.174 \times \text{AR}}$	4 h	146	27.1
Log10 Tebuconazole (WAG)	$1.91 + 1.87 \times \text{Exp}^{-0.249 \times \text{AR}}$	31 d	46	NA
Tebuconazole (CA-B)	$1064.6 \times \text{Exp}^{-0.129 \times \text{AR}}$	31 d	46	NA
Tebuconazole (O-MCA)		31 d	46	NA
Tebuconazole (A-MCA)		31 d	46	NA
Log10 Propiconazole (WAG)	$1.93 + 1.81 \times \text{Exp}^{-0.254 \times \text{AR}}$	85 d	111	NA
Propiconazole (A-MCA)		85 d	111	NA

NA = not available at this time; AR = accumulated rainfall, measured in inches.

between 5.0 and 9.0 and of temperatures between 5 and 25°C. Tebuconazole has a relatively short degradation half-life and losses from treated wood decline quickly (-0.191 d^{-1}). Therefore, maximum accumulations of this compound are low (2.77 to 8.85 $\mu\text{g TEB}/\text{cm}^2$ immersed product) and the maxima occur 9.5 to 26.5 d after immersion.

$$\text{TEB Loss Rate from CA-B} = 0.212 + 5.529 \cdot \exp^{(-0.191 \cdot \text{time(d)} + 0.039 \cdot T(\text{C}) - 0.281 \cdot \text{pH})} \quad [9.7]$$

$$\text{Accumulation at } t_n = M_{(t=0)} \cdot D_{(t=n)} + M_{(t=1)} \cdot D_{(t=n-1)} + M_{(t=2)} \cdot D_{(t-2)} + \dots + M_{(t=n)} \cdot D_{(t-n=0)} \quad [9.8]$$

where,

M_t is the loss of active ingredient at time t

D_t is the degradation of the active ingredient at t_n that has occurred since release

9.3 SEDIMENT ACCUMULATION OF ORGANIC CONTAMINANTS RELEASED FROM TREATED WOOD

The accumulation of organic contaminants that degrade in sediments over time and whose loss is a function of fixed factors and time can be modeled at any time ($t = n$) using the series described in Equation [9.8]. At any given time (t_n), the active ingredient lost from the treated wood on day zero will have been degraded for a period of (n) days and the contaminant lost on day (n) will not be degraded at all. This series was evaluated numerically to determine the maximum accumulation of organic contaminants, given a predicted degradation half-life and the temporal changes in loss rates from pressure-treated wood.

The Microsoft Excel® spreadsheet described in this section has been developed to predict the accumulation of existing and future organic active ingredients released from pressure-treated wood to aquatic environments. Prior to reaching a maximum, organic contaminants are being added to sediments faster than the existing contaminant load is being degraded. Contaminant concentrations decline after the maximum because the accumulation is degrading faster than new contaminant is being released from the wood. Output from the model describes the amount of organic contaminant accumulating from each

square centimeter of pressure-treated wood at any time t . These are not environmental concentrations because the actual concentration in sediments depends on the total leaching surface area of treated wood and on the dispersion of contaminants in sediments around the structure, which is primarily a function of current speeds and water depth. The model also provides a prediction of the time at which maximum concentrations should be expected in sediments near pressure-treated wood structures. Use of the model for assessing other organic preservatives requires an understanding of the preservative migration rates from pressure-treated wood as a function of time and those factors that affect migration rates. The model would also require an understanding of the degradation of the organic contaminant in sediments as a function of time and those environmental factors that influence degradation rates.

9.3.1 A spreadsheet model for estimating the accumulation of organic compounds in sediments associated with immersed treated wood

The Sediment Accumulation Workbook (available electronically at WWPIInstitute.org) is general in nature and can be used to predict the maximum amount and timing of accumulations in sediment of organic active ingredients released from pressure-treated wood. The spreadsheet requires knowledge of the loss rate of the organic compound from pressure-treated wood and its degradation rate in sediments. The factors influencing loss and degradation rates will vary by preservative. The spreadsheet described herein includes inputs important to assessing creosote, pentachlorophenol, tebuconazole, imidacloprid, and propiconazole. New organic active ingredients may require the addition of new independent variables. The results are based on an expansion of the series described in Equation [9.8]. Creosote is used as an example in Appendix 9.1.

User inputs are entered in Column H, Rows 2 through 6 (Table 9.8)

$E2$ = day interval (Δt) in days used in the accumulation calculation. This can be varied by the user

$\Delta t = 1 \text{ d}$ for active ingredients whose loss rates decline quickly and that have short degradation time constants to intervals of 60 d or more for those organics whose loss rates remain elevated for long periods or that degrade slowly. Short Δt values provide more precise

Table 9.8 Inputs for development of factors affecting the temporal characteristics of the degradation of sedimented PAH associated with creosote-treated wood structures.

	G	H	I	J
1	Time constant (exp-1)	3650	Factors for half-life	
2	pH			
3	Temperature (C)	15	1.418	
4	Salinity (PSU)	30		
5	Retention (kg/m ³)	359.1		
6	RPD (cm) or eH (mV)	2	1.345	
8				
9	PAH migration = (24.4 + 0.78*T - 0.58* S)*exp ^{(R/359.1 - 1)/2} * exp ^{-t/3650} (mg TPAH/cm ² -d)			
10				
11		Delta t	200	
12		Day	Loss rate	Proportion
13		0	18.7	1.00
14		200	17.7	0.95
15		400	16.8	0.90
16		600	15.9	0.85
17		800	15.0	0.80
18		1000	14.2	0.76
19		1200	13.5	0.72
20		1400	12.7	0.68
21		1600	12.1	0.65
22		1800	11.4	0.61
23		2000	10.8	0.58
24		2200	10.2	0.55
25		2400	9.7	0.52
26		2600	9.2	0.49
27		2800	8.7	0.46
28		3000	8.2	0.44
29		3200	7.8	0.42
30		3400	7.4	0.39
31		3600	7.0	0.37
32		3800	6.6	0.35
33		4000	6.3	0.33
34		4200	5.9	0.32
35		4400	5.6	0.30
36		4600	5.3	0.28
37		4800	5.0	0.27

predictions of the amount and timing of accumulation. However, MS Excel® limits the number of characters in cells to 1,040 requiring longer Δt values when more than 110 iterations are necessary.

H2 = Loss rate Time Constant (TC in days) defining when losses are reduced by a factor of exp⁻¹ in the expression exp^{-TC/t}. Values for each organic contaminant are described in Chapter 7.

H3 = pH of the sediment pore water estimated as the pH of the receiving water.

H4 = Temperature (°C) of the receiving environment (water temperature).

H5 = Salinity (PSU) of the receiving water

H6 = Preservative retention in the treated wood (kg/m³)

H7 = Redox potential of the sediments measured as the depth (cm) of the RPD for creosote or as redox potential (mV) for pentachlorophenol.

I3 through I7 provide calculated factors for degradation of the organic active ingredient being evaluated in association with each of the input factors entered in column H. In the case of PAH, the half-life is shorter by a factor of 0.608 at 35°C than it is at 20°C. The degradation factor associated with redox for creosote is 1.0 when the RPD is ≥ 4 cm.

G10 is the algorithm describing the loss of the organic preservative being considered.

I12 (Δ t) is the time interval assigned for the loss rate assessment.

The loss-rate time constant for creosote of 3,650 d used in this example deserves additional discussion. Two algorithms describing the migration of creosote from immersed pressure-treated wood are available. Based on a literature review, Brooks (1995, 2005a) estimated the temporal factor as exp^{-t/3650}. In contrast, the results of Kang et al. (2005) suggested a temporal factor of exp^{-t/30}. The long-term Sooke Basin study (Goyette and Brooks 1998, 2001) provides empirical data for evaluating these alternatives. Figure 9.7 describes the results, which have been normalized to the maximum predicted TPAH concentration obtained in each analysis. The 3,650-d factor results in predicting a peak at 825 d post immersion, which is consistent with the apparent peak in the normalized Sooke Basin data. A 30-d temporal factor predicts a peak concentration at 75 d, which is clearly too early. The Sooke Basin data is too sparse to precisely determine when the peak occurred. However, the original estimate of 3,650 d provides a closer fit and has been retained in this model.

Why was there a difference in estimates of creosote migration as a function of time between Kang et al. (2005) and Goyette and Brooks (1998, 2001)? Kang et al. (2005) was a carefully controlled laboratory study conducted using fresh water at a constant temperature. In contrast, the Sooke Basin Study was conducted in a natural marine environment where the piling became heavily fouled with invertebrates and where air temperatures were not mea-

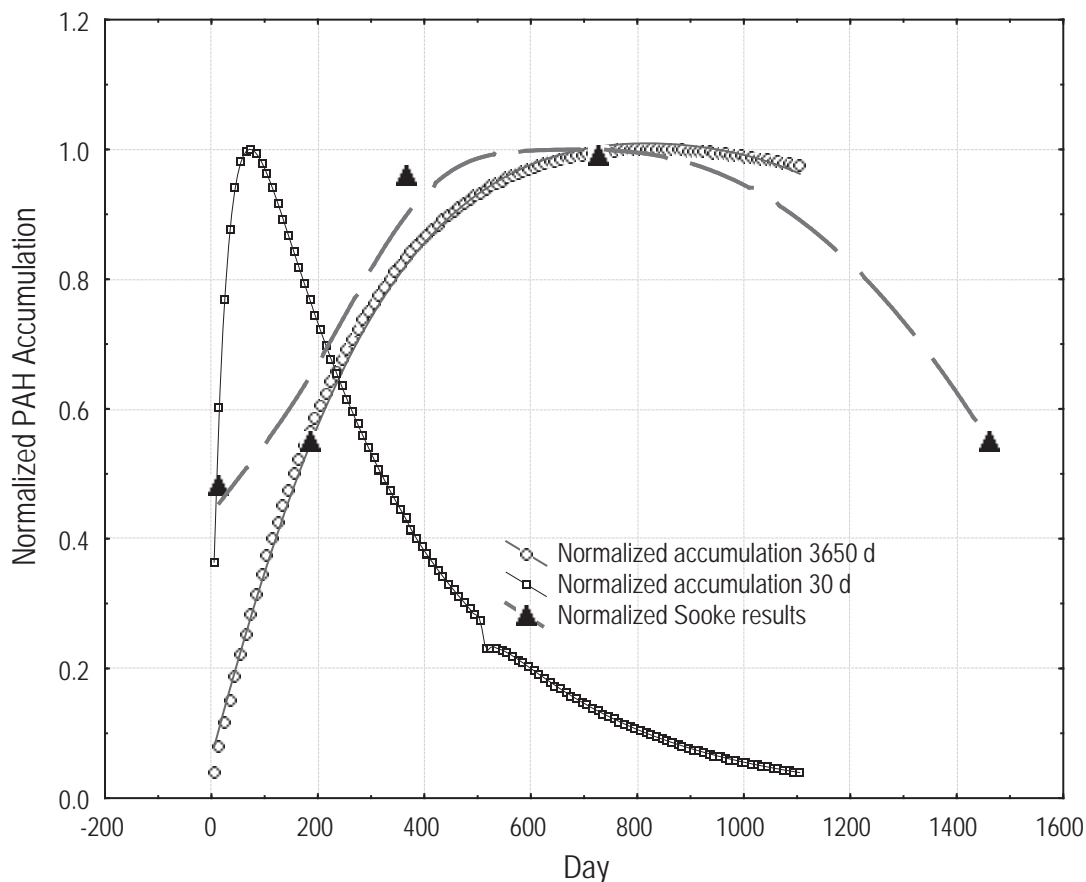


Figure 9.7 Comparison of predicted relative accumulation of sedimented PAH when migration rates decline with temporal factors of 30 d and 3,650 d with data from Sooke Basin (Goyette and Brooks 1998, 2001).

sured, but likely varied between 0° and 40°C. A limited suite of mostly low-molecular-weight compounds was detected by Kang et al. (2005), whereas all 18 PAH analyzed in the Sooke Basin Study were detected during the 10-y study. It is hypothesized that the higher intermediate and high molecular weight PAH in creosote are lost at such slow rates that they are not detected during short-term studies, but because they degrade more slowly than the low-molecular-weight compounds, they are detected in sediments after accumulating for months or years. The time factor of 3,650 d adopted by Brooks (1995, 2005a) is supported by the Sooke Basin data and for that reason will continue to be used in this model.

9.3.1.1 Loss rate output

The loss rate output describing the loss rate of the active ingredient (see Chapter 7) is provided in rows I14 through I38 of the spreadsheet (Table 9.8). The example is for wood treated with 359.1 kg creosote/m³ and immersed in seawater with a salinity of 30 PSU at 15°C. A loss rate of 18.7 µg TPAH/cm²-d is predicted on the first day. The loss rate

declines to 5.0 µg TPAH/cm²-d after the wood has been immersed for 4,800 d (13.2 y).

9.3.1.2 Maximum accumulation of organic active ingredients in sediments.

Columns A through F of the spreadsheet are described in Table 9.9. The time interval used in the calculation is entered in cell E1. In this case, iterations were made using a Δt of 100 d. The half-life of the compound being considered is calculated for the user in cell B2. In this case, the calculations were for creosote-treated wood installed in seawater (30 PSU) at a mean annual temperature of 15°C. Sediments had a distinct color discontinuity at 2 cm depth (the RPD) indicating that surficial sediments were marginally aerobic. The degradation half-life in this case is 409.8 d.

The model predicts that 8% of the sedimented TPAH will have degraded on d 50, leaving 91.9% of the creosote deposited on d 1 still in the sediments. On d 3,150, only 0.5% of the TPAH sedimented on d 1 remains in the sediment. The preservative loss rates during each time interval are provided in column C. In this case, the TPAH loss rate

Table 9.9 Predicted accumulation of TPAH in sediments adjacent to a creosote-treated wood structure immersed in seawater (30 PSU) with an average annual temperature of 15°C and sediments having an RPD at 2.0 cm depth. The time and amount ($\mu\text{g TPAH}/\text{cm}^2$) are highlighted.

	A	B	C	D	E	F
1		Half-life followed by proportion remaining	Creosote loss ($\mu\text{g}/\text{cm}^2$ leaching surface)	Day interval accumulation	Difference	Normalized accumulation
2	Days	409.8				
3	50	0.919	18.4	1844.558		0.237
4	150	0.776	17.9	3080.366	1235.808	0.396
5	250	0.655	17.5	4205.601	1125.235	0.541
6	350	0.553	17.0	5112.365	906.764	0.658
7	450	0.467	16.5	5835.828	723.463	0.751
8	550	0.394	16.1	6405.655	569.827	0.824
9	650	0.333	15.6	6846.865	441.209	0.881
10	750	0.281	15.2	7180.550	333.686	0.924
11	850	0.237	14.8	7424.495	243.945	0.956
12	950	0.201	14.4	7593.687	169.192	0.977
13	1050	0.169	14.0	7700.753	107.065	0.991
14	1150	0.143	13.6	7756.327	55.575	0.998
15	1250	0.121	13.3	7769.365	13.038	1.000
16	1350	0.102	12.9	7747.402	-21.964	0.997
17	1450	0.086	12.6	7696.775	-50.627	0.991
18	1550	0.073	12.2	7622.812	-73.963	0.981
19	1650	0.061	11.9	7529.988	-92.824	0.969
20	1750	0.052	11.6	7422.059	-107.929	0.955
21	1850	0.044	11.3	7302.174	-119.885	0.940
22	1950	0.037	11.0	7172.971	-129.203	0.923
23	2050	0.031	10.7	7036.656	-136.315	0.906
24	2150	0.026	10.4	6895.072	-141.585	0.887
25	2250	0.022	10.1	6749.753	-145.319	0.869
26	2350	0.019	9.8	6601.977	-147.775	0.850
27	2450	0.016	9.6	6452.805	-149.172	0.831
28	2550	0.013	9.3	6303.112	-149.692	0.811
29	2650	0.011	9.0	6153.622	-149.490	0.792
30	2750	0.010	8.8	6004.927	-148.695	0.773

is predicted to be $18.4 \mu\text{g TPAH}/\text{cm}^2\text{-d}$ during the middle of the first time interval. It declines to $8.8 \mu\text{g TPAH}/\text{cm}^2\text{-d}$ on d 2750. The heart of the output is provided in column D, where the accumulation of TPAH associated with each cm^2 of immersed treated wood is calculated. The accumulations slowly increase until they peak 1,250 d after immersion. After that, degradation exceeds the delivery of newly migrating TPAH from the treated wood and the total sediment burden decreases. Column E is simply the difference in accumulating TPAH in sediments from the previous time to the current time over the interval Δt . It is provided as an aid to finding the peak, which is identified

when the positive difference changes to negative differences. Column F provides accumulations normalized to the peak concentration. The peak occurs when this value is 1.00. In this case, the peak accumulation is predicted to be $7,769.4 \mu\text{g TPAH}/\text{cm}^2$ of immersed treated wood. This is not a concentration in the sediment. The concentration will be determined in the model based on water depth and current speeds, which distribute the active ingredient over a site-specific area.

Table 9.10 is a three-dimensional matrix describing the predicted maximum accumulation of TPAH in sediments as a function of temperature, salinity, and depth of the

Table 9.10 Maximum accumulation of TPAH in sediment from creosote-treated wood as a function of depth of the RPD, temperature, and salinity. (µg TPAH/cm² of leaching surface area).

Salinity = 0							
RPD/ Temp	5	10	15	20	25	30	35
0	64,193	57,772	54,615	52,801	51,552	50,704	50,106
0.5	49,006	40,601	36,358	33,795	32,081	30,848	29,932
1	37,658	29,057	25,046	22,688	21,124	20,024	19,189
2	25,372	18,123	14,999	13,225	12,082	11,276	10,671
3	21,495	14,965	12,216	10,682	9,688	8,996	8,481
4	20,980	14,548	11,850	10,351	9,376	8,699	8,201
Salinity = 10 PSU							
RPD/ Temp	5	10	15	20	25	30	35
0	51,037	47,366	45,840	45,145	44,741	44,349	44,330
0.5	38,962	33,288	30,517	28,895	27,842	27,113	26,577
1	29,940	23,824	21,022	19,398	18,333	17,601	17,049
2	20,172	14,858	12,589	11,307	10,486	9,930	9,512
3	17,090	12,269	10,254	9,133	8,408	7,942	7,577
4	16,680	11,928	9,946	8,850	8,137	7,672	7,352
Salinity = 20 PSU							
RPD/ Temp	5	10	15	20	25	30	35
0	37,881	36,960	36,948	37,268	37,713	38,224	38,728
0.5	28,919	25,974	24,577	23,969	23,606	23,369	23,219
1	22,222	18,590	17,000	16,113	15,554	15,170	14,894
2	14,972	11,594	10,184	9,402	8,905	8,559	8,310
3	12,685	9,574	8,300	7,598	7,153	6,845	6,620
4	12,380	9,307	8,054	7,364	6,927	6,627	6,404
Salinity = 30 PSU							
RPD/ Temp	5	10	15	20	25	30	35
0	24,724	26,546	28,201	29,657	30,941	32,100	33,127
0.5	18,865	18,552	18,759	19,074	19,367	19,625	19,860
1	14,504	13,323	12,976	12,823	12,761	12,739	12,740
2	9,772	8,333	7,773	7,482	7,306	7,188	7,108
3	8,279	6,880	6,335	6,046	5,869	5,749	5,662
4	8,081	6,687	6,139	5,860	5,683	5,566	5,494
Salinity = 35 PSU							
RPD/ Temp	5	10	15	20	25	30	35
0	18,146	21,351	23,903	26,005	27,714	29,170	30,432
0.5	13,853	15,005	15,913	16,644	17,246	17,747	18,179
1	10,645	10,739	10,962	11,174	11,356	11,520	11,654
2	7,172	6,698	6,564	6,513	6,495	6,487	6,481
3	6,076	5,530	5,347	5,261	5,208	5,176	5,151
4	5,931	5,377	5,187	5,098	5,040	5,005	4,981

Table 9.11 Statistical output from analysis of the model data shown in Table 9.10.

	Estimate	Standard error	t-value df = 205	p-level	Confidence limit	
					Lower	Upper
a	54,973.63	1689.4	32.54	0.000	51,642.77	58,304.50
b	-237.34	56.6	-4.19	0.000	-348.95	-125.74
c	729.47	45.3	16.10	0.000	640.15	818.78
d	0.56	0.0	24.97	0.000	0.52	0.61

RPD. Retention was not included in this matrix to reduce its complexity. The assumed retention of 359.1 kg/m³ (22.4 pcf) is the mean retention recorded in several thousand creosote-treatment charges in the Pacific Northwest. It is conservatively used because AWWA Standard U1(AWWA 2008) currently specifies a minimum retention of 256 kg/m³ (16 pcf) for Douglas-fir piling in both southern and northern waters. The final model allows for correction of predicted sediment concentrations of TPAH associated with differing creosote retentions. The data in Table 9.10 was analyzed in the non-linear prediction module of Statistica™ Version 6 to minimize the residuals leading to Equation [9.9], which explains 86% of the variation in the database. Statistics associated with each of the coefficients are provided in Table 9.11. A single outlier was observed in association with Case 1 describing the accumulation of TPAH in anaerobic sediments (RPD = 0) in cold environments having an average annual temperature of 5°C. The regression underestimates the accumulation of TPAH in that case (the series estimated 57,772 and the fitted regression predicts only 53,607.1 µg TPAH/cm² leaching surface area). However, it should be noted that creosote-treated wood is not generally recommended as a construction material in environments having anaerobic sediments.

$$\begin{aligned}
 \text{PAH Max. Acc.} &= (54,973.6 - 237.3 * T & [9.9] \\
 &- 729.5 * S) * \exp^{-0.56 * \text{RPD}} \text{ (}\mu\text{g TPAH/cm}^2\text{)} \\
 R^2_a &= 0.864
 \end{aligned}$$

9.3.1.3 Future uses and availability of this model

The spreadsheet can be used to predict the accumulation of any organic contaminant as a function of time, degradation half-lives, and time constants describing the loss of active ingredients from pressure-treated wood or other sources. Future wood preservatives may use new organic compounds to protect the wood, and this spreadsheet will facilitate developing risk-assessment models for those new preservatives.

9.3.2 Sediment accumulations of organic contaminants associated with rainwater runoff

Contaminants in rainwater runoff from overhead pressure-treated wood structures described in Chapter 7 are described as a function of accumulated rainfall. Annual rainfall amounts and rates vary regionally as well as temporally. Developing an understanding of the accumulation of organic contaminants in sediments associated with rainfall runoff using this model requires some assumptions allowing conversion of contaminant concentrations as a function of accumulated rainfall to contaminant concentrations as a function of time. Brooks (2006b) examined two rainfall-rate scenarios in developing a timber-bridge model for pentachlorophenol. The first scenario assumed that rain fell steadily at a rate of 0.1 cm/h (2.4 cm or 1 inch/d) for the first 35 d, followed by 10 d without rain. Rainfall after this initial event was assumed to fall at 0.1 cm/h for 5 d followed by 10 d without rain in a cyclical pattern for a total period of 150 d. This pattern results in an initial rainfall of 84 cm/35 d, plus another 84 cm falling in the next 115 d, for a total of 168 cm (66.14 inches) of rainfall in the first 150 d following construction. The second scenario assumed that a light rain of 0.1 cm/h fell continuously for 150 d (360 cm or 142 inches total). Other scenarios are possible, but these were considered representative of worst cases. The maximum predicted penta accumulation was then determined in a two-by-two matrix of pH (range 5.0 to 9.0, in 0.5 increments) and temperature (5 to 25°C, in 5°C increments) and entered into a Statistica database. This database was analyzed using linear and non-linear regression analysis to predict the timing and maximum amount of sedimented pentachlorophenol as a function of receiving water pH and redox potential. The highest accumulations of pentachlorophenol were predicted to occur in anaerobic sediments (-300 mV) at high pH (8.5). However, the range was relatively small: 50.2 µg penta/L at pH = 5.5 and 300 mV redox in rainfall scenario one to 116.4 µg penta/L at pH = 8.5 and -300 mV redox in rainfall scenario two. Maximum concentrations were predicted to occur 18 d after construction with cyclical rain and 58 d after construction for 150 days of steady rain. Because of the rather fast declines in penta loss and relatively short half-lives, maximum sediment concentrations were predicted to occur at times ≤ 58 d following construction. Differences in the predicted accumulation of penta between scenarios were not great. For instance, with intermittent rain at pH = 6.5 and +100 mV redox potential, a maximum of 97.68

µg penta/cm² of exposed treated wood was expected to accumulate in sediments at the end of the first prolonged rainfall event (d 35). Continuous rainfall, produced a maximum predicted concentration of 99.04 µg/L after 42 d of rain. Because these differences were relatively small throughout the database, only the worst case of 2.4 cm/d steady rain for 150 d was used in the model, and that convention will be used herein. A critical reader might ask whether increased preservative losses should be expected with renewed rainfall following prolonged dry periods. Algorithms describing concentrations of wood preservative contaminants in rainwater have been developed from rainwater runoff studies (see chapter on migration) for 10 currently used preservatives (Xiao et al. 2001; Brooks, 2003, 2005a, 2005b, 2005c, 2006b, 2007, 2009a, 2009b). The results for CCA-C (Figure 9.8) are typical and indicate an exponential decline in runoff concentrations with no significant increases during fall rainfall events following typically dry summers in the Pacific Northwest.

9.3.2.1 Spreadsheet model for predicting the accumulation of organic contaminants in sediments associated with rainwater runoff

The previously described model (Tables 9.8–9.10) was modified to allow prediction of the accumulation of organic contaminants in sediments as a function of rainwater runoff. The model is included in the Sediment Accumulation Workbook. Table 9.12 reproduces portions of the Microsoft Excel® model.

User inputs are described in column H (rows 3–11) and entered in column I (rows 3–11). Half-life factors are cal-

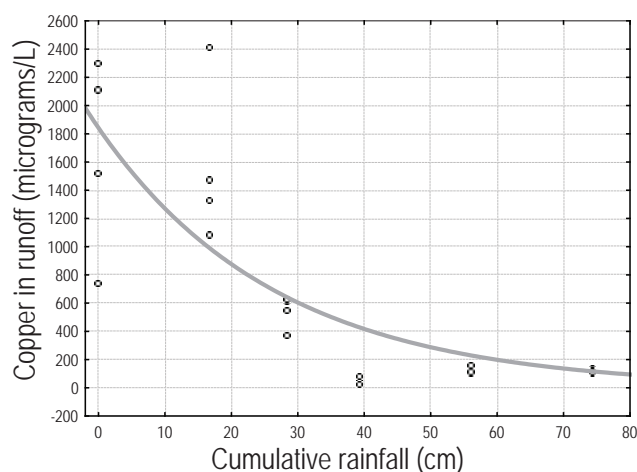


Figure 9.8 Copper concentrations in rainfall runoff from CCA-C treated decking exposed to rainfall in the Pacific Northwest as a function of the cumulative amount of rain. $y = (1841.5) * \exp(-0.037126 * x)$. $R^2 = 0.66$.

culated in column J for those inputs that influence the half-life of the compound in question. Inputs are available for rainwater pH, temperature (°C), salinity (PSU), preservative retention (kg/m³) and depth of the RPD (cm) or redox potential (mV), whichever is appropriate for the preservative in question.

Calculation of compound half-life

Independent factors that are necessary to compute a compound half-life using an algorithm are entered by the user in C3 where the calculated half-life will then be displayed. Users enter the fixed half-life directly in C3 for compounds whose half-lives are not a function of independent variables.

Concentration of a compound in rainwater runoff

The algorithm describing rainwater concentrations of the compound must be entered in column D. Concentrations have typically been determined in µg/L as a function of accumulated rainfall (AR). In this model, the annual rainfall (cm) is entered in cell I8. The steady state rainfall is computed and described in cell I10. This value is copied into cell I9. However, the user can vary the rainfall rate in cell I9 to examine changes in compound accumulation as a

function of different rainfall rates. The day interval over which calculations are made is entered by the user in cell F2. In this case calculations are made every 3 d with the first interval set at half the day interval value (1.5 d, in this case).

Assessing storm events

The user can enter the number of centimeters of rain anticipated during a Δt as a storm event in cell I11. In this case, a storm event of 5 cm over a 3-d interval beginning on d 43.5 was assessed.

9.3.2.2 Concentration of PAH in rainwater runoff from creosote-treated wood

Xiao et al. (2001) exposed Douglas-fir lumber that had been treated to a retention of 492 kg/m³ with P1/P13 creosote to deionized rainwater containing a bacterial control agent and measured the concentration of PAH in the runoff with 6.7 cm of rainwater applied during 40-min showers that were applied once every 12 h for 10 cycles. The authors did not detect any difference in detected PAH concentrations as a function of heating of the wood to 68–70°C. They hypothesized that the temperature of the wood declined to the rainwater's temperature immediately

Table 9.12 Portions of the Microsoft Excel™ spreadsheet model for predicting the accumulation of PAH in sediments associated with rainwater runoff from overhead structures constructed of wood pressure treated with creosote.

A	B	C	D	E	F	G	H	I	J
Days	Accumulated rain (cm)	Half-life 3260	PAH loss to rainwater (µg PAH/L)	Day interval accumulation	Difference	Normalized accumulation	Time constant (exp-1) pH	3650	Half-life factors
1.5	0.8	1.000	654.1	537		0.014	Temperature (°C)	15	1.42
4.5	2.5	0.999	642.9	1,593	1055.3	0.043	Salinity (PSU)	0	
7.5	4.1	0.998	632.0	2,629	1036.8	0.071	Retention (kg/m ³)	192	
10.5	5.7	0.998	621.1	3,648	1018.4	0.098	RPD (cm)	0	10.70
13.5	7.4	0.997	610.5	4,648	1000.3	0.125	Annual rainfall (cm)	200	
16.5	9.0	0.996	600.1	5,630	982.5	0.152	Rainfall rate (cm/h)	0.013	
19.5	10.7	0.996	589.8	6,596	965.0	0.178	Steady rain rate (cm/h)	0.023	
22.5	12.3	0.995	579.7	7,543	947.8	0.203	Storm event (cm/d)	5	
25.5	14.0	0.995	569.8	8,474	930.9	0.229	Creosote concentration in rainwater (µg/L) = $659.8 \cdot \exp(-0.0105 \cdot \text{AR (cm)})$		
28.5	15.6	0.994	560.1	9,389	914.4	0.253			
31.5	17.2	0.993	550.5	10,287	898.0	0.277			
34.5	18.9	0.993	541.1	11,169	882.0	0.301			
37.5	20.5	0.992	531.8	12,035	866.3	0.325			
40.5	22.2	0.991	522.7	12,886	850.8	0.347			
43.5	28.8	0.991	487.5	16,115	3229.2	0.435			
46.5	25.5	0.990	505.0	14,410	-1705.2	0.389			
49.5	27.1	0.990	496.4	15,216	806.0	0.410			
52.5	28.7	0.989	487.9	16,007	791.5	0.432			
55.5	30.4	0.988	479.5	16,784	777.3	0.453			
58.5	32.0	0.988	471.3	17,539	754.6	0.473			

after starting the shower. Figure 9.9 describes the concentration of the detected PAH in the runoff as a function of accumulated rainfall. The residuals associated with the fitted non-linear regression line (Equation [9.10]) were normal, with no evidence of heteroschedasticity, and both coefficients were highly significant ($p < 0.000$). The regression was significant ($p < 0.000$), but the high variability between the three replicates resulted in the regression explaining only 34% of the variability in the data. These results predict that rainwater runoff from creosote-treated lumber will initially contain 659.8 μg TPAH/L. Assuming annual rainfall of 45 cm/y, the concentration of PAH in rainwater runoff is predicted to be reduced to 5.85 μg PAH/L at the end of 10 y (450 cm of rainfall). The high rainfall rate of 10 cm/h (4 inches/h) in this study may have exacerbated losses by physically dislodging creosote from the wood's surface. However, this is the only data available and the methodology is consistent with the worst-case analyses undertaken in developing these models.

$$\begin{aligned} \text{Detected PAH } (\mu\text{g PAH/L}) & \quad [9.10] \\ = 659.8 * \exp^{-0.0105 * \text{AR (cm)}}; R^2_a = 0.34 \end{aligned}$$

9.3.2.3 Accumulation of detected PAH in sediments associated with rainwater runoff

Predicted maximum accumulations of PAH in sediments were predicted by substituting the degradation algorithm (Equation [9.5]) and predicted concentration given by Equation [9.10] into the Equation [9.8] series and solving for concentrations at annual rainfall rates of 2, 50 100, 150, 200, and 250 cm/y; temperatures of 5, 10, 15, 20, 25, 30, and 35°C; and RPD depths of 0.5, 1.0, 2.0, 3.0, and 4.0 cm. In Appendix 9.1, tables 9.1A through 9.1F provide output describing the maximum accumulation/1000 cm² of rainwater-exposed surface area. The denominator is 1000 cm² because the units in Equation [9.10] are $\mu\text{g/L}$ and the rainfall rates are in cm/y. One centimeter of rainfall must occur over an area of 1,000 cm² to produce one liter of diluent. As previously noted, the model assumes that the annual rainfall occurs steadily over the entire year, allowing for the use of a constant rate. Appendix 9.2 describes the days of constant rainfall when the maximum concentration is achieved. Loss rates decline as rainfall accumulates. However, degradation rates are a function of depth of the RPD and temperature. Therefore, at higher rainfall rates, higher initial PAH loadings occur, but the loss rates decline more quickly in a temporal sense; the degradation rates remain constant for a particular RPD and temperature.

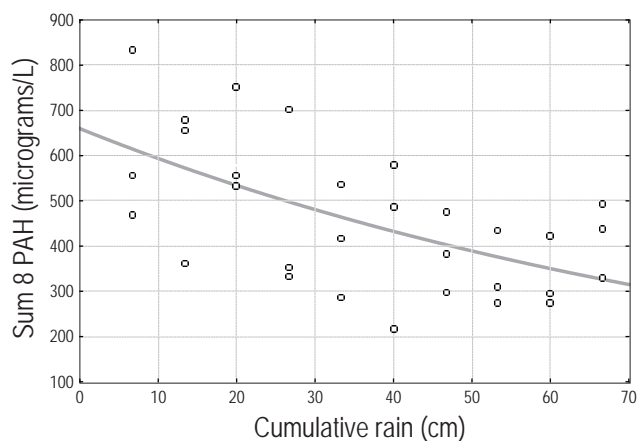


Figure 9.9 Concentration of detected PAH in rainwater runoff from creosote-treated lumber = $659.8 * \exp^{-0.0105 * \text{Accumulated Rainfall (cm)}}$. Data from Xiao et al. (2001).

This allows degradation to exceed the delivery of new PAH at earlier times. For instance, at 10°C in sediments having at RPD at 2.0 cm depth, the maximum accumulation of 265,099 μg PAH/1000 cm² leaching surface area occurs following 1,050 d of steady rain associated with an annual rate of 25 cm/y. Maximum accumulation level is predicted to decline to 95,122 μg PAH/1000 cm² and occurs after only 405 d when annual rainfall increases to 150 cm/y (59.1 inches).

The output detailed in Appendix 9.1 was entered into a Statistica™ Version 6 database and analyzed using non-linear regression analysis to develop Equation [9.11] to predict the maximum amount of PAH accumulation in association with rainwater runoff from over-water structures constructed with creosote-treated wood. Statistics describing the coefficients in this algorithm are summarized in Table 9.13. The prediction and each of its coefficients were significant ($p < 0.000$). The residuals were normally distributed with no evidence of heteroschedasticity. Figure 9.10 describes the values predicted by Equation [9.11] versus the modeled (observed) values developed using Equations [9.5, 9.8 and 9.10]. There is no evidence of significant bias in the predicted results at any level of accumulation. However, maximum accumulations predicted by Equation [9.11] were slightly higher than the modeled accumulations, at very low accumulations and again at high predicted accumulations associated with low flows, anaerobic sediments, and low temperatures. This suggests that Equation [9.11] is conservative for environmental protection. Equation [9.12] was developed to predict the day on which maximum PAH accumulation occurs in sediments as a function of annual rainfall, RPD, and temperature.

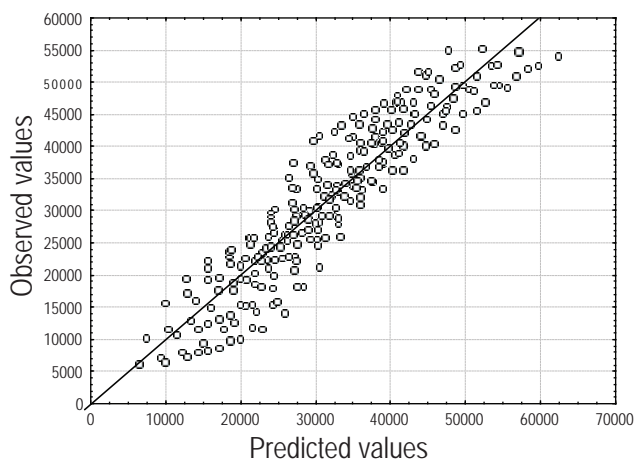


Figure 9.10 Pentachlorophenol sediment values predicted by Equation 9.11 versus modeled predictions developed using Equations 9.5, 9.8, and 9.10 (observed values).

$$\begin{aligned} &\text{Maximum accumulation (}\mu\text{g TPAH/1000 cm}^2 \text{ [9.11]} \\ &\text{of rainwater-exposed creosote-treated wood)} \\ &= 42,649 * [\exp^{-(0.002 * \text{Annual rainfall (cm)} + 0.172 * \text{RPD (cm)})} \\ &\quad - 0.01 * \text{Temp (C)}]; R^2_a = 0.86 \end{aligned}$$

$$\begin{aligned} &\text{Day of maximum} = 3,825.3 * \text{ [9.12]} \\ &\exp^{-0.008 * \text{Annual rainfall (cm)} - 0.331 * \text{RPD (cm)} - 0.029 * \text{Temp (C)}}; \\ &R^2_a = 0.90 \end{aligned}$$

Table 9.13 Statistical output for analysis of PAH sediment concentration predicted by Equation [9.12] vs. those developed using Equations [9.5], [9.8], and [9.11]. Model is $V4 = a * (\exp(-b * V1 - c * V2) - d * V3)$ (accumulation of contaminants from rainwater). Dep. Var.: Maximum PAH accumulation (mmg/1000 cm²). Level of confidence: 95.0% ($\alpha = 0.050$).

	Estimate	Standard error	t-value df = 248	p-level	Confidence limit	
					Lower	Upper
a	42,649.060	900.8434	47.3435	0.000	40,874.78	44,423.34
b	-0.002	0.0001	-19.6301	0.000	-0.00	-0.00
c	0.131	0.0056	23.5893	0.000	0.12	0.14
d	0.013	0.0005	24.3371	0.000	0.01	0.01

9.3.2.4 Accumulation of pentachlorophenol in sediments associated with rainwater runoff from treated wood

Equation [9.6] describing pentachlorophenol half-life in sediments and Equation [7.38] from Chapter 7 describing the concentration of penta in rainwater runoff were used in Equation [9.8] to derive Equation [9.13] predicting the accumulation of penta in sediments as a function of water pH (5.5 to 9.0), redox potential (-200 to +200 mV), and annual rainfall (25 to 250 cm/y). Maximum concentrations

were lowest in aerobic sediments at low pH and low rainfall. Maximum accumulations were highest in anaerobic sediments at high pH where loss rates to rainfall were highest. However, the range was rather narrow (9.82 to 43.26 $\mu\text{g penta/1000 cm}^2$ rainwater-exposed area).

$$\begin{aligned} &\text{Maximum penta accumulation in sediments [9.13]} \\ &(\mu\text{g/1000 cm}^2 \text{ rainwater exposed area}) = \\ &6.35 - 0.023 * \text{Redox (mV)} + 1.45 * \text{pH} + \\ &0.068 * \text{Rainfall Rate (cm/y)} \end{aligned}$$

Table 9.14 Output from the statistical analysis of the output predicted by Equation [9.14] vs. that predicted by Equations [9.6], [9.8], and [9.13].

	Estimate	Standard error	t-value (df = 176)	p-level	Confidence limit	
					Lower	Upper
a	-0.023	0.001	-21.715	0.000	-0.026	-0.021
b	1.446	0.104	13.924	0.000	1.241	1.652
c	0.068	0.002	35.586	0.000	0.065	0.072
d	6.351	0.783	8.106	0.000	4.804	7.897

9.3.2.5 Accumulation of Imidacloprid, Tebuconazole and Propiconazole in sediments associated with rainwater runoff from treated-wood products

Table 9.7 provides algorithms describing concentrations of these three organic compounds in rainwater runoff from pressure-treated decking as a function of accumulated rainfall (Brooks 2007) and published half-lives in sediments. This information was used together with Equation [9.8] to describe the accumulation of these compounds in sediments as a function of time and rainfall rates for Wolman AG™ (WAG) and copper azole (CA-B) preservatives to develop the information in Table 9.15.

9.3.3 Summary of algorithms describing the maximum accumulation of organic active ingredients in sediments associated with the use of pressure-treated wood in and over aquatic environments

The data generated by the accumulation models was entered into a Statistica™ Version 6 database and analyzed to produce the following algorithms describing the accumulation of organic active ingredients as a function of the independent variables that are known to influence them.

9.3.3.1 Accumulation of organic compounds from immersed pressure-treated wood ($\mu\text{g}/\text{cm}^2\text{-day}$)

Creosote = $(54,973.6 - 237.3 \cdot T - 729.5 \cdot S) \cdot \exp^{-0.56 \cdot \text{RPD}}$
 ($\mu\text{g TPAH}/\text{cm}^2$); $R_a^2 = 0.864$

Pentachlorophenol =
 $10^{(1.054 - 0.00041 \cdot \text{Redox (mV)} + 0.310 \cdot \text{pH} + 0.769 \cdot \text{AR (cm)})}$; $R_a^2 = 0.91$

Table 9.15 Predicted maximum accumulation and the time required to reach it for propiconazole, tebuconazole, or imidacloprid in freshwater sediments as a function of annual rainfall.

Maximum propiconazole accumulation in sediments associated with WAG (microg PROP/1000 cm ²)		
Annual rainfall (cm)	Accumulation	Day of maximum
25	6,788.6	53.0
50	8,832.5	38.5
100	10,682.5	27.5
150	11,575.7	22.5
200	12,089.2	19.5
250	12,408.6	18.5

Maximum propiconazole accumulation in sediments associated with WAG (microg PROP/1000 cm ²)		
Annual rainfall (cm)	Accumulation	Day of maximum
25	7,396.7	53.3
50	9,567.2	38.3
100	11,532.7	27.5
150	12,469.0	22.5
200	12,999.0	19.5
250	13,320.0	17.5

Maximum imidacloprid accumulation in sediments associated with WAG (microg IMID/1000 cm ²)		
Annual rainfall (cm)	Accumulation	Day of maximum
25	1,119.3	136.5
50	1,395.7	100.5
100	1,676.1	77.0
150	1,818.7	73.0
200	1,920.9	75.0
250	2,021.5	99.0

Maximum TEB accumulation in sediments associated with CA-B (microg TEB/1000 cm ²)		
Annual rainfall (cm)	Accumulation	Day of maximum
25	2,250	85
50	3,223	61
100	4,317	42
150	4,752	33
200	5,315	15
250	5,587	24

Tebuconazole from CA-B = $11.75 \cdot \exp(0.019 \cdot T^\circ\text{C} - 0.140 \cdot \text{pH})$ $R_a^2 = 0.95$

9.3.3.2 Accumulation of organic compounds associated with rainwater runoff ($\mu\text{g}/1,000 \text{cm}^2\text{-day}$).

Creosote = $42,649 \cdot [\exp^{-(0.002 \cdot \text{AR (cm)} + 0.172 \cdot \text{RPD (cm)})} - 0.01 \cdot \text{Temp (C)}]$; $R_a^2 = 0.86$

Penta = $6.35 - 0.023 \cdot \text{Redox (mV)} + 1.45 \cdot \text{pH} + 0.068 \cdot \text{AR (cm/y)}$; $R_a^2 = 0.92$

Tebuconazole from CA-B = $-1.09 + 3.35 \cdot \text{Log}_{10}(\text{AR (inches)})$; $R_a^2 = 0.99$

Tebuconazole from WAG = $4.10 + 4.52 \cdot \text{Log}_{10}(\text{AR (inches)})$; $R_a^2 = 0.98$

Propiconazole from WAG = $3.78 + 4.20 \cdot \text{Log}_{10}(\text{AR (inches)})$; $R_a^2 = 0.99$

Imidacloprid from WAG =
 $0.61 + 0.67 \cdot \text{Log}_{10}(\text{AR (inches)})$; $R_a^2 = 0.99$

9.4 DILUTION OF CONTAMINANTS IN WATER AND SEDIMENTS

While chemical components clearly migrate from wood during immersion, rainfall volumes of water and sediment dilute contaminants released from treated wood. The dilution rates are a function of site-specific factors.

9.4.1 Estimation of site specific current speeds

Current speeds may vary significantly as a function of season, geomorphology of the bottom and shoreline, time, water depth, rainfall history, wind, depth, and distance from shore. These models allow for significant simplification; however, it should be noted that the aforementioned factors will influence actual current speeds and resulting contaminant concentrations measured in the field.

9.4.1.1 Harmonically driven marine environments (V_{harmonic})

Current speeds in mixed semi-diurnal tidal (marine) environments are estimated using a sine function with t expressed in radians and the maximum speed (V_{max}) observed 3 h before and after slack tide on an exchange to mean low water (MLW; see Equation [9.14]). Integrating Equation

[9.14] over a 6-h exchange from low to high or high to low tide gives a mean speed of $0.64 * V_{max}$ during the exchange. (Brooks 2005).

$$V_t = V_{max} * \text{Sin}(\pi/12) \text{ with an average speed of } 0.64 * V_{max} \text{ (cm/sec)} \quad [9.14]$$

9.4.1.2 Steady-state current regimes (V_{ss})

Most freshwater environments are primarily influenced by steady-state currents (V_{ss}). Typically these flow along the shore of streams, lakes, and even ponds in response to the water budget, winds, and other factors. The V_{ss} in tidally influenced marine and estuarine systems should be determined as the mean of the speeds recorded at high slack and low slack tides on an exchange to MLW (the 18.6 y average of all low tides). V_{ss} in streams and rivers, should be measured at mid depth at intervals across the width of the proposed project and an average speed estimated. The water channel's cross-sectional area in streams or rivers that are gauged can be determined and divided into the recorded volume of flow to estimate an average current speed. Risk assessments should be based on current speeds estimated at the time of construction and for several months afterward. The model does not account for higher current speeds associated with significant rainfall because unit hydrographs depend on a number of factors including watershed size, channel morphology, and permeability of watershed soils. Increased current speeds during high rainfall events would reduce the concentration of contaminants.

9.4.1.3 Combined steady state and harmonic regimes (V_{model})

Current speeds in some marine and estuarine environments, are a combination of steady-state and harmonic factors. Equation [9.15] combines these contributions to more accurately define site-specific current speeds. Tidal flows may be in the same direction as steady-state flows—usually on ebb tides—or they may oppose V_{ss} —usually on flood tides. Consistent with the worst-case approach taken in this model, V_{model} considers only the case where tidal flows are opposed to steady-state flows reducing V_{model} resulting in increased water column concentrations and sediment accumulations of contaminants.

$$V_{model} = \text{Absolute Value} (0.64 * V_{max} - V_{ss}) \text{ (cm/sec)} \quad [9.15]$$

9.4.2 Dilution volumes for estimating concentrations of dissolved contaminants

Two types of models described by Brooks for use in predicting water column and sediment concentrations of contaminants. The Proximity Model estimated concentrations of contaminants within a few centimeters or meters of immersed treated wood members. The dilution volume is simply the cross-sectional area (CSA) of the treated-wood member, orthogonal to the current vector, multiplied by the appropriate current speed for the environment being evaluated. A unit depth of water (Δh) was used because immersed treated wood contributes contaminants in proportion to the depth of the dilution water. The dilution water is proportional to the same depth. The current speed (cm/s) is multiplied by 86,400 s/d to give results that are consistent with the temporal factors in the loss algorithms (Equation [9.16]). The Proximity Model is useful for understanding the spatial distribution of contaminants in close proximity to immersed treated wood. However, structures are complex and may contain dozens or hundreds of treated-wood members, making the use of this model for understanding the overall effects of actual structures very complicated. In addition, rainwater runoff from overhead structures constructed with treated wood represents a diffuse source of contaminants that is not amenable to the Proximity Model approach.

$$\text{Dilution Volume}_{proximity} = \Delta h * \text{CSA} * (V_{ss} \text{ or } V_{model}) * 86,400 \text{ (cm}^3/\text{day)} \quad [9.16]$$

9.4.3 Box model

A box model was developed by Brooks (2005a) to better assess the environmental response to timber bridges in association with all inputs of contaminants from pressure-treated wood originating in immersed and above-water (rainwater exposed) portions of the structure. Dilution volumes for the box model for assessing water column concentrations of contaminants from all sources, are defined in two ways:

- (a) If the environment is dominated by steady state currents ($V_{ss} > V_{harmonic}$), dilution water volume is determined using Equation [9.17].

$$\text{Volume}_{box} \text{ for immersed wood} = h * \text{Width} * (V_{model}) * 86,400 \text{ (cm}^3/\text{day)} \quad [9.17]$$

(b) The dilution water volume for environments dominated by tidal currents ($V_{ss} < V_{\text{harmonic}}$), is the volume of water within 30 min on either side of slack tide contained within the project's width (W in cm) and its length parallel to the currents (L in cm). Current speeds at slack tide are chaotic in direction, but the speed is not zero. To account for this mixing, the instantaneous current speed ($V_t = V_{\text{max}} * \text{Sin}(\pi t/12)$) was integrated from 30 min before slack tide to 30 min after slack tide to predict an average current speed during this time of $0.0645 * V_{\text{max}}$. This average speed is multiplied by 1,800 s and applied to the upstream and downstream dispersion of contaminants and by 3,600 s to the dimension offshore (Equation [9.18]). This adds 1.7 m to the upstream and downstream box dimension and 3.4 m to the offshore dimension when the maximum current speed is 15 cm/s.

$$\text{Volume}_{\text{box-tidal}} = (W + 0.0645 * V_{\text{model}} * 3600) * (L + 2 * 0.0645 * V_{\text{model}} * 1800) * h / 1000 \quad [9.18]$$

Contaminants in rainwater runoff are assumed to be mixed into the upper 20 cm of the receiving water, unless the water depth is < 20 cm when mixing occurs to the depth of the water. Water depth (h) for both steady-state and tidal regimes is replaced with 20 cm if $h > 20$ or by the water's depth if $h < 20$.

9.4.4 Sediment volumes receiving contaminants from immersed treated wood

Contaminants are assumed to permanently accumulate in sediments at their first point of contact and are assumed to be mixed into the top 2 cm of the sediment column. These are both conservative estimates as bioturbation is expected to mix surficial sediments to depths of 3 to 4 cm and high flows or wave action are expected to resuspend and redistribute surficial sediments downcurrent. These activities should result in reduced environmental concentrations. Contaminants are assumed to adsorb to silt or clay and to settle in sediments with a vertical velocity (V_v), conceptualized in Figures 9.4 and 9.11. The model makes no allowance for contaminant adsorption to dissolved or suspended organic molecules or matter having lower V_v resulting in further transport and greater dilution downstream because longitudinal dispersal is proportional to (V_{ss}/V_v). Contaminants in a horizontal plane are assumed

to be mixed into a trapezoid having an original width equal to the width of the project footprint orthogonal to the current vector and increasing 0.5° in width for each cm of current speed as they settle to the bottom (Figures 9.4, 9.11, and 9.12). All contaminants are assumed to be released in a curtain oriented orthogonal to the current vector at the center of the project (Figures 9.11 and 9.12). Rainwater contaminants are initially mixed into the upper 20 cm of the water or to the water's depth if $h < 20$ cm. Driplines will be on the perimeter of structures covered with impermeable surfaces. Rainwater will drip in a diffuse pattern from within the entire structure for structures with exposed treated-wood decking, such as some piers, floats, and walkways. In either case, contaminants will likely enter the box at many locations, resulting in reduced environmental concentrations when compared with model predictions. All of the contaminants will be carried downstream in environments with steady-state current vectors. In tidally dominated environments, half the contaminants are assumed to be released in each of the two directions of the prevailing currents. As previously discussed, only the worst case where the tidal and steady-state vectors are in opposition is assessed in environments influenced by overlaid tidal and steady-state current vectors.

Note that the distribution of contaminants released from a differential unit of height Δh at the curtain are distributed downstream over the sediments a distance of $\Delta h * V_{\text{harmonic}} / V_v$. Rainwater-derived contaminants are initially distributed in the top 20 cm of the water column. Setting $\Delta h = 20$ cm, and letting $V_v = 0.05$ for creosote-derived PAH or 0.005 cm/s for metals and other organics, including pentachlorophenol, show that rainwater contaminants will be distributed over a reach of sediments downstream equal to $20 \text{ cm} / V_{v=0.05} * V_{\text{(model)}}$ or $400 \text{ cm} * V_{\text{(model)}}$ for PAH. The model assumes a settling velocity of 0.005 cm/s for metals and pentachlorophenol, and predicts that contaminants suspended in rainwater will be spread over a distance downstream of $4,000 * V_{\text{(model)}}$. Also note that, in the absence of turbulence, rainwater-entrained contaminants will first reach sediments a distance equal to $(h - 20) * V_{\text{(model)}} / V_v$. If the water depth (h) is less than 20 cm, contaminants will be distributed downstream a distance equal to $h * V_{\text{(model)}} / V_v$. These models show that rainwater-derived contaminants deposited in deep water will not reach sediments until they are some distance downstream from the structure. This must be considered in designing sediment monitoring protocols.

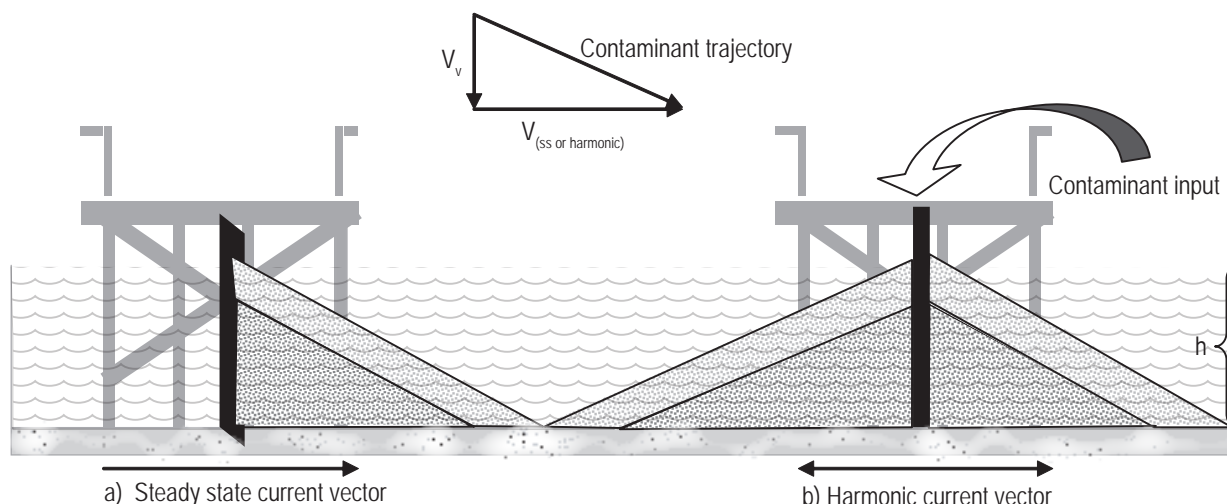


Figure 9.11 Conceptual diagram describing the assumptions used in modeling contaminants released from pressure treated wood to aquatic environments using the box model in (a) steady state current regimes and (b) at sites with tidally driven currents.

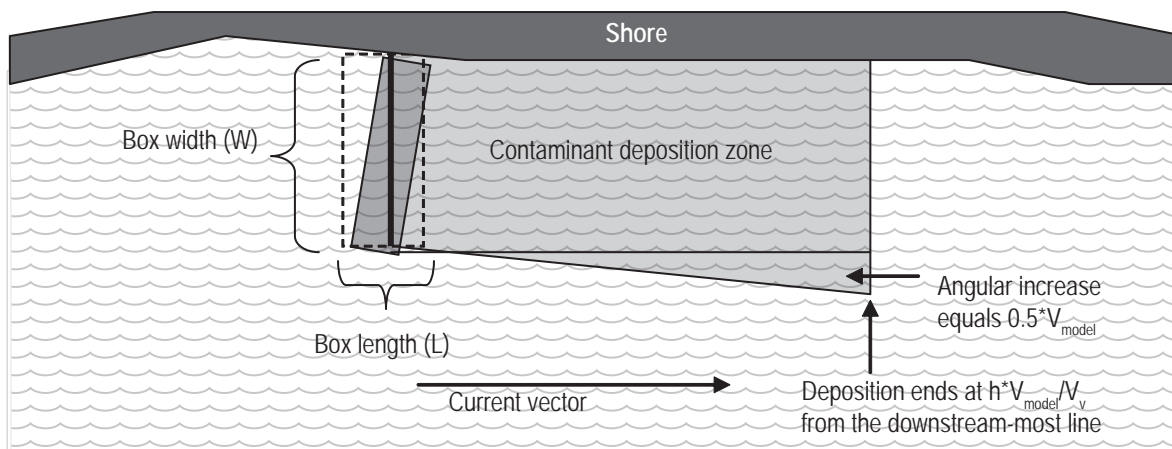


Figure 9.12 Plan view describing the horizontal distribution of contaminants as they settle to the bottom in association with pressure-treated wood structures constructed over water.

9.5 USER INPUTS FOR A MICROSOFT EXCEL® SPREADSHEET MODEL PREDICTING ENVIRONMENTAL CONCENTRATIONS OF CONTAMINANTS ASSOCIATED WITH PRESSURE-TREATED WOOD STRUCTURES

This section describes the model from a user’s point of view. The algorithms used in each cell can be obtained from the electronic version of this General Risk Assessment Model, which is available at WWPinstitute.org.

Preservative

1. Enter a preservative identification code from Model Table 1 of the spreadsheet (column P) into cell K1. The

name of the preservative will then appear in either cell H1 or H2. When this is accomplished, the spreadsheet calculations will be for that preservative. Table 9.16 describes the User Input section of the model for site- and project-specific assessments. Not all of the user inputs are necessary for every type of preservative. The model can function without all inputs without jeopardizing the results.

Piling

- (a) Piling retention (kg/m^3). Enter the piling preservative retention provided by the producer. If this information is not available, then enter the retention specified in the latest version of the American Wood Protection Standards.

Table 9.16 User inputs for running the treated-wood box model for a CCA-C treated timber bridge constructed over a slow-flowing freshwater stream marginally influenced by tides.

Piling	
1. Piling retention (kg/m ³)	12.8
2. Number of piling in a row paralleling the currents	3
3. Number of piling bents	4
4. Average piling radius (cm)	15
5. Distance between piling in a row paralleling currents(cm)	200
6. Reserved	
Immersed lumber	
7. Surface area of sawn lumber that is immersed (cm ²)	725,000
8. Immersed Lumber Retention (kg/m ³)	9.6
Rainwater exposed lumber and piling	
9. Surface area of sawn lumber and piling exposed to rainfall (cm ²)	1,500,000
10. Above water lumber retention (kg/m ³)	4.95
Box dimensions	
11. Box width or width of a stream channel under an overhead structure (cm)	1,000
12. Box length paralleling the currents	600
13. Mean water depth in the box (cm)	300
14. Maximum tidal current speed or V_{harmonic} (cm/s)	2
15. Steady State Current Speed or V^{ss} (cm/s)	8
16. Model speed or V_{model} (cm/s)	6.72
Water characteristics	
17. Average annual water temperature (°C)	15.0
18. Freshwater pH	6.5
19. Water hardness (mg CaCO ₃ /L)	100.0
20. Salinity (PSU)	0.0
21. Background dissolved copper concentration (μ/L)	0.6
22. Background dissolved arsenic concentration (μ/L)	1.5
23. Background dissolved chromium concentration (μ/L)	0.3
24. Background dissolved zinc concentration (μ/L)	0.8
25. Background dissolved penta concentration (μ/L)	0.0
Rainfall characteristics	
26. Annual rainfall (cm/y)	114.3
27. Steady state rainfall rate (cm/d)	0.313
28. Storm event (cm/h)	2.5
29. Duration of the Storm event (h)	1.0
Sediment characteristics	
30. Sediment total organic carbon (%)	2.1
31. Sediment density (g/cm ³)	2.6
32. Sediment redox potential (mV) for penta or depth of the RPD for creosote (cm)	4
33. Background sediment copper concentration (mg/kg)	12
34. Background sediment arsenic concentration (mg/kg)	2.8
35. Background sediment chromium concentration (mg/kg)	1.1
36. Background sediment zinc concentration (mg/kg)	10.5
37. Background sediment penta concentration (mg/kg dry)	0
38. Background sediment PAH concentration (mg/kg)	0.2
Other	
39. Days since construction for determining contaminant concentrations in water	0.5
40. Settling velocity (0.005 cm/s for clay and 0.05 cm/s for creosote)	0.005
41. Modeled lifespan of the project in excess of 35 y (additional years)	35.00
42. Angular increase in width of the sediment deposition zone downstream (°)	3.36
43. Channel width (cm)	1000

(b) Number of piling in a row paralleling the currents. Enter the number of piling in rows that most closely parallel the current vector.

(c) Number of piling rows. Enter the number of rows of pilings.

(d) Average piling radius (cm). Enter the average radius of the piling used in the project. For Class A piling on the Pacific Coast, this is typically 30 cm.

(e) Distance between piling in a row paralleling the currents (cm). Enter the average distance between the centers of pilings driven in rows paralleling the currents.

(f) Distance between rows of piling (cm). Enter the distance between the bents of piling in cm.

Immersed lumber

(g) Surface area (cm²) of sawn lumber that is immersed at mean high water (MHW). This requires access to the project plans. Sum the surface areas of all sawn lumber (all wood excepting piling) that is immersed in water when the tide is ≤ MHW. Tidal heights are published by the National Oceanographic and Atmospheric Agency (NOAA). For bulkheads that are backed by earth, enter the surface area facing the water plus the two sides of each board. The side in contact with the soil is considered non-leaching with respect to the water body.

(h) Immersed lumber retention (kg/m³). When available, enter the average measured retention provided by the treated-wood producer. When that information is not available, enter the retention specified for this use in the latest version of the American Wood Protection Association Standards.

Rainwater exposed lumber and piling

(i) Surface area above MHW exposed to rainfall (cm²). Enter the surface area (cm²) of all piling and lumber in the structure that is exposed to rainfall. Figure 9.3 is provided as a guide for the lumber. The surface area for piling is that area located on all perimeters of the structure. This is $\pi * r * \text{height}$ above MHW for each perimeter piling because only the outer half of the piling is exposed to rain. The inner half is assumed to be under the structure. This is provided only as a guide. Special circumstances, such as the use of pin piling, will require other approaches.

(j) Above water lumber retention (kg/m³). This is generally the same as the immersed lumber retention.

Box dimensions

- (k) Box width or width of a stream channel under an overhead structure (cm). Refer to Figure 9.11 because the box width may be less than the structure's width when the structure is oriented at an angle to the prevailing currents. Box width for structures crossing rivers, streams, or estuaries, is the channel full width of the stream at the flow used to define current speed. Box width for bulkheads is one meter, which assumes that mechanical mixing associated with the bulkhead will initially distribute contaminants to a distance of one meter from the bulkhead. Users may choose higher widths for bulkheads located in energetic environments or lower widths for bulkheads associated with ponds or other quiescent water bodies.
- (l) Box length (cm) paralleling the currents. Figure 9.11 can be used as a guide because the length of a project may be greater than the width of a bridge or pier, depending on its orientation. However, the width decreases with increasing angle as the length increases for projects in which the orientation is not orthogonal to the current vector, and the area of contamination, which is important for determining sediment contaminant concentrations, does not significantly change.
- (m) Mean water depth in the box (cm). This is the mean depth of water within the box. It can be determined by using a measured wading staff in shallow waters or with a weighted tape measure in moderately deep waters. In deeper waters, the depth is most easily determined by using a boat-mounted depth sounder. Transects must be run orthogonal and parallel to the current vector through the center of the project and then averaged. At least six measurements spaced equally across the channel are recommended for streams. Where depths vary greatly, it may be necessary to partition the box into segments representing different depths. In this case, the partitions must be assessed as individual boxes; however, this is not usually necessary.
- (n) Maximum tidal current speed (V_{\max} in cm/s). Current speeds can be measured with a number of staff-mounted or weighted electromagnetic or mechanical devices. Rough estimates can be obtained by placing a container that is three-quarters full of water about 2 m up current from a mark on the shore (or the upstream edge of a bridge) and measuring the time required to move past a distance defined by the width of a bridge

or two marks on the shore. The model requires an assessment of the maximum current speed in a tide cycle (V_{\max}). Assuming a mixed, semidiurnal tidal regime, at least three measurements should be made 3 h before and after slack tide and the six or more datapoints averaged. Measurements should be made on an exchange to mean low water (MLW).

- (o) Steady-state current speed or V_{ss} (cm/s). The same methods described for user input 14 are appropriate for determining steady-state current speeds. A current speed determination should be made in streams and rivers at each of the points where water depth is measured, giving six values, which are averaged. In tidally driven systems, V_{ss} is measured at slack tide. The value at slack tide should be approximately equal to the difference in V_{harmonic} measured 3 h before and after slack tide. Three or more measurements of V_{ss} are recommended in tidally dominated systems.
- (p) Model speed or V_{model} (cm/s). This is not a user input. The value is determined by the model as the absolute value of $(0.64 * V_{\max} - V_{ss})$. This predicts concentrations on the side of the project in which the steady state and tidal currents are in opposition to each other and is therefore the worst case. Note in those instances where V_{ss} is approximately twice V_{\max} , V_{model} can be close to zero, requiring additional consideration by the user. If V_{\max} and V_{ss} vary by less than a factor of 4, it is recommended that the speed best characterizing the site be used and the alternate speed be ignored. For example, if V_{\max} is 8 cm/s and V_{ss} is 3 cm/s, then the evaluation should be conducted with V_{\max} set to 8 cm/s and the V_{ss} is ignored (is set to zero).

Water characteristics

The effects of contaminants are cumulative and inputs from pressure-treated wood structures must be added to existing concentrations to achieve a meaningful assessment. Background concentrations can sometimes be determined by using existing U.S. Geological Survey (USGS) or state databases. Unless there is reason to believe that there is significant existing contamination, screening assessments do not need to determine background concentrations of dissolved contaminants associated with pressure-treated wood. However, these endpoints should be evaluated appropriate to the preservative being considered if the screening assessment indicates that a site-specific risk assessment is required. For example, there is no need to consider PAH or penta if a metal-based pre-

servative is being considered. Likewise, metals do not need to be considered if an organic-based preservative is being considered. The Puget Sound Estuary Protocols (PSEP 1996) provide detailed guidance for the collection, handling and analysis of most parameters evaluated in aquatic environments. Contaminants should be collected in properly cleaned glass bottles at mid-depth, taking care to avoid contamination. Triplicate 100-ml samples are sufficient to complete all of the inorganic analyses required as user inputs when dealing with fresh water. Seawater analyses may require concentration and therefore triplicate 500 ml samples are recommended. Water samples should be filtered at 0.045 μm prior to analysis to exclude particulate-bound metal that is not biologically available. This does not exclude metal ions bound to other ions and/or dissolved organic molecules, which also reduces their bioavailability. The Biotic Ligand Model (BLM) (HydroQual 2007) provides a more accurate assessment of bioavailable copper, but this requires measurement of numerous parameters. Use of the BLM is recommended when model predictions suggest that a project may be marginally unsuitable or for waters known to contain high levels of humic acid or other dissolved organic molecules.

- (q) Average annual water temperature ($^{\circ}\text{C}$). For purposes of evaluating long-term sediment accumulation of contaminants, an average annual temperature is appropriate. This can be determined for major river systems from USGS records. State records are useful for determining average temperatures in many water bodies. In areas where temperatures fluctuate significantly, users may want to evaluate water column concentrations of contaminants at water temperatures appropriate for the time of year when construction is anticipated. This will require two assessments, one at the average temperature for sediments and another at the temperature expected during construction.
- (r) Freshwater pH. This can be measured using any one of the available field or laboratory pH meters. USGS and state records can also be useful. Where large fluctuations in pH occur, users should enter a value appropriate for the time of year when construction is anticipated because it can affect metal loss rates from pressure-treated wood.
- (s) Water hardness ($\text{mg CaCO}_3/\text{L}$). Water hardness is important for determining the bioavailability and toxicity of metals in fresh waters. It can be measured in the field by using selective ion probes or in the laboratory by using inductively coupled plasma (ICP) spectroscopy for determination of calcium and magnesium. Hardness is reported in $\text{mg CaCO}_3/\text{L}$ equivalents and is used by the model to calculate EPA water-quality criteria for comparison with model predictions.
- (t) Salinity (PSU or parts per thousand). Salinity can be measured electrometrically by using any one of a number of salinity and/or conductivity meters (Standard Method 2520) or by titration in the laboratory (SM 210C). Water having a salinity <2.0 PSU is considered fresh water.
- (u) Background dissolved copper concentration ($\mu\text{g Cu}/\text{L}$). Copper is typically evaluated in a laboratory with ICP (EPA Method 200.7).
- (v) Background dissolved arsenic concentration ($\mu\text{g As}/\text{L}$). Aquatic organisms are less sensitive to arsenic, zinc, and chromium than they are to copper. However, these other contaminants may be important, especially when the water may be used by humans or livestock. Arsenic is typically measured with ICP (EPA Method 200.7).
- (w) Background dissolved chromium concentration ($\mu\text{g Cr}/\text{L}$). Dissolved chromium is determined by using EPA Method 200.7.
- (x) Background dissolved zinc concentration ($\mu\text{g Zn}/\text{L}$). Zinc is also evaluated using ICP (EPA Method 200.7).
- (y) Background dissolved penta concentration. Pentachlorophenol is not typically found outside of industrial areas or in some cases adjacent to railway rights of way. When there is reason to believe that penta may exist in the background, triplicate water samples should be evaluated. Penta is measured using EPA (8151) by gas chromatography using an electron capture detector (GC/ECD).

Rainfall characteristics

- (z) Annual rainfall (cm/y). Rainfall data are available from the U.S. Natural Resources Conservation Service (NRCS) in soil surveys or from NOAA. In the United States, this is usually given in inches/day, which must be multiplied by 2.54 cm/inch to convert to cm/d .
- (aa) Steady-state rainfall rate (cm/d). This value is provided by the model as User Input 26/365.25. A steady-state rainfall rate is assumed for predicting long-term accumulation of contaminants in sediments.
- (bb) Storm event (cm/hour). Trial runs with the model

suggest that contaminated rainwater runoff from pressure-treated wood structures during storm events has little effect on the predicted concentration of contaminants in water—unless unrealistic amounts of rainwater runoff are introduced to a small body of water whose flow does not respond to the storm. The model allows users to evaluate the effects of increased rainfall during storm events. User Input 28 defines the rate of rainfall. Realistic inputs should not exceed 5 cm/h.

- (cc) Duration of the storm event (h). The length of the storm event is entered here. Because water body flows are not programmed to increase during storm events, this input has little effect on the prediction. In reality, high rainfall events lasting more than a few hours will increase stream flows as the unit hydrograph responds to increased rainfall in the watershed.

Sediment characteristics

The same comments made for dissolved contaminants also apply to sediment determinations. The need for specific analyses depends on the results of preliminary modeling and site- and preservative-specific factors. PSEP (1996) recommends analysis of the upper 2.0 cm of sediments because they are representative of “recent” sediments. This is also the zone where bioturbation and porewater movement are likely to distribute contaminants. This assessment assumes that contaminants are distributed in these surficial sediments. As a result, sediments should be collected to a depth of 2 cm for analysis. Triplicate 100-ml (250 g) sediment samples are sufficient to conduct the required analyses. Samples can be stored at 4°C for up to 2 wk or frozen for holding times of up to 6 mo. PSEP (1996) provides detailed guidance for the collection and analysis of contaminants in sediments. Sediments are digested in acids of varying strengths and at varying temperatures. Strong acid digestion (EPA Method 3000 Series) is recommended for these analyses. This approach may overestimate the bioavailable fraction of sedimented metals—but it will not liberate metals that are natural constituents of many minerals found in sediments. Total digestion using hot hydrofluoric acid is not recommended as it essentially mines the sediments for metals. In addition, total digestion is not available at most commercial laboratories. All sediment endpoints are reported as mg/kg dry sediment.

- (dd) Sediment total organic carbon (TOC in percent). TOC should be measured in sediments whenever either creosote- or pentachlorophenol-treated wood is proposed. Non-polar organic contaminants, like penta

and PAH, bind to organic carbon—reducing their bioavailability and toxicity. Few governmental jurisdictions have published marine sediment quality criteria (SQC). Washington State is an exception and their SQC have been adopted for this risk assessment. Sedimented PAH in the SQC are based on sediment TOC. At 1% TOC, the SQC for HPAH is 9.6 mg HPAH/kg dry sediment. The SQC for HPAH at 2% TOC is 19.2. The model uses User Input 30 to determine SQC for both PAH and pentachlorophenol. Total organic carbon is determined in a laboratory by using available elemental analyzers.

- (ee) Sediment density. The recommended value of 2.6 g/cm³ should not be changed unless site-specific information indicates otherwise.
- (ff) Sediment redox potential (mV) for penta assessments and depth of the RPD for creosote (cm). These endpoints should be determined for all projects involving either creosote- or pentachlorophenol-treated wood. The RPD is easy to measure in the field, and Table 9.2 provides a method for estimating redox potentials using the depth of the RPD. Redox potential can be measured with probes for full risk assessments (see Brooks 2001). These measurements are typically made in the field. The depth of the RPD is determined in the field by measuring the depth in the sediments where the matrix chroma declines sharply and becomes dull or black due to the accumulation of iron sulfide in anaerobic layers.
- (gg) Background sediment copper concentration (mg Cu/kg). When required, triplicate samples should be analyzed in the laboratory, using ICP and EPA Method 6010 following a strong acid digestion. The results are reported as mg Cu/kg dry sediment.
- (hh) Background sediment arsenic concentration (mg As/kg). When required, triplicate samples should be analyzed in the laboratory, using ICP and EPA method 6010 following a strong acid digestion.
- (ii) Background sediment chromium concentration (mg Cr/kg). When required, triplicate samples should be analyzed in the laboratory, using ICP and EPA Method 6010 following a strong acid digestion.
- (jj) Background sediment zinc concentration (mg Zn/kg). When required, triplicate samples should be analyzed in the laboratory, using ICP and EPA Method 6010 following a strong acid digestion.

- (kk) Background sediment penta concentration (mg penta/kg). When required, sediment concentrations of pentachlorophenol can be determined by using GC/ECD and EPA Method 8151 to evaluate triplicate sediment samples. Background concentrations of this compound need only be determined if there is reasonable cause to suspect some previous or ongoing contamination.
- (ll) Background sediment PAH concentration (mg PAH/kg). Sediment concentrations of PAH can be determined by using either high performance liquid chromatography (HPLC) with EPA Method 8310 or gas chromatography/mass spectrometry (GC/MS) analyses, using EPA Method 8270.
- (mm) Days since construction for determining contaminant concentrations in water. Preservative loss rates from pressure-treated wood decline with time, and the highest losses occur immediately after construction. Acute WQC are 1-h concentrations and a user entry of 0.5 d is recommended for comparison of predictions with acute criteria. Chronic criteria are generally a 4-d average, and a user entry of 2.0 d is recommended for comparison with these criteria. This user entry has no effect on predicted sediment accumulation of contaminants. However, preservative loss rates and water column concentrations can be evaluated for any day during the life of the project by manipulating this entry.
- (nn) Settling velocity (0.05 cm/s for creosote and 0.005 cm/s for other contaminants). These inputs are based on the results of the Sooke Basin Study, unpublished laboratory observations for creosote, and an assumption that metals bind to clay while other organic contaminants bind to particulate or dissolved organic matter or molecules.
- (oo) Anticipated lifespan of the project. The default project lifespan is 35 y, with a minimum of 10 y. If a project is expected to remain in place for longer than 35 y, enter the larger expected lifespan here. If the project is temporary or it is expected that periodic storm events will refresh sediments through erosion or accretion of new sediment, the user may enter the period at which these events are expected to occur. However, entries of < 10 y will result in errors. An expected lifespan of 35 y is recommended for normal use.
- (pp) Angular increase in width of the sediment deposition zone downstream and offshore. The model assumes

that contaminants are dispersed downstream by the project's width orthogonal to the current vector plus an angle on the offshore side that is dependent on V_{model} . Experience working in aquaculture indicates that the angular dispersion of water downcurrent from structures is dependent on the nature of the structure, water depth, and primarily on current speeds. Near slack tide, the distribution is chaotic and the dispersion is circular around the structure. The model uses this for calculating water column concentrations of contaminants in harmonically driven current speed environments. As current speeds increase, the angular displacement downcurrent decreases. The model estimates the half-angle increase by using the following algorithm. The half-angle increase downcurrent equals 180° if V_{model} is < 0.5 cm/s. If V_{model} is ≥ 0.5 cm/s, then the half-angle is $180^\circ / (4 * V_{\text{model}})$. If V_{model} is < 0.5 cm/s, then sediment contamination is modeled as a circle around the structure. As current speeds increase, the half-angle decreases. In current speeds of 20 cm/s, the half-angle is estimated at 2.25° . It is emphasized that this algorithm is conceptual and not based on an analysis of empirical data.

- (qq) Channel width (cm). For projects crossing streams or those located in narrow channels, the sediment deposition zone is constrained by the boundary conditions imposed at the shoreline. The sediment deposition zone in the model will not exceed the entered channel width.

9.6 MODEL OUTPUT

The model provides output as a series of tables.

Model Table 1. Preservative loss rates

Loss rates for metals and organic active ingredients used in pressure-treated wood are provided in cells \$O\$8 to \$AG\$20 for the 10 wood preservatives commonly used over and/or in water. Only data for the preservative being examined is shown. Cells providing loss rates from other preservatives are marked as not applicable (NA). Data is provided for metal loss from immersed wood ($\mu\text{g}/\text{cm}^2\text{-d}$) and rainwater runoff inputs for each contaminant are given in $\mu\text{g}/\text{L}$. These values are derived from the algorithms previously described in this chapter and in Chapter 7. The algorithms rely on the user inputs in column E where necessary. Note that some preservatives do not have AWWPA Standards for use in water. Only rainwater runoff concentrations ($\mu\text{g}/\text{L}$) are provided for these preservatives.

Model Table 2. Maximum accumulation of wood preservative active ingredients in sediments

Metals

Metal accumulation in sediments is accomplished by numerically integrating the loss-rate algorithms from t = 0 to 10 y and then adding the additional accumulation predicted during the remainder of the user-determined project lifespan (User Input 41) multiplied by the long-term loss rate for the active ingredient or preservative being assessed (User Input 41). This is accomplished in the “Metal Accumulation Worksheet” included with the model, which is linked to the appropriate cells in \$Q\$27:\$AG\$29.

Organics

The maximum accumulation of degradable organic active ingredients was described earlier in this chapter and the value is determined in a separate Sediment Accumulation Workbook available from WWPinstitute.org. Appropriate values were copied into these cells. Maximum accumulations are provided in Table 2 of the Risk Assessment Model for immersed treated wood and for rainwater runoff from overhead treated structures.

Model Table 3. Benchmarks for assessing active ingredients

This table provides water and sediment quality criteria adopted for this risk assessment (See Chapter 6 for a more detailed discussion of how and why these benchmarks were adopted). The values are corrected for water hardness (metals) and sediment total organic carbon (PAH and pentachlorophenol) based on user inputs in column E. The sediment half-life is calculated and/or listed in column V for the organic active ingredients currently used in wood preservatives. These values are corrected for depth of the RPD, redox potential, and temperature based on user inputs.

Model Table 4. Preservative loss rates from immersed treated wood

Cells \$I\$6 through \$K\$16 summarize the loss rates of the active ingredients from immersed wood at the conditions specified by the user in column E. (See Table 9.17 for CCA-C.) The immersed portions of the project will lose 3.4 µg Cu; 0.7 µg As; and 0.02 µg Cr/cm² of immersed wood per day on the first day of immersion (d 0.5 entered in User Input 39).

Table 9.17 Predicted preservative migration rates on the first day of immersion from CCA-C pressure-treated piling exposed in freshwater having a pH of 6.5 and a temperature of 15°C. (See Figure 9.16 for a description of the site and project.)

Contaminant	Migration rate (µg/cm ² -day)
Copper	3.405
Arsenic	0.707
Chromium	0.024
Zinc	0.000
TEB	0.000
PROP	0.000
IMID	0.000
Creosote (PAH)	0.000
PENTA	0.000
DDAC	0.000

Table 9.18 Predicted copper, arsenic, and chromium concentrations in rainwater runoff from above-water portions of the structure treated with CCA. (See Figure 9.17 for a description of the site and project.)

Contaminant	Concentration (µg/L)
Copper	1831.4
Arsenic	1593.8
Chromium	206.0
Zinc	0.0
TEB	0.0
PROP	0.0
IMID	0.0
Creosote (PAH)	0.0
PENTA	0.0
DDAC	0.0

Model Table 5

Cells \$I\$20:\$K\$30 summarize the predicted concentrations of active ingredients in rainwater runoff from overhead portions of a structure under the conditions specified by the user in column E. See Table 9.18 for CCA-C. The runoff is predicted to contain 1,831 µg Cu/L; 1,594 µg As/L; and 206 µg Cr/L on first exposure to rain. The basic information in Model Tables 3 and 4 can be very useful to knowledgeable users when encountering unusual projects or situations.

Model Table 6

Dilution water volume factors Output describing the predicted volume of dilution water for the project described in Figure 9.12 of this chapter is summarized in Table 9.19. Predictions include the following.

Table 9.19 Dilution water volume factors.

Volume of rainwater runoff from pressure-treated wood (L/d)	312.9
Dilution water passing through the box with steady-state currents (L/d)	174,182,400
Dilution water in the box within 30 min of slack tide (L)	1,659,424
Rainwater dilution (20 cm deep) water passing through the box with steady state currents (L/day)	11,612,160
Rainwater dilution (20 cm deep within 30 min either side of slack tide (L)	110,628

Volume of rainwater runoff from pressure-treated wood (L/d)

This value is determined by multiplying User Input 9 [with guidance from Figure 9.3 of this chapter, which describes the surface area of sawn lumber and piling above MHW that is exposed to rainfall (cm²)] by the steady state rainfall (cm/d) computed for users in User Entry 44 [based on the annual rainfall (cm/y) that users provide in User Entry 43]. This value is divided by 1,000 to convert from cm³ (ml) to liters. All of the surface area of treated wood exposed to rainfall is assumed to be horizontal for this computation, which likely overestimates the actual runoff because vertical surfaces encounter much less precipitation than do horizontal surfaces. In this case, an annual rainfall of 114.3 cm/y (User Entry 26) and a rainwater-exposed treated-wood surface area of 1,000,000 cm² (User Entry 9) will result in rainwater runoff from the overhead portion of the structure of 312.9 L/d.

Dilution water passing through the box with steady state currents (L/d)

This is the volume of water passing through a vertical cross section of the box [box width (cm) × mean water depth (cm) × current speed (cm/s) × 86,400 s/d/1000 cm³/L]. In this case, $V_{\text{model}} = 6.72$ cm/s (a computed value given in User Input 16); the box width (User Entry 11) is 1,000 cm; and the mean water depth is 300 cm (User Entry 13).

Dilution water in the box within 30 min of slack tide (L)

This output is based on a harmonic evaluation of V_{model} for the period ± 30 min either side of slack tide. If current vectors are not influenced by tides (User Entry 14 = 0), then an “NA” will appear in this output. Contaminant concentrations will be calculated with either the steady-state dilution factor or the tidal dilution factor given in this cell, depending on which speed dominates the flow. In this case, the steady-state current speed is 8 cm/s and the

maximum tidal speed is 2 cm/s. Therefore, contaminant concentrations will be based on the dilution factor for steady-state flows. However, note that V_{model} is used to determine the steady-state dilution factor (174,182,400 L/d) and is computed when tidal flows and steady-state currents are in opposition to each other (the minimum flow rate through the project). In this case, the $V_{\text{ss}} = 8$ cm/s and $V_{\text{model}} = 6.72$ cm/s.

Rainwater dilution (20 cm deep) water passing through the box with steady-state currents (L/d)

This dilution factor is computed in a manner similar to the steady-state dilution factor, except that water depth is restricted to a maximum of 20 cm. For depths >20 cm, the model assigns a depth of 20 cm. For depths <20 cm, the model uses the depth entered in User Input 26.

Rainwater dilution (20-cm deep within 30 min either side of slack tide (L)

For mean water depths >20 cm, this is the volume of water defined by expected water movement within 30 min of slack tide multiplied by 20 cm. The model uses actual depth for mean water depths <20 cm (User Input 26).

Model Table 7. Dissolved contaminant concentrations leaving the box (µg/L).

Comparisons between predicted water column concentrations of contaminants and water quality criteria are provided in spreadsheet cells \$G\$43:\$M\$52 (Table 9.20). Output is provided only for those contaminants associated with the preservative being considered in the assessment. Background concentrations of the contaminants are automatically copied from User Inputs 21 to 25. Background concentrations of TEB, PROP, IMID, and DDAC are assumed to be zero because these are uncommonly encountered organic compounds. Hydrophobic PAH are also rarely found dissolved in water, except in oil spills, and their concentrations are assumed to be zero.

Dissolved contaminants from immersed treated wood

These values are based on contaminant loss rates on the day entered in User Entry 39 and the independent factors influencing those loss rates entered in other user entries, divided by the dilution volumes that are appropriate to the environment being considered. In this case, copper will be lost from the immersed wood at a rate equal to 3.405 µg Cu/cm²-d. It will be diluted by the 174,182,400 liters of water flowing through the project each day, giving a predicted increase of 0.022 µg Cu/L.

Dissolved contaminants from rainwater runoff

These values are based on algorithms describing the concentration of contaminants in rainwater runoff from commodity-size decking samples exposed for several years to rainfall in the Pacific Northwest. The predicted concentration in the runoff on the day being evaluated (d 0.5, in this case) is multiplied by the volume of rainwater calculated in cell \$L\$34 to determine inputs to the box. These inputs are divided by the volume of water included in the upper 20 cm of the water column flowing through the project. In this case, the concentration of copper in runoff from exposed wood on first exposure to rain is predicted to be 1,831 µg Cu/L. The volume of rainwater striking the exposed wood (Cell \$L\$34) is 312.94 L/d and the total contaminant reaching the receiving water from rainwater runoff is 0.57 grams of Cu/d. Assuming no turbulent mixing of rainwater after its initial dilution in the upper 20 cm of water results in a predicted increased in concentration of 0.049 µg Cu/L. The background concentration at this site was 0.60 µg/L. The project will add 0.071 µg/L additional copper on the first day in the upper 20 cm of the water column and 0.022 µg Cu/L to the entire 300 cm depth. Total copper from all sources is predicted to be 0.67 µg Cu/L in the upper 20 cm of the water column. Actual water hardness at this site was 100 mg CaCO₃/L, resulting in an acute EPA WQC of 17.02 µg/L. When the day of evaluation is changed to two (User Entry 39), the project is expected to result in an increased copper concentration of 0.05 µg/L, giving a total concentration of 0.65 µg/L. The chronic EPA Water Quality Criterion (WQC) at the water’s hardness is 11.4 µg Cu/L. In either case, the predicted concentration is a very small fraction of the WQC, and copper lost from this project could not be expected to

cause any adverse environmental response in the water column. Copper is most problematic for most aquatic systems not already contaminated by metal from other sources or for those that have unusually high natural background concentrations. That is true in this example, and the concentrations of arsenic and zinc added by this project result in total concentrations that were several orders of magnitude less than respective EPA acute or chronic WQC.

Model Table 8

Predictions of the area of sediment contamination (cm²)

Sediment concentrations of contaminants are described in mg/kg. The model assumes that contaminants from treated wood are mixed into the upper 2 cm of sediments and uses a default sediment density of 2.6 g/cm³. Users can modify this value in User Input 31. The horizontal area over which contaminants are dispersed is described qualitatively in Figures 9.4–9.5 and 9.10–9.11. Quantitative predictions based on project width, water depth, current speed, and settling speed are provided in spreadsheet Cells \$G\$59:\$M\$62 (Table 9.21).

Effective width of the sediment footprint (cm)

The minimum width (cm) is the width of the project orthogonal to the currents. The maximum width (cm) is the minimum width increased by a half-angle displacement (see item 42 in the User Inputs) as the contaminants are carried downstream while settling to the substrate. In this case, the project width is 1,000 cm = the minimum width. For metals, the assumed settling speed is 0.005 cm/s and $V_{model} = 6.72$ cm/s. When added to the project’s width orthogonal to the current vector, the angular displacement

Table 9.20 Comparisons between predicted sum of contaminants leaving the box and concentrations with acute and chronic water quality criteria. A separate worksheet is provided and linked with the model for calculating ΣTU for evaluating dissolved PAH.

Model Table 7. Dissolved contaminant concentrations leaving the box (µg/L)						
Contaminant	Background	From immersed	From rain	Total	Acute benchmark	Chronic benchmark or ΣTU for PAH
Copper	0.60	0.022	0.049	0.67	17.016	11.351
Arsenic	1.50	0.0047	0.04295	1.55	360.00	190.00
Chromium	0.30	0.0002	0.00555	0.31	548.74	178.00
Zinc	0.80	-	0.00000	0.80	114.45	104.51
TEB	0.00	-	0.00000	-	FA	FC
PROP	0.00	-	0.00000	-	FA	FC
IMID	0.00	-	0.00000	-	FA	FC
Creosote (PAH)	0.00	-	0.00000	-	ΣTU<0.186	0.000
PENTA	0.00	-	0.00000	0.00	5.49	3.46
DDAC	0.00	-	0.00000	-	FA	FC

Table 9.21 Spatial dimensions of the sediment area receiving contaminants from immersed treated wood and rainwater runoff from overhead structures.

	Minimum (cm)	Maximum (cm)	Area (cm ²)
Effective width of sediment footprint (cm)	1,000	1,000	
Distribution downcurrent of rainwater contaminants (cm)	376,320	403,800	27,480,000
Distribution downcurrent of contaminants from immersed wood (cm)	0.0	403,800	403,800,000
Maximum width of the sediment footprint (cm)	1,000	24,771	

of 3.36° increases the sediment impact zone by 23,771 cm (or 237 m) as the contaminants settle to the bottom (last row in Table 9.21). However, channel width (User Entry 43) is only 1,000 cm. In cases where channel width is less than the computed width of the sediment receiving zone, the model constrains the effective width to that of the receiving channel.

Distribution downcurrent of rainwater contaminants (cm)

Contaminants in rainwater at this site do not reach the sediments until they are a minimum distance of 3,763 m downstream. At this distance, it is the rainwater contaminants initially mixed 20 cm deep in the water that reach the sediments. Rainwater contaminants mixed into the surface of the receiving water are carried a maximum of 4,038 m downstream as they settle to the substrate. The horizontal area over which rainwater contaminants mix in sediments at this site is 1,000 cm wide (channel width) by 27,480 cm long (403,800 cm–376,320 cm). The area of deposition of rainwater contaminants is 27,480,000 cm² (or 2,748 m²). These “displaced footprints” are not uncommon, and the deeper the water, the farther downstream the rainwater contaminant footprint will be displaced.

Distribution downcurrent of contaminants from immersed wood (cm)

Contaminants released from piling or bulkheads that are buried in the substrate are captured in sediments starting at their point of release (zero distance). Contaminants released from near the water’s surface in this 3-m-deep river traveled a maximum distance of 4,038 m downstream—the same distance downstream as rainwater contaminants mixed into surface water. The area within this footprint is 403,800,000 cm² (or 40,380 m²). The shal-

lower the water, the smaller the sediment receiving area. However, the treated wood will be immersed to a shallower depth and contaminants will be proportionally reduced, giving essentially the same final concentrations. The same is not true for rainwater contaminants, unless the water depth is <20 cm.

Model Table 9. Surface areas (cm²) of pressure-treated wood for determining total contaminant loading (Table 9.22)

The surface area of immersed piling is computed as the number of immersed pilings (User Entry 2*User Entry 3) multiplied by their diameter (2*User Entry 4) and their depth of immersion below MHW in tidal environments (User Entry 13). This is added to the surface area of immersed sawn lumber determined by the user and entered in User Entry 7). The project described in Figure 9.12 has 5 pilings in a row in each of 3 bents for a total of 15 pilings. The pilings have an average radius of 15 cm. In addition, the project includes 725,000 cm² of immersed timbers and lumber—all treated with CCA-C preservative. The water depth is 300 cm. The model determined that there are 1,148,900 cm² of immersed, treated-wood surface, as well as 1,000,000 cm² of pressure-treated wood (piling above MHW, timbers, lumber, etc.) exposed to rainfall, using Figure 9.3 as a guide.

Model Table 10. Maximum contaminant concentrations in sediment (mg/kg)

Predicted maximum sediment concentrations of active ingredients in treated-wood are provided in Cells \$G\$71:\$L\$81 (Table 9.23). The predictions are based on the maximum accumulations in Model Table 2 of the Risk Assessment Model (µg contaminant/cm² leaching surface area) times the immersed surface area of treated wood (cm²) given in Model Table 9 divided by the 2-cm-high depth of sediment times sediment density (g/cm³) times the sediment receiving area (cm²) given in Model Table 8. This calculation provides the maximum predicted sediment concentrations (µg/g = mg/kg). Output in Model Table 10 includes the following:

Table 9.22 Surface areas (cm²) of pressure-treated wood predicted to be exposed to immersion or rainfall for determining total contaminant loading (Model Table 9).

Immersed treated wood (cm ²)	1,148,900
Rainwater exposed wood (cm ²)	1,000,000

Table 9.23 (Model Table 10) Comparison between predicted maximum sediment concentrations of contaminants from pressure-treated wood and sediment quality criteria.

Contaminant	Background (mg/kg)	From immersed (mg/kg)	From rain (mg/kg)	Total (mg/kg)	Sediment quality criterion (mg/kg)
Copper	12.00	1.70	0.83	14.54	80.000
Arsenic	2.80	0.0032	2.6441	5.45	20.000
Chromium	1.10	0.0050	0.8358	1.94	95.000
Zinc	10.50			10.50	140.000
TEB	0.00				FS
PROP	0.00				FS
IMID	0.00				FS
Creosote (PAH)	0.20			0.20	37.600
PENTA	0.00				0.840
DDAC	0.00				FS

Background (mg/kg)

Biological effects of contaminants are cumulative; the background concentrations (measured or from available data sources) that were entered in User Entries 33 through 38 are linked to the second column in Model Table 10. Background concentrations of TEB, PROP, IMID, and DDAC are assumed to be zero. Only contaminants appropriate to the preservative being considered in the model will be shown.

Sedimented contaminants from immersed wood

In this case, the immersed wood loses $3.405 \mu\text{g Cu/cm}^2\text{-d}$, leading to a maximum copper accumulation in sediments of $3,112 \mu\text{g Cu/cm}^2$ of immersed leaching surface area during the 35-y lifespan of the project. There is a total of $1,148,900 \text{ cm}^2$ of immersed CCA-C treated wood, giving a sediment loading of 3.57 kg of copper at the end of 35 y. This copper is distributed over an area of $40,380 \text{ m}^2$ of sediments, whose density is 2.6 g/cm^3 . The 2-cm-deep section of sediments in which the contaminants are distributed therefore weighs 2,099,760 kg, giving a predicted maximum sediment concentration increase of 1.7 mg Cu/kg dry sediment associated with immersed sections of wood.

Sedimented contaminants originating in rainwater runoff

Model Table 2 (Cell \$U\$27) predicts that $119.3 \mu\text{g Cu}$ will accumulate in sediment over the project's 35-y lifespan for every cm^2 of CCA-C-treated wood exposed to rain. User Inputs used the default project lifespan of 35-y, with an annual rainfall rate of 114.3 cm. In this example, there are $1,000,000 \text{ cm}^2$ of treated wood exposed to rainfall, leading to an increase in the sediment's total load of copper of

119.3 g associated with rainwater runoff. The copper is received by a sediment surface area of $2,748 \text{ m}^2$. The 2-cm depth of the receiving sediments underlying this area weighs 142,896 kg ($2.6 \text{ g/cm}^3 \times 2 \text{ cm} \times 27,480,000 \text{ cm}^2$) and the rainwater runoff adds another 0.83 mg Cu/kg dry sediment ($119,300 \text{ mg Cu}/142,896 \text{ kg dry sediment}$).

Total sediment concentrations of contaminants

The predicted contamination from immersed and rainwater-exposed pressure-treated wood ($1.70 + 0.83 = 2.54 \text{ mg Cu/kg}$) is added to the background concentration of 12.0 mg Cu/kg (entered at User Input 33) to obtain a total predicted sediment concentration in this example of 14.54 mg/kg. This prediction can then be compared with the SQC given in the last column of the table (80 mg Cu/kg dry sediment for fresh water). In this case, 82.5% of the copper in the sediments at the end of the project's lifespan is due to the background. In any case, the model predicts that the 15 piling will increase copper levels by 18% of the benchmark.

It should be noted that it is the total copper concentration in the environment that can stress biological resources. In some instances, background sediment concentrations of a contaminant may already approach or exceed the SQC, leading to the denial of a permit to add even a small amount of additional metal. A total of 5.45 mg/kg arsenic is predicted at the site. About half (2.8 mg As/kg) is from background and the other half (2.64 mg As/kg) will be added by rainwater runoff from the overhead structure. Chromium losses from CCA-C treated wood have always been low as long as the wood passes the Chromotropic Acid Test (a requirement of the CCA-C BMP), and should not appreciably alter total chromium at the site.

Model Table 11. Dissolved contaminants in the upper 20 cm of the water during a storm event

Metal accumulation in sediments is a decades-long process that is dependent on annual rainfall—not the distribution of that rainfall in time. However, water column concentrations of contaminants should be expected as the input of contaminants in rainwater runoff increases during short storm events. Long-lasting storms (days to weeks long) result in increases in current speeds as the volume of water increases. Table 9.24 describes the Model Table 11 output associated with short-term storm events that do not appreciably increase the dilution water flowing in a stream or river. The output assumes that the volume of dilution water remains constant, resulting in constant current speed, channel depth, and width. In this example, the project described in Table 9.16 is subjected to a storm that increases rainfall from the steady-state rate of 0.313 cm/d to 2.5 cm/h (User Entry 28). The storm is predicted to last for 1.5 h (User Entry 29). Rainwater runoff during the storm is assumed to have the same contaminant concentrations described in Model Table 5. However, the increased runoff volume will increase the total contaminant loading, resulting in increased predictions. Under steady-state rainfall, the copper concentration of the receiving water is predicted to be 0.049 µg Cu/L (Table 9.20), but the level during the storm will increase to 0.394 µg/L.

9.7 ASSESSING PROJECTS INVOLVING MULTIPLE TYPES OF PRESERVATIVES

Several new preservatives are intended only for above-ground uses and may be used for decks and handrails on

Table 9.24 Predicted dissolved contaminants in water during a storm event with an intensity of 2.5 cm/h lasting for 1.5 h (Model Table 11).

Contaminant	Concentration (µg/L)
Copper	0.39428
Arsenic	0.34312
Chromium	0.04435
Zinc	0.00000
TEB	0.00000
PROP	0.00000
IMID	0.00000
Creosote (PAH)	0.00000
PENTA	0.00000
DDAC	0.00000

structures that use another type of pressure-treated wood for water- or ground contact. The model examines only one preservative at a time. The project must be partitioned when more than one preservative is employed and separate runs made for each preservative. If the above-water and in-water preservatives contain the same active ingredients, then users will have to manually add the predictions for the active ingredients to obtain an overall prediction. For instance, a project may use CCA-C treated piling and timbers for construction below the waterline and another copper-containing preservative for above-water construction. In that case, one model run should be made for the CCA-C preserved wood that is in and above the water and a second run should be made to predict copper concentrations in rainwater runoff from the material preserved with the second preservative. The contributions of copper from each of the two preservatives must then be added in order to predict the increase above background level associated with the project.

9.8 EXPECTATIONS AND UNCERTAINTIES

One way to look at realistic expectations for this model is to compare it with the results from meteorological models. Hundreds of millions of dollars have been spent to develop very sophisticated atmospheric models designed to predict the weather. Those models do a good job of alerting society to oncoming storms, but they don't function well for predicting whether or not it will rain on my farm in a given one- or two-week period. It may rain a mile from the farm and it may be dry here when the weather forecast is for a rainy day in western Washington. When the forecast is for a significant storm, I batten down the hatches and prepare appropriately—and usually that has proven to be wise. However, when it comes to non-event forecasts, I get up in the morning and look outside. Forecasting weather on anything but a large geographic scale and within fairly wide bounds of intensity is still not possible.

The predictions made by any model are only as good as the inputs used to run the model. Users are encouraged to provide high-quality, conservatively developed data in the User Input section. If water hardness varies significantly as a function of season, then ensure that the entry is consistent with the season in which construction is anticipated. In some cases, it would be wise to make several model runs to mimic anticipated environmental conditions. For instance, if construction is planned in August when predicted pH is 6.5, hardness is 125 mg CaCO₃, and current speed is 5.5 cm/s, make one run for those conditions and

set User Input 39 to $d = 0.5$ or 2.0 . Then conduct another run for conditions expected in June of the next year when pH is 5.6, hardness is 35 mg CaCO_3 , and current speeds are 11.2 cm/s . User Input 39 would then be set to $\sim 180 \text{ d}$ and compared against both the acute and chronic WQC. Once the project is defined in the user inputs, it takes only a few minutes to assess each of a variety of possible environmental conditions. The point is that users are encouraged to provide accurate inputs and to use the model to assess a suite of expected environmental conditions. Users are encouraged to be conservative on behalf of the environment. However, the model can be abused with User Inputs that are outside reasonable expectations for the environment being considered.

This model was designed as a risk-assessment tool to help alert project proponents and permit writers when a project has a potential to cause environmental harm on a site-, project-, and preservative-specific basis. It is unrealistic to expect the model to predict precise sediment or water column concentrations of a contaminant at some point in time. The assumptions used in building the model are intentionally conservative from an environmental protection point of view. For instance:

Factors that may cause model predictions to be too high

- Evaluation of real-world projects indicates that contaminants are generally mixed deeper in sediments than 2.0 cm , reducing observed concentrations below predictions.
- It is unlikely that contaminants will remain at their initial site of deposition for a 35-y lifespan. It is more likely that storm events or seasonal high flows in streams will resuspend sediments and contaminants, moving them farther offshore or downstream and reducing their concentrations below those predicted by the model. The accretion of new sediment in depositional environments will also reduce sediment concentrations below predictions.
- Projects are rarely constructed in half a day, and evaluations that assume all of the treated wood is in place on $d 0.5$ will likely overestimate the actual maximum dissolved concentrations that might be observed.
- The model assumes that it is raining on the day of construction. Most (but not all) preservative loss rates decline exponentially with time. Assuming that the first flush of rainwater occurs on the same day that all of the pressure-treated wood is installed—so that initial loss rates from rainwater-exposed and immersed wood occurs at the same time—is possible, but unlikely. It is more likely that the first flush of treated wood members will happen over a period of time as the wood is put in place in the project. Upon completion, some of the treated wood will have been in place for a week or more, whereas only treated wood members installed on the last day of construction will be in a first-flush stage of leaching.
- Depending on current speeds and water course or shoreline geomorphology, turbulent mixing of contaminants is highly likely. This will increase both the horizontal dispersion of contaminants and the vertical distribution of contaminants in rainwater. The model assumes laminar flows with no turbulent mixing, which may result in significantly higher predicted concentrations than are actually observed.
- The model assumes that metals are adsorbed to clay particles rather than to dissolved organic or inorganic molecules. Clay is far heavier than a molecule of humic acid or a hydroxyl ion, and the clay will settle much closer to the project—leading to higher predicted sediment concentrations than will likely occur for metals adsorbed to other material. The deposition field for sediment assessments is defined, in part, by V_{model}/V_v , making it sensitive to the assigned settling speed of contaminants. The model was originally based on a silt-settling speed for metals and pentachlorophenol, but that assumption has been modified over the years to bring predictions closer to the results of field trials.
- The model uses the EPA hardness-based WQC. This WQC assumes that carbonate ions bind with copper, zinc, chromium, or arsenic to reduce their bioavailability and toxicity. In fact, there are many particulate and dissolved organic and inorganic molecules that bind metals and organic contaminants. HydroQual's Biotic Ligand Model (BLM) provides a more accurate assessment of the proportion of dissolved copper that is in the most toxic cupric ion (Cu^{2+}) state. However, use of the BLM requires a significant amount of expensive chemical analysis and is recommended only when a project's biological effects are problematic.

- The catabolism of some organic contaminants (like PAH) is facilitated by the presence of co-metabolites supporting PAH degrading microorganisms. Creosote-treated piling in the Pacific Northwest typically becomes heavily fouled with abundant and diverse communities of invertebrates within a year or two of construction. These communities create an organic film around the immersed sections of the piling that binds PAH migrating from the wood and provides a ready source of co-metabolites that facilitate breakdown of the trapped PAH—interdicting its path to the sediments.
- The determination of the surface area of rainwater-exposed wood guided by Figure 9.3 is very conservative. The model assumes that all of the potentially wetted surfaces are exposed horizontally to rainfall. In fact, only a portion of the rainwater-exposed wood surface is horizontal. This significantly increases the amount of rainwater runoff predicted by the model. The model could have been constructed with the assumption that only the area subsumed by the project's width and length was receiving rain. That would have more accurately described the predicted volume of rainwater runoff. However, no data describing the concentration of contaminants in rainwater runoff from complex geometries including vertical, horizontal, and diagonal surfaces was available. To be conservative, all of the potentially rainwater-wetted surfaces were assumed to be horizontally exposed to rain. This could lead to significant overestimates of the contaminant load from rainwater. However, the assumption makes the model more manageable by eliminating the need to include rainwater contact time with the treated wood and by obviating the need to understand the saturation constants for contaminants in rainwater runoff.

Factors that may cause the model to underestimate concentrations and/or biological effects

- When these models were first developed, information describing the concentration of wood-preserved active ingredients in rainwater runoff was not available. The models were designed to predict environmental concentrations based solely on the contribution from immersed wood. The Proximity Models were designed to predict contaminant concentrations from piling as a

function of distance. They predicted higher concentrations immediately adjacent to the piling, with decreased contamination away from the piling. Pressure-treated wood projects are sometimes large and contain hundreds of treated wood members located at various elevations above the sediments and in the overhead portions of the structure. Rainwater runoff studies were begun a decade ago and the results of these several-year-long studies provide a basis for including rainwater runoff contributions to the assessment. However, rainwater runoff is characterized as a diffuse source that is not amenable to the proximity model approach. For these reasons, the box model used herein has been adopted because it more easily enables assessments of all of the inputs from a structure. However, the box model does not account for the fact that concentrations of contaminants will be higher close to those portions of the structure that are buried in sediments. The box model loses the ability to discriminate predicted changes in concentration on a small scale. If users are concerned in this respect, the proximity models can be downloaded from WWPIInstitute.org for a closer examination of this issue. Despite this limitation, the box model presented in this chapter does provide good agreement with field data from real-world treated-wood projects.

- The model does not account for abraded treated wood, which would increase the apparent sediment concentration of a wood preservative. However, wood chips and splinters will leach preservative somewhat like the commodity; not all of the preservative in a chip will be released at one time. Moreover, unless treated wood structures are prevented from significant abrasion, as suggested by Best Management Practices, they may contribute more preservative to the environment than predicted by the models.
- The models assume that all of the pressure-treated wood used in a project has been produced using BMPs. Model predictions are not valid for non-BMP products.
- The models assume that conditions during construction are accurately depicted at the time environmental measurements are made in support of the required User Entries. Water flow changes

dramatically with season in some streams and rivers. If current speeds and channel profiles are made during the rainy season and construction occurs during the dry season, then model predictions may underestimate actual concentrations because of the reduced dilution water. One way to overcome this is to use stream gauging data to predict current speeds and water depths during the anticipated time of construction.

9.9 MODEL VERIFICATION STUDIES

In the absence of detailed background concentrations of contaminants (on a scale of a meter or less in sediments), assessments conducted in industrial or urban areas, where there are multiple sources of contaminants, cannot be used to evaluate the predictions made using this model because the sources of contaminants are widespread and spatially variable. Goyette and Brooks (1998, 2000) and Brooks et al. (2006c) assessed the proximity model based CREORISK approach (Brooks 1995) for predicting sediment concentrations at the Sooke Basin site (see Figure 9.1). Brooks (2005a) conducted three additional model-verification studies during the development of the Timber Bridge Model for the U.S. Forest Service. These four verification studies are reviewed below and are re-assessed using the model presented herein. Other model-verification studies have been completed. However, all have resulted in predictions that were higher than observed concentrations.

9.9.1 Sooke Basin

In 1994, Environment Canada commissioned the Creosote Evaluation Study conducted by Goyette and Brooks (1998, 2000; Brooks et al. 2006c). Pim Head in Sooke Basin was chosen after screening 17 sites in British Columbia. Three dolphins consisting of six piling each were driven into the pristine sediments of the basin. One dolphin was constructed of BMP-produced piling, the second of 8-y-old piling pulled by the Port of Vancouver for the project, and the third (the Mechanical Control dolphin) of untreated Douglas-fir piling. Figure 9.13 shows the BMP dolphin in 2005, 10 y after construction. The inset shows an example of the abundant and diverse epibenthic community that developed after the first 4 y of immersion. Sediment PAH concentrations were compared with proximity model predictions and the predictions always exceeded the observed concentrations.



Figure 9.13 Sooke Basin dolphins constructed in support of Environment Canada's creosote evaluation study.

9.9.1.1 User inputs

Table 9.25 describes the user input sections of the current model used for a new evaluation. The BMP pilings were overtreated to 432.8 kg/m^3 , which was nearly twice the required retention of 256 kg/m^3 . The base of the dolphin was measured at 410 cm wide orthogonal to the currents. The current vector at Pim Head was west southwest (258°M) at an average speed of 1.89 cm/s with little evidence of harmonic motion. Based on periodic measurements, water temperature was found to average 11.4°C and the salinity was 28.3 PSU. Annual rainfall in Sooke Basin is 95 cm/y . The sediments contained 0.92% TOC and the background concentration of PAH was $0.027 \text{ mg } \Sigma \text{PAH/kg}$ dry sediment. Initially, the redox potential discontinuity (RPD) was observed at 3.0 cm depth. A copy of the model output is provided in Table 9.26.

Hydrophobic PAH are not expected to dissolve in the water column. The model predicts a total of $0.15 \text{ } \mu\text{g } \Sigma \text{PAH/L}$. Dissolved PAH was measured during the Sooke Basin study using semi-permeable membrane devices (SPMD), which indicated total concentrations of $\sim 20 \text{ ng/L}$ with no significant increase within 15 cm of the dolphins. Model predictions were low, but exceeded the actual concentrations measured. Also note that the ΣTU at the predicted con-

Table 9.25 User inputs for the Sooke Basin Creosote Study model verification.

Piling	
1. Piling retention (kg/m ³)	432.8
2. Number of piling in a row paralleling the currents	2.4
3. Number of piling bents	2.4
4. Average piling radius (cm)	15
5. Distance between piling in a row paralleling currents (cm)	120
6. Receiving water channel width (cm)	100000
Immersed lumber	
7. Surface area of sawn lumber that is immersed at mean high water (MHW) in cm ²	0
8. Immersed Lumber Retention (kg/m ³)	0
Rainwater exposed lumber and piling	
9. Surface area of sawn lumber and piling above MHW exposed to rainfall (cm ²)	141,372
10. Above water lumber retention (kg/m ³)	432.8
Box dimensions	
11. Box width or width of a stream channel under an overhead structure (cm)	410
12. Box length paralleling the currents (cm)	240
13. Mean water depth in the box (cm) (measured as the depth at MHW in tidal systems)	810
14. Maximum tidal current speed or V_{harmonic} (cm/s)	0
15. Steady State Current Speed or V_{ss} (cm/s)	1.89
16. Model speed or V_{model} (cm/s)	1.89
Water characteristics	
17. Average annual water temperature (°C)	11.4
18. Freshwater pH	7.8
19. Water hardness (mg CaCO ₃ /L)	100.0
20. Salinity (PSU or parts per thousand)	28.3
21. Background dissolved copper concentration (µg Cu/L)	0.0
22. Background dissolved arsenic concentration (µg As/L)	0.0
23. Background dissolved chromium concentration (µg Cr/L)	0.0
24. Background dissolved zinc concentration (µg Zn/L)	0.0
25. Background dissolved penta concentration (µg penta/L)	0.0
Rainfall characteristics	
26. Annual rainfall (cm/y)	95.0
27. Steady state rainfall rate (cm/d)	0.260
28. Storm event (cm/h)	0
29. Duration of the storm event (h)	0
Sediment characteristics	
30. Sediment total organic carbon (%)	0.92
31. Sediment density (g/cm ³)	2.6
32. Sediment redox potential (mV) for penta or depth of the RPD for creosote (cm)	2
33. Background sediment copper concentration (mg/kg)	0
34. Background sediment arsenic concentration (mg/kg)	0
35. Background sediment chromium concentration (mg/kg)	0
36. Background sediment zinc concentration (mg/kg)	0
37. Background sediment penta concentration (mg/kg dry)	0
38. Background sediment PAH concentration (mg/kg)	0.027
Other	
39. Days since construction for determining contaminant concentrations in water	0.5
40. Settling velocity (0.05 cm/s for creosote and 0.005 cm/s for other contaminants)	0.05
41. Anticipated lifespan of the project; default is 35 y with a minimum of 10 y	35
42. Angular increase in width of the sediment deposition zone downstream and offshore	0.95
43. Channel width (cm)	100000

centrations of PAH is 0.019, or 10 times less than the recommended maximum of 0.186 TU. Figure 9.14 describes the history of Σ PAH accumulation in sediments. At the end of the first year, sediments were aerobic and the maximum Σ PAH observed was 18 mg Σ PAH/kg dry sediment. At the end of 3 y, sediments within a few meters of the dolphins had reduced redox potential due to organic enrichment from the epifaunal community that took up residence on the piling after the first year. At the end of 10 y, sediments throughout the PIM Head area of Sooke Basin had become anaerobic, with heavy patches of *Beggiatoa* to distances of at least 200 m from all three dolphins. Redox potentials were generally negative, averaging -157.1 mV within 3.0 cm of the BMP dolphin, where free sulfide concentrations up to 1,428 µM were measured. Brooks et al. (2006c) attributed this organic enrichment to unknown environmental factors, possibly including a known major fish kill at a nearby salmon farm and/or input from the Sooke River. Redox potential was reduced between 1999 and 2005, increasing the half-life of sedimented PAH.

The model assumes that contaminants are retained in the upper 2.0 cm of sediment and that there is no accretion of new sediment to dilute the contaminants. During the 2005 evaluation (10 y after construction), sediments in Sooke Basin cores were sectioned at 3.0 cm over the 21 cm core depth and analyzed (N = 39 total) for PAH along with sediment grain size (SGS). The SGS analyses indicated significant accumulations of mussel shell and barnacle tests to depths of 15 cm. Sediment Σ PAH concentrations were highest at depths of 0.0 to 12.0 cm depths, but remained elevated to 15 cm depth. When the results for distances \leq 2.5 m were summed over all sediment core depths to 15 cm, the total accumulation was 7.85 mg Σ PAH, giving an average concentration in the contaminated zone of 17.7 mg Σ PAH/kg. When all of the accumulated PAH is confined in the upper 2.0 cm of the sediments, the equivalent concentration would be 132.6 mg Σ PAH/kg.

The model presented herein predicted a maximum Σ PAH concentration of 25.2 mg Σ PAH/kg, when observed concentrations were 16 to 18 mg Σ PAH/kg in aerobic sediments. Running the model with the RPD equal to 0.0 cm (i.e., $<$ -100 mV eH) predicts a maximum accumulation of 131.7 mg Σ PAH/kg dry sediment, which was close to the 132.6 mg Σ PAH/kg accumulation calculated based on measured concentrations in the core. This analysis supports the previous assertion that creosote-treated wood should not be used in environments having anaerobic sediments.

Table 9.26 Model output for the Sooke Basin Project.

Model Table 7. Dissolved contaminant concentrations leaving the box ($\mu\text{g/L}$)

Contaminant	Background	From immersed	From rain	Total	Acute	Chronic
					Benchmark	Benchmark or ΣTU for PAH
Copper	0.00				4.800	3.100
Arsenic	0.00				69.00	36.00
Chromium	0.00				110.00	50.00
Zinc	0.80			0.80	90.00	81.00
TEB	0.00				MA	MC
PROP	0.00				MA	MC
IMID	0.00				MA	MC
Creosote (PAH)	0.00	0.1515	0.00002	0.1516	$\Sigma\text{TU} < 0.186$	0.019
PENTA	0.00				13.00	7.90
DDAC	0.00				MA	MC

Box Model for predicting sediment accumulation of contaminants from pressure treated wood (mg/kg)

Model Table 8. Predictions of the area of sediment contamination (cm^2)

	Minimum	Maximum	Area (cm^2)
Effective width of sediment footprint (cm)	240	750.4	
Distribution downcurrent for rainwater contaminants (cm)	29862	30,858	493,200
Distribution downcurrent for contaminants from immersed wood (cm)	0.0	30,858	15,280,275
Maximum width of the sediment footprint (cm)	240	750.4	

Model Table 9. Surface areas (cm^2) of pressure treated wood for determining total contaminant loading

Immersed treated wood (cm^2)	439,500
Rainwater exposed wood (cm^2)	141,372

Model Table 10. Maximum contaminant sediment concentrations (mg/kg)

Contaminant	Background	From immersed	From rain	Total (mg/kg)	Sediment quality criterion (mg/kg)
Copper	0.00				390.000
Arsenic	0.00				57.000
Chromium	0.00				260.000
Zinc	0.00				410.000
TEB	0.00				MS
PROP	0.00				MS
IMID	0.00				MS
Creosote (PAH)	0.03	24.27	0.86	25.16	12.236
PENTA	0.00				0.360
DDAC	0.00				MS

9.9.1.2 Observed sediment concentration

It should also be noted from Figure 9.14, that significant increases in sedimented PAH occurred only at distances < 7.5 m. The contaminated area shrank in 2005 because significant organic loading from the epifaunal community reduced oxygen tension in the sediments, but only within a few meters of the dolphin. At about 5 m from the dolphin,

sediment concentrations decreased over time (as predicted by the model) because microbial catabolism in the marginally oxic sediments exceeded the delivery of new PAH lost from the piling.

The model predicted increased sediment concentrations to distances of 30,858 cm or 309 m at this site. With the exception of one sample (with a concentration of 1.05

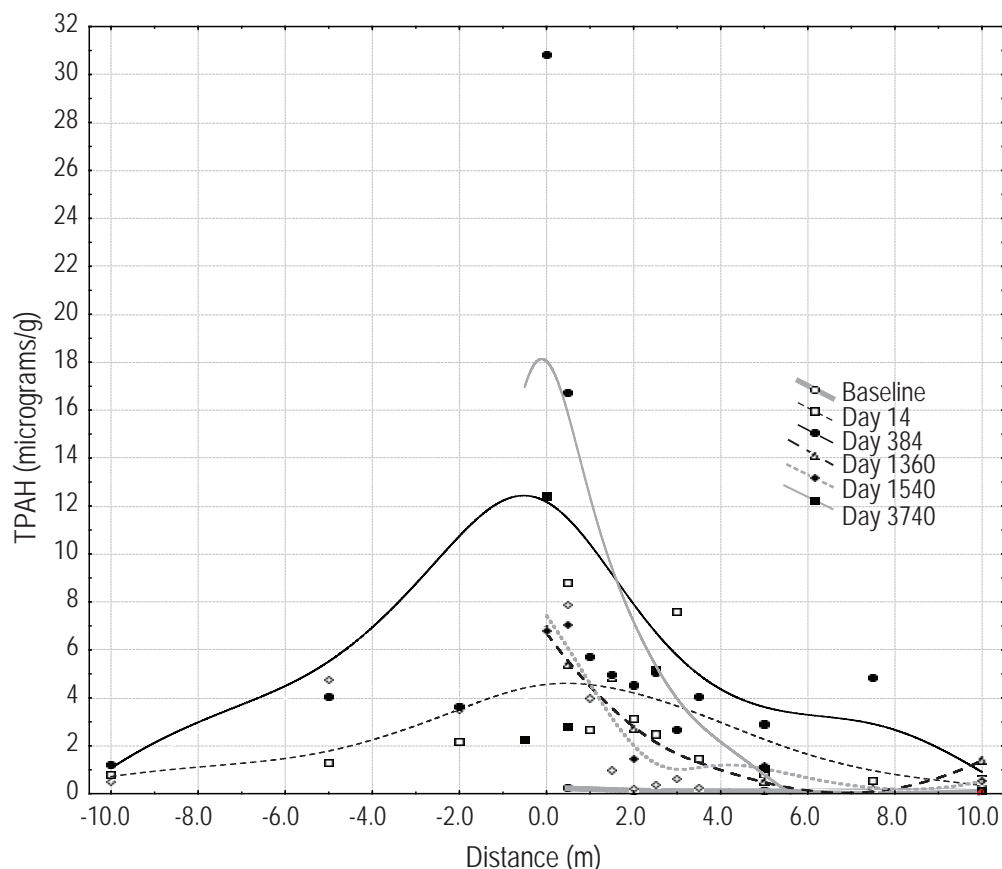


Figure 9.14 Trends in observed Σ PAH concentrations in surficial sediments at the Sooke Basin BMP dolphin along upcurrent (left) and downcurrent (right) transects as a function of time following construction. TPAH (micrograms/g) = distance weighted least squares.

mg Σ PAH/kg), increases >0.5 mg Σ PAH/kg dry sediment were not observed beyond 2.5 m from the BMP dolphin in 2005, suggesting that the model does a reasonable job of predicting the maximum PAH that will be observed near a site; however, it significantly over-predicts the total accumulation of PAH in sediments. As noted previously, the model is designed to use worst-case assumptions, which appear satisfactory with respect to identifying the maximum risks, but may predict more PAH than will be observed at distances greater than a few meters from the structure.

9.9.1.3 Biological response

The Sooke Basin site was chosen in part because the dense cluster of piling and very slow currents were expected to result in sediment accumulations of PAH that would exceed SQC—allowing the researchers to observe effects in bioassays and in the macrofaunal community. Adverse effects at a distance of 0.5 m from the piling were seen in laboratory bioassays, but not in the macrofaunal community—

likely because much of the sedimented PAH was buried by the biodeposits from the epifaunal community. This kept concentrations in the biologically active zone at or only slightly above effects concentrations. No adverse effects were observed in macrofaunal communities at any distance.

9.9.2 Meadowbrook Creek Bridge

This highway bridge was constructed in 1961 and is load-rated at 38 tons (Figure 9.15). The bridge was first examined on October 15, 2004 and samples were collected on October 18, 2004. The bridge is 671 cm long and spans the creek for a distance of 579 cm. The deck width (curb to curb) is 808 cm and the total width of the bridge is 972 cm. Meadowbrook Creek drains a small watershed dominated by agricultural lands. The stream is heavily impacted by fine-grained sediments and fecal coliform bacteria. Its high nutrient load supports a significant aquatic flora dominated by reed canarygrass (*Phalaris arundinacea* L.). A unit hydrograph was not available for the stream, which



Figure 9.15 Meadowbrook Creek Bridge in Clallam County, Washington, showing the span across the creek and a view of the underside.

Table 9.27 Creosote-treated timber and piling used in construction of the Meadowbrook Creek Bridge in Clallam County, Washington. Dimensions are in centimeters and retention in pcf.

Component	Number	Retention ^a	Thickness or radius	Width	Length or height
Piling	12	192	30.0		157.0
Piling caps	2	128	30.0	35.6	952.5
Stringers	16	128	15.0	55.9	795.0
Bulkheads	14	160	7.6	30.5	1,227.0
Decking	32	128	10.2	30.25	665.5
Stringer blocking	1	128	15.0	30.25	952.5

a. This is an assumed retention based on current AWPA Standards.

appears to flow at <20 cfs. The creosote-treated wood members listed in Table 9.27 were identified during the site evaluation and in plans provided by Clallam County. Table 9.28 describes user inputs for the Timber Bridge Model determined during the site evaluation.

9.9.2.1 Model output

The predicted water column concentration of Σ PAH in the box was 0.091 $\mu\text{g/L}$ and the ΣTU is 0.0123. No adverse effects on biota could be anticipated at this low concentration of dissolved Σ PAH. Predicted sediment concentrations of Σ PAH are summarized in Table 9.29. The maximum predicted concentration is 25.33 mg Σ PAH/kg, which is only 67% of the SQS. According to the model, this project likely would not adversely affect the stream's biological resources. However, it should be noted that maximum accumulations are predicted to occur about 2 y after construction and then decline. The Meadowbrook Bridge was 43 y old when this evaluation was made and lower than predicted concentrations of PAH should be anticipated.

9.9.2.2 Observed sediment concentration

A single high sample was collected under the bridge (23.8 mg Σ PAH/kg), which was close to the predicted maximum accumulation of 25.33 mg Σ PAH/kg. The contamination was noted in the field as several small sheens with diameters of 2 to 3 mm, suggesting that the PAH was at least partially in a droplet form. The other two samples from this same location were 2.7 and 0.5 mg Σ PAH/kg, giving a mean at this station of 9.02 mg Σ PAH/kg dry sediment. These three samples were collected 15 cm from the creosote-treated bulkhead on the downcurrent side of the bridge. Except for a single sample containing 8.6 mg Σ PAH/g in sediment collected 457 cm downstream, accumulated PAH appeared to be restricted to an area within 1.37 m of the bridge. The Σ PAH collected at the reference location was uniformly low, varying between 0.13 and 0.16 mg Σ PAH/kg. Taken as a whole, the concentrations present 43 y after construction were much lower than the maximum accumulation predicted by the model, and PAH

Table 9.28 User inputs determined by an examination of plans and site evaluation for Meadowbrook Creek Bridge 8 y after installation.

Piling	
1. Piling retention (kg/m ³)	192
2. Number of piling in a row paralleling the currents	6
3. Number of piling bents	2
4. Average piling radius (cm)	15
5. Distance between piling in a row paralleling currents (cm)	190
6. Receiving water channel width (cm)	579
Immersed lumber	
7. Surface area of sawn lumber that is immersed at mean high water (MHW) (cm ²)	15,545
8. Immersed lumber retention (kg/m ³)	160
Rainwater exposed lumber and piling	
9. Surface area of sawn lumber and piling above MHW exposed to rainfall (cm ²)	166,264
10. Above water lumber retention (kg/m ³)	128
Box dimensions	
11. Box width or width of a stream channel under an overhead structure (cm)	579
12. Box length paralleling the currents (cm)	972
13. Mean water depth in the box (cm) (measured as the depth at MHW in tidal systems)	32.2
14. Maximum tidal current speed or V_{harmonic} (cm/s)	0
15. Steady State Current Speed or V_{ss} (cm/s)	9.0
16. Model speed or V_{model} (cm/s)	9.0
Water characteristics	
17. Average annual water temperature (°C)	10.0
18. Freshwater pH	6.8
19. Water Hardness (mg CaCO ₃ /L)	100.0
20. Salinity (PSU or parts per thousand)	0.0
21. Background dissolved copper concentration (µg Cu/L)	0.0
22. Background dissolved arsenic concentration (µg As/L)	0.0
23. Background dissolved chromium concentration (µg Cr/L)	0.0
24. Background dissolved zinc concentration (µg Zn/L)	0.0
25. Background dissolved penta concentration (µg penta/L)	0.0
Rainfall characteristics	
26. Annual rainfall (cm/y)	83.8
27. Steady State Rainfall rate (cm/d)	0.229
28. Storm event (cm/h)	0
29. Duration of the storm event (h)	0
Sediment characteristics	
30. Sediment total organic carbon (%)	3.7
31. Sediment density (g/cm ³)	2.6
32. Sediment redox potential (mV) for penta or depth of the RPD for creosote (cm)	2
33. Background sediment copper concentration (mg/kg)	0
34. Background sediment arsenic concentration (mg/kg)	0
35. Background sediment chromium concentration (mg/kg)	0
36. Background sediment zinc concentration (mg/kg)	0
37. Background sediment penta concentration (mg/kg dry)	0
38. Background sediment PAH concentration (mg/kg)	0.08
Other	
39. Days since construction for determining contaminant concentrations in water	0.5
40. Settling velocity (0.05 cm/s for creosote and 0.005 cm/s for other contaminants)	0.05
41. Anticipated lifespan of the project. Default is 35 y with a minimum of 10 y	55
42. Angular increase in width of the sediment deposition zone downstream and offshore	4.5

concentrations were restricted to an area much nearer the structure (< 12 m) than the 67-m distance downstream predicted by the model. These results highlight the conservative nature of the predictions.

9.2.2.3 Biological response

A total of 16,980 macrofauna representing 57 taxa were retrieved from the 18 Meadowbrook Creek samples. Consistent with the fine-grained sediments and eutrophic state of the watershed, the community was dominated by oligochaetes (3,997) representing 23.5% of the total. The heavy vegetation (reed canarygrass) hosted a large number (3,765 = 22.2% of the total) of amphipods (*Gammarus* sp.) and isopods (Caecidotea = 1,687 or 9.9%). Most of the remaining taxa were midges or gastropods. The arthropods and gastropods were found on vegetation, whereas the midges were likely to be found in the fine-grained sediments. This is a robust community typical of eutrophic environments in North America. More sensitive taxa, including mayflies (Ephemeroptera) and numerous caddisfly species (Trichoptera) were found in low abundance. The results indicate that the measured physicochemical variables, including those attributable to PAH lost from the creosote-treated wood, did not cause adverse effects in the macrobenthic community.

Meadowbrook Creek summary

This eutrophic stream is highly impacted by agricultural nutrients and the loss of riparian vegetation. As a result, the sediments are dominated by silt and clay and the channel supports a dense floral community dominated by reed canarygrass. The robust macrofaunal community downstream from the bridge and at the upstream reference location is dominated by chironomids, gastropods, and oligochaetes with very few of the more pollution sensitive EPT taxa. Increased concentrations of PAH were observed under and downstream from the bridge, which is constructed of creosote-treated wood, including solid bulkheading on either side of the stream channel. The highest increase was observed 15 cm from the creosote-treated bulkhead. None of the observed PAH concentrations exceeded the biological effects benchmark used in this evaluation, and no adverse biological effects were predicted or observed. The results of modeling this bridge prior to construction predict that it would be unlikely to adversely affect Meadowbrook's biological resources, and 43 years after construction, no evidence of harm was apparent.

Table 9.29 Model output for the Meadowbrook Creek Bridge evaluation.

Table 7. Dissolved contaminant concentrations leaving the box ($\mu\text{g/L}$)

Contaminant	Background	From immersed	From rain	Total	Acute benchmark	Chronic benchmark or $\sum\text{TU}$ for PAH
Copper	0.00				4.800	3.100
Arsenic	0.00				69.00	36.00
Chromium	0.00				110.00	50.00
Zinc	0.80			0.80	90.00	81.00
TEB	0.00				MA	MC
PROP	0.00				MA	MC
IMID	0.00				MA	MC
Creosote (PAH)	0.00	0.0914	0.00002	0.091	$\sum\text{TU}<0.186$	0.012
PENTA	0.00				13.00	7.90
DDAC	0.00				MA	MC

Box Model for predicting sediment accumulation of contaminants from pressure-treated wood (mg/kg)

Table 8. Predictions of the area of sediment contamination (cm^2)

	Minimum	Maximum	Area (cm^2)
Effective width of sediment footprint (cm)	579	579	
Distribution downcurrent for rainwater contaminants (cm)	2,196	6,768	493,200
Distribution downcurrent for contaminants from immersed wood (cm)	0.0	6,768	15,280,275
Maximum width of the sediment footprint (cm)	579	1,113	

Table 9. Surface areas (cm^2) of pressure treated wood for determining total contaminant loading

Immersed treated wood (cm^2)	51,944
Rainwater exposed wood (cm^2)	166,264

Table 10. Maximum contaminant sediment concentrations (mg/kg)

Contaminant	Background	From immersed	From rain	Total (mg/kg)	Sediment quality criterion (mg/kg)
Copper	0.00				390.000
Arsenic	0.00				57.000
Chromium	0.00				260.000
Zinc	0.00				410.000
TEB	0.00				MS
PROP	0.00				MS
IMID	0.00				MS
Creosote (PAH)	0.03	24.99	0.26	25.33	37.6
PENTA	0.00				0.360
DDAC	0.00				MS

9.9.3 Seabeck Lagoon

This bridge (Figure 9.16) crosses a natural saltwater lagoon that was partially isolated from Hood Canal, Washington, during the 1880s, when the lagoon was used for log storage in support of a local sawmill. Seawater enters the lagoon through a culvert and tide gate located approximately 38 m south of the bridge. The bridge was evaluated on October 19, 2004. Seabeck Lagoon is a shallow marine pond. The privately owned bridge was originally constructed in the 1880s. It has been well maintained, and underwent renovation in 1989.

9.9.3.1 User Inputs

The bridge is 503 cm wide and 5,593 cm long. Plans were not available for the bridge; the materials list provided in Table 9.30 was based on measurements made during the site evaluation. Sawn ACZA-treated decking boards were spaced about 1.0 cm apart, resulting in wetting of all of the above-water creosote-treated wood. User inputs for this evaluation are provided in Table 9.31.

9.9.3.2 Model Output

Table 9.32 describes water dilution factors and predicted water column concentrations of Σ PAH on the first day after construction at Seabrook Lagoon. The model output predicts an initial (d 0.5) PAH migration rate of $20.2 \mu\text{g}/\text{cm}^2\text{-d}$ from the immersed, creosote-treated wood portions of the structure. After 15 y (i.e., since the 1989 renovation), the loss rate is predicted to be $4.49 \mu\text{g}/\text{cm}^2\text{-d}$. The predicted concentration of Σ PAH in rainwater runoff on the first day after construction was $0.719 \mu\text{g} \Sigma\text{PAH}/\text{L}$. At the time of the evaluation, the predicted rainwater concentration was $0.302 \mu\text{g} \Sigma\text{PAH}/\text{L}$. The model predicts a concentration of $0.091 \mu\text{g} \Sigma\text{PAH}/\text{L}$ from the immersed sections of the bridge and $< 0.000 \mu\text{g} \Sigma\text{PAH}/\text{L}$ from the overhead structure, giving a total of $0.091 \mu\text{g} \Sigma\text{PAH}/\text{L}$. The resulting $\Sigma\text{TU} = 0.015$, which is 8% of the maximum recommended value of 0.186. No biological effects would be expected in the box at concentrations this low.

Predicted sediment concentrations of PAH are provided in Table 9.33. The minimum and maximum effective



Figure 9.16 Seabeck Lagoon bridge, located in Seabeck, Washington, on Hood Canal.

Table 9.30 List of materials used in the construction of the Seabeck Lagoon Bridge.

Component	Preservative type	Dimension	Number	Surface area (cm ²)
Piling	Creosote	Class A (30 cm diameter)	30	Above water = 430,901
Bent caps	Creosote	25.4 x 30.48 x 487.7 cm	10	545,054
Longitudinal stringers	Creosote	10.2 x 30.48 x 5,593.1 cm	6	2,730,328
Wheel guards	Creosote	30.48 cm dia. x 5,593.1 cm long	2	1,071,143
Wheel guard blocking	Creosote	20.32 x 20.32 x 30 cm	60	146,304
Total surface area (cm ²) of creosote-treated wood exposed to rainfall				4,923,730
Decking	ACZA	10.2 x 30.48 x 487.7 cm	184	7,300,986

Table 9.31 User inputs determined during a site evaluation of the Seabrook Lagoon bridge conducted on October 19, 2004.

Piling	
1. Piling retention (kg/m ³)	321
2. Number of piling in a row paralleling the currents	3
3. Number of piling bents	10
4. Average piling radius (cm)	15
5. Distance between piling in a row paralleling currents (cm)	240
6. Receiving water channel width (cm)	5,593
Immersed lumber	
7. Surface area of sawn lumber that is immersed at mean high water (MHW) (cm ²)	0
8. Immersed lumber retention (kg/m ³)	160
Rainwater exposed lumber and piling	
9. Surface area of sawn lumber and piling above MHW exposed to rainfall (cm ²)	4,923,730
10. Above water lumber retention (kg/m ³)	128
Box dimensions	
11. Box width or width of a stream channel under an overhead structure (cm)	5,593
12. Box length paralleling the currents (cm)	503
13. Mean water depth in the box (cm) (measured as the depth at MHW in tidal systems)	45.3
14. Maximum tidal current speed or V_{harmonic} (cm/s)	14.1
15. Steady state current speed or V_{ss} (cm/s)	
16. Model speed or V_{model} (cm/s)	9.02
Water characteristics	
17. Average annual water temperature (°C)	13.0
18. Freshwater pH	7.8
19. Water Hardness (mg CaCO ₃ /L)	150.0
20. Salinity (PSU or parts per thousand)	22.9
21. Background dissolved copper concentration (µg Cu/L)	0.0
22. Background dissolved arsenic concentration (µg As/L)	0.0
23. Background dissolved chromium concentration (µg Cr/L)	0.0
24. Background dissolved zinc concentration (µg Zn/L)	0.0
25. Background dissolved penta concentration (µg penta/L)	0.0
Rainfall characteristics	
26. Annual rainfall (cm/y)	152
27. Steady state rainfall rate (cm/d)	0.416
28. Storm event (cm/h)	0
29. Duration of the storm event (h)	0
Sediment characteristics	
30. Sediment total organic carbon (%)	2.2
31. Sediment density (g/cm ³)	2.6
32. Sediment redox potential (mV) for penta or depth of the RPD for creosote (cm)	4
33. Background sediment copper concentration (mg/kg)	0
34. Background sediment arsenic concentration (mg/kg)	0
35. Background sediment chromium concentration (mg/kg)	0
36. Background sediment zinc concentration (mg/kg)	0
37. Background sediment penta concentration (mg/kg dry)	0
38. Background sediment PAH concentration (mg/kg)	0.11
Other	
39. Days since construction for determining contaminant concentrations in water	0.5
40. Settling velocity (0.05 cm/s for creosote and 0.005 cm/s for other contaminants)	0.05
41. Anticipated lifespan of the project. Default is 35 y with a minimum of 10 y	55
42. Angular increase in width of the sediment deposition zone downstream and offshore	4.51
43. Channel width (cm)	5593

contaminated-sediment width is the width of the channel or 5,593 cm. Because bridge width equals to the channel width, there is no angular increase in the area of contaminated sediments. However, because the water is relatively shallow, contaminants are distributed from the up-current edge of the structure downcurrent a distance of 86.8 m. The very long bridge results in a large area of contamination (2,300 m² for contaminants in rainwater and 4,854 m² for contaminants from the immersed portions of the bridge).

The bridge's length and well-oxygenated sediments (RPD > 4.0 cm and eH = 164.9 ± 34.9 mV) result in low predicted maximum sediment accumulations of 1.9 mg ΣPAH/kg from immersed portions of the structure and 0.65 mg ΣPAH/kg for above-water areas receiving precipitation. When the background concentration of 0.11 mg ΣPAH/kg is added, the total maximum sediment accumulation within the box is predicted to be 2.66 mg ΣPAH/kg. This value is less than 10% of the SQC in these 2.2% TOC sediments. No macrofaunal effects are anticipated at this low concentration. Note that the sediment proximity model used by Brooks (2005a) predicted a maximum sediment concentration of 2.87 mg ΣPAH/kg within 15 cm of the piling, with an increase to 6.6 mg ΣPAH/kg at 46 to 82 m from the upstream dripline associated with rainwater runoff. However, that assessment assumed that the bridge decking, covering 7,300,986 cm², was originally treated with creosote rather than ACZA. The point is that the proximity model for immersed treated wood and this box model gave similar results for the immersed wood (Table 9.33).

9.9.3.3 Observed sediment concentration

The results for the sum of all 18 PAH species identified in the Seabrook Lagoon analysis are summarized in Figure 9.17. Three of the observed ΣPAH concentrations exceeded those predicted by the model. However, the differences are not large (i.e., < 1.5 µg/g), except the value of 3.87 µg/g observed 3.0 m south of the bridge. Several hypotheses can be invoked to explain the higher-than-predicted concentrations, including uneven distribution and migration of creosote solution (bleeding). The most likely is that the model assumes a uniform distribution of ΣPAH within the box, which extends well beyond the limits of this assessment. The average ΣPAH concentration observed at all sampling stations was 1.32 ± 0.61 mg/kg (N = 18), which is about half of that predicted by the model.

Table 9.32 Model output describing dilution water volume factors used in the computations and predicted water column concentrations of Σ PAH on the first day of exposure.

Model Table 6. Dilution Water Volume Factors

Volume of rainwater runoff from pressure treated wood (L/d)	2,049.03
Dilution water passing through the box with steady state currents (L/d)	197,540,364
Dilution water in the box within 1/2 hour of slack tide (L)	904,970
Rainwater dilution (20 cm deep) water passing through the box with steady state currents (L/day)	87,214,289
Rainwater dilution (20 cm deep within 1/2 hour either side of slack tide (L)	399,545

Model Table 7. Dissolved contaminant concentrations leaving the box ($\mu\text{g/L}$)

Contaminant	Background	From immersed	From rain	Total	Acute benchmark	Chronic benchmark or Σ TU for PAH
Copper	0.00				4.800	3.100
Arsenic	0.00				69.00	36.00
Chromium	0.00				110.00	50.00
Zinc	0.80			0.80	90.00	81.00
TEB	0.00				MA	MC
PROP	0.00				MA	MC
IMID	0.00				MA	MC
Creosote (PAH)	0.00	0.0914	0.00002	0.0914	Σ TU<0.186	0.015
PENTA	0.00				13.00	7.90
DDAC	0.00				MA	MC

Table 9.33 Model output predicting sediment accumulation of Σ PAH in Seabeck Lagoon.

Box Model for predicting sediment accumulation of contaminants from pressure treated wood (mg/kg)

Model Table 8. Predictions of the area of sediment contamination (cm^2)

	Minimum	Maximum	Area (cm^2)
Effective width of sediment footprint (cm)	5,593	5,593	
Distribution downcurrent for rainwater contaminants (cm)	4,566	8,679	23,001,772
Distribution downcurrent for contaminants from immersed wood (cm)	0.0	8,679	48,540,215
Maximum width of the sediment footprint (cm)	5,593	6,279.7	

Model Table 9. Surface areas (cm^2) of pressure treated wood for determining total contaminant loading

Immersed treated wood (cm^2)	51,944
Rainwater exposed wood (cm^2)	166,264

Model Table 10. Predicted maximum contaminant sediment concentrations (mg/kg)

Contaminant	Background	From immersed	From rain	Total (mg/kg)	Sediment quality criterion (mg/kg)
Copper	0.00				390.000
Arsenic	0.00				57.000
Chromium	0.00				260.000
Zinc	0.00				410.000
TEB	0.00				MS
PROP	0.00				MS
IMID	0.00				MS
Creosote (PAH)	0.08	1.90	0.65	2.66	29.260
PENTA	0.00				0.360
DDAC	0.00				MS

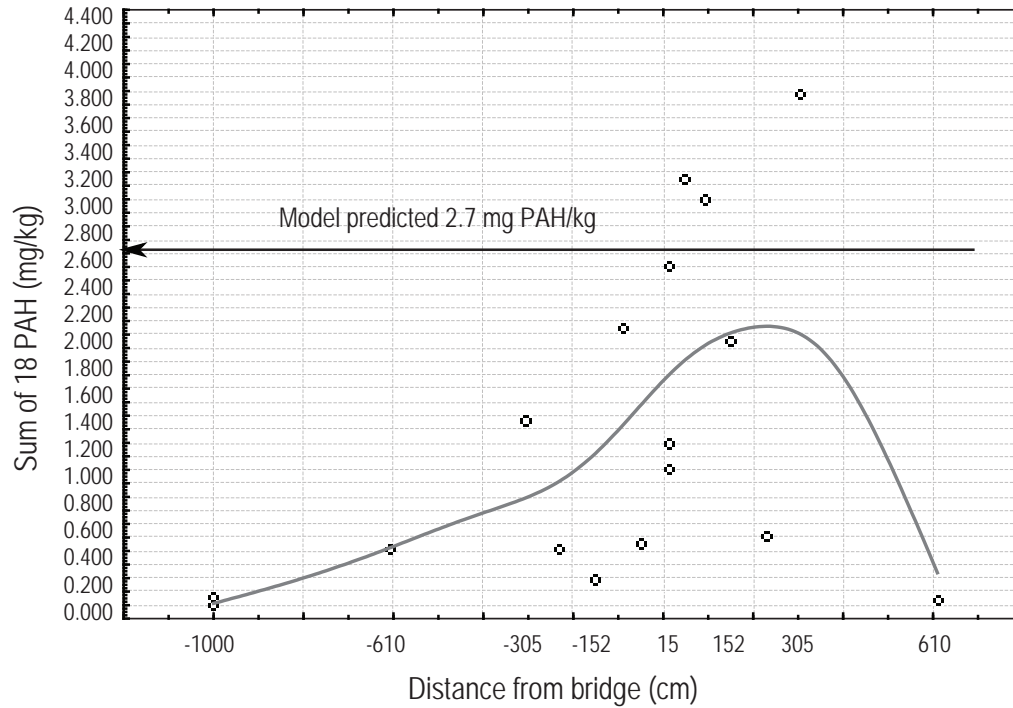


Figure 9.17 Comparison of predicted and observed Σ PAH concentrations (mg Σ PAH/kg dry sediment) in sediments north and south of the Seabeck Lagoon timber bridge. Scatterplot (Model Verification Database 86v*56c). TPAH = Distance Weighted Least Squares.

9.9.3.4 Biological response

In eighteen 0.0225-m² sediment samples from Seabeck Lagoon, 39 taxa and 6,588 macrofaunal organisms were identified. The high organic content in the sediments should effectively bind PAH, reducing bioavailability and, therefore, toxicity. As noted in Table 9.33, the effects benchmark chosen for this assessment was 29.26 μ g Σ PAH/g dry

sediment at the observed TOC. The concentrations of PAH observed at Seabeck Lagoon were not predicted to have any adverse effects on local biota, and none were observed. Typical of other creosote-treated structures assessed in Puget Sound, higher macrofaunal community abundance, species richness, and diversity were observed near the Seabeck Lagoon Bridge than at the reference location.

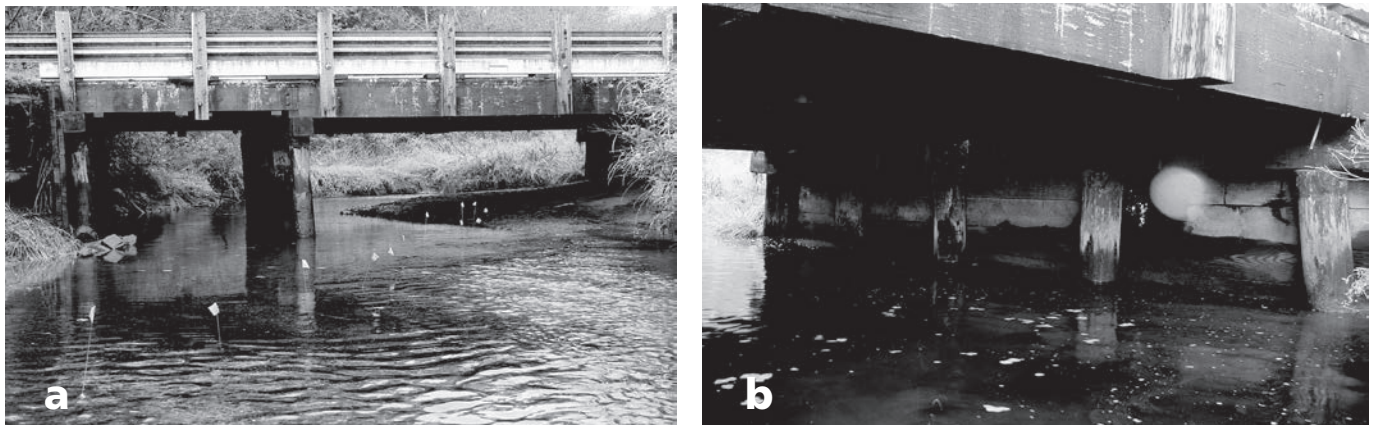


Figure 9.18 Anderson Creek Bridge viewed from (a) downstream looking east and (b) from the south shore looking at the north bulkhead.

9.9.4 Anderson Creek Bridge

This bridge (Figure 9.18) carries Miami Beach Road across Anderson Creek as it flows into Stavis Bay on Hood Canal, WA. The bridge is 843 cm wide and 1,250 cm long. At low tide, the stream channel was 640 cm wide under the bridge and at high tide, water marks on the bulkheads indicated that the channel has been flooded to the length of the bridge (1,250 cm). Anderson Creek is an active salmon spawning stream and numerous redds were observed between the bridge's upstream dripline and the reference location. This site is hydrodynamically complex because Anderson Creek is flooded by seawater creating mixed salinities and slow current speeds during high tides. The stream flows unimpeded to sea at low tide. Visual observations during high tide suggested that surface currents, dominated by lower density fresh water with respect to higher density saltwater, continued to flow seaward—but at significantly reduced speed. Samples were collected during the later stages of an ebb tide when the stream could be waded. The site is reasonably well shaded by riparian vegetation at most times, except at high noon during summer. Substrates at this site were complex, with deep rocky channels where sediment samples could not be collected and sandy substrates along the banks of the stream above the channel at low tide.

The sampling transect was chosen to maintain homogeneity in substrate composition at the upstream reference and downstream sample stations. Substrates along the sampling transect were dominated by gravel (74.5%) and sand (20.5%) with very little silt or clay (5.0%), indicating an erosional environment dominated for much of the time by relatively fast currents, despite their slowing during high tides. Water depths varied between 0 and 81.3 cm across the channel. Water depths along the sampling transect averaged 19.6 cm. The redox potential was variable, ranging from -101.0 to +382.2 mV—a range that may affect infauna but not epifauna. Three water samples indicated that temperature averaged of 9.9°C, salinity was 0.00 PSU, and saturated oxygen was 10.2 mg O₂/L. Three measurements of current speed under the bridge at low tide when the stream was free flowing were 25.5, 21.1, and 20.6 cm/s, giving a mean speed of 22.4 cm/s. The depth of immersion of the bulkheads and pilings at high tide was estimated at 60 cm by taking measurements at slack flood tide and by examining watermarks on the structure.

9.9.4.1 User inputs

Plans for this bridge, constructed in 1951, along with a Bill of Materials were provided by the Kitsap County Department of Public Works (Table 9.34). The exposure assessment to determine the amount of wood exposed to rainfall was based on the site visit. The bulkheads were constructed of a double layer of 3-inch-thick, rough-sawn material. Only the outer surface and top and bottom of the outer layer of creosote-treated bulkhead sheeting were considered wetted by rainfall. User inputs for the model are provided in Table 9.35. An average current speed of 22.4 cm/s was recorded. Tidal current speeds were not measured, but were assumed to be 5 cm/s in opposition to stream flow during flood tide.

9.9.4.2 Model output

The model predicted a PAH migration rate of 26.51 μg ΣPAH/cm²-d from the immersed wood and a rainwater

Table 9.34 Creosote-treated timber and piling used in construction of the Anderson Creek Bridge in Kitsap County, Washington.

Preservative type/ Component	Dimension (cm)	Number	Surface area (cm ²) exposed to rain
Creosote (321 kg/m ³)			
Support piling	Class A (30-cm dia)	15	33,929.2
Wingwall piling	Class A (30-cm dia)	8	45,992.9
Creosote (8 pcf)			
Bent caps	30.48 × 35.6 × 914.4	3	0
Creosote (160 kg/m ³)			
Bulkheads	7.6 × 30.5 × 914.4	50	0
Creosote (128 kg/m ³)			
Longitudinal stringers	10.2 × 40.6 × 365.8	17	0
Longitudinal stringers	15.2 × 55.9 × 853.4	17	121,353.5
Wingwall bulkheads	7.6 × 30.5 × 365.8	101	167,243.8
Top of wingwalls	10.2 × 20.3 × 304.8.0	5	49621.4
Bridging	10.2 × 35.6 × 609.6	1	0
Bridging	10.2 × 55.9 × 609.6	3	0
Spreader beam	5.1 × 15.2 × 853.4	1	0
Rail/post fillers	8.89 × 19.1 × 731.5	1	40,949.4
Stringer splice fillers	5.1 × 40.6 × 121.9	1	0
Stringer splice	10.2 × 40.6 × 243.8	1	0
Stringer blocking	15.2 × 30.5 × 914.4	1	0
Total area exposed above water to rainfall			459,090.2
Untreated			
Decking	10.2 × 30.5 × 853.4	42	0

Table 9.35 User inputs for Anderson Creek determined through an examination of plans and the site evaluation on October 19, 2004.

Piling	
1. Piling retention (kg/m ³)	321
2. Number of piling in a row paralleling the currents	9
3. Number of piling bents	3
4. Average piling radius (cm)	15
5. Distance between piling in a row paralleling currents (cm)	202
6. Receiving water channel width (cm)	1,250
Immersed lumber	
7. Surface area of sawn lumber that is immersed at mean high water (MHW) (cm ²)	25,301
8. Immersed lumber retention (kg/m ³)	160
Rainwater exposed lumber and piling	
9. Surface area of sawn lumber and piling above MHW exposed to rainfall (cm ²)	459,090
10. Above water lumber retention (kg/m ³)	128
Box dimensions	
11. Box width or width of a stream channel under an overhead structure (cm)	1,250
12. Box length paralleling the currents (cm)	843
13. Mean water depth in the box (cm) (measured as the depth at MHW in tidal systems)	59.5
14. Maximum tidal current speed or V_{harmonic} (cm/s)	5.0
15. Steady state current speed or V_{ss} (cm/s)	
16. Model speed or V_{model} (cm/s)	22.4
Water characteristics	
17. Average annual water temperature (°C)	12.0
18. Freshwater pH	7.8
19. Water hardness (mg CaCO ₃ /L)	150.0
20. Salinity (PSU or parts per thousand)	10.0
21. Background dissolved Cu concentration (µg Cu/L)	0.0
22. Background dissolved arsenic concentration (µg As/L)	0.0
23. Background dissolved chromium concentration (µg Cr/L)	0.0
24. Background dissolved zinc concentration (µg Zn/L)	0.0
25. Background dissolved penta concentration (µg penta/L)	0.0
Rainfall characteristics	
26. Annual rainfall (cm/year)	152
27. Steady state rainfall rate (cm/d)	0.416
28. Storm event (cm/h)	0
29. Duration of the storm event (h)	0
Sediment characteristics	
30. Sediment total organic carbon (%)	0.8
31. Sediment density (g/cm ³)	2.6
32. Sediment redox potential (mV) for penta or depth of the RPD for creosote (cm)	4
33. Background sediment copper concentration (mg/kg)	0
34. Background sediment arsenic concentration (mg/kg)	0
35. Background sediment chromium concentration (mg/kg)	0
36. Background sediment zinc concentration (mg/kg)	0
37. Background sediment penta concentration (mg/kg dry)	0
38. Background sediment PAH concentration (mg/kg)	0.11
Other	
39. Days since construction for determining contaminant concentrations in water	0.5
40. Settling velocity (0.05 cm/s for creosote and 0.005 cm/s for other contaminants)	0.05
41. Anticipated lifespan of the project. Default is 35 y with a minimum of 10 y	55
42. Angular increase in width of the sediment deposition zone downstream and offshore	4.51
43. Channel width (cm)	1,250

concentration of 0.719 µg ΣPAH/L in runoff from the overhead structure (Table 9.36). Computed dilution water volumes are summarized in Table 9.36. The model predicts a maximum concentration of dissolved ΣPAH of 0.038, giving a ΣTU = 0.005, which is 2.0% of the benchmark (<0.186 ΣTU) value.

The model predicted maximum accumulation of ΣPAH in Anderson Creek sediments (Table 9.37). The effective width of the sediment contamination zone was defined by the channel width at high tide (1,250 cm). Rainwater entrained PAHs are predicted to first reach the sediments 151 m downstream, and should not extend beyond 237 m downstream. Contaminants from immersed portions of the bridge begin at the bridge and extend 237 m downstream. Maximum predicted PAH accumulation from the immersed portions of the bridge is 5.47 mg ΣPAH/kg, and rainwater entrained contaminants add another 0.13 mg ΣPAH/kg, giving a total of 5.61 mg ΣPAH/kg within the box. At 0.8% TOC, the SQC is 10.64 mg ΣPAH/kg, and no adverse biological effects should be anticipated.

9.9.4.3 Observed sediment concentrations

Annual rainfall on this portion of the Kitsap Peninsula is heavy (152 cm/y) and high stream flows are likely to occur every winter. The coarse nature of the sediments suggests that fines (and PAH) do not accumulate at this site from year to year. Instead, they appear to be resuspended, diluted, and dispersed downstream. Fluoranthene (0.006 µg/g) and pyrene (0.00578 µg/g) were detected in the sample collected 914 cm downcurrent from the bridge. Polycyclic aromatic hydrocarbons were not detected in any other sediment sample. Detection limits for individual PAH were ≤0.00467 mg PAH/kg in all samples. These analyses support PAH dispersion at this site.

9.9.4.4 Biological response

The macrofaunal community near the mouth of Anderson Creek was complex in that it was dominated by marine amphipods, isopods, and polychaetes. However, large numbers of chironomid larvae and oligochaetes were also observed living sympatrically with the marine species. Typical of other creosote-treated structures in Puget Sound, a significant trend in abundance was observed downstream from the bridge's dripline, with higher abundance under and within 4 m of the bridge than at farther distances. Species richness and Shannon's index were also highest under the bridge, but the trends were not statisti-

Table 9.36 Dilution water volume factors used in the computations and predicted water column concentrations of Σ PAH on the first day of exposure at the Anderson Creek Bridge.

Model Table 6. Dilution water volume factors

Volume of rainwater runoff from pressure treated wood (L/d)	191.05
Dilution water passing through the box with steady state currents (L/d)	123,379,200
Dilution water in the box within 1/2 hour of slack tide (L)	1,800.5
Rainwater dilution (20 cm deep) water passing through the box with steady state currents (L/d)	41,472,000
Rainwater dilution (20 cm deep within 1/2 hour either side of slack tide (L)	605,215

Model Table 7. Dissolved contaminant concentrations leaving the box ($\mu\text{g/L}$)

Contaminant	Background	From immersed	From rain	Total	Benchmark	
					Acute	Chronic or Σ TU for PAH
Copper	0.00				4.800	3.100
Arsenic	0.00				69.00	36.00
Chromium	0.00				110.00	50.00
Zinc	0.80			0.80	90.00	81.00
TEB	0.00				MA	MC
PROP	0.00				MA	MC
IMID	0.00				MA	MC
Creosote (PAH)	0.00	0.0380	<0.000	0.0380	Σ TU<0.186	0.015
PENTA	0.00				13.00	7.90
DDAC	0.00				MA	MC

Table 9.37 Predicted sediment accumulation of Σ PAH downstream from the Anderson Creek Bridge.

Box Model for predicting sediment accumulation of contaminants from pressure-treated wood (mg/kg)

Model Table 8. Predictions of the area of sediment contamination (cm^2)

	Minimum	Maximum	Area (cm^2)
Effective width of sediment footprint (cm)	1,250	1,250	
Distribution downcurrent for rainwater contaminants (cm)	15,165	23,691	10,653,750
Distribution downcurrent for contaminants from immersed wood (cm)	0.0	23,691	29,613.750
Maximum width of the sediment footprint (cm)	1,250	5,268	

Model Table 9. Surface areas (cm^2) of pressure treated wood for determining total contaminant loading

Immersed treated wood (cm^2)	176,633
Rainwater exposed wood (cm^2)	459,090

Model Table 10. Maximum contaminant sediment concentrations (mg/kg)

Contaminant	Background	From immersed	From rain	Total (mg/kg)	Sediment quality criterion (mg/kg)
Copper	0.00				390.000
Arsenic	0.00				57.000
Chromium	0.00				260.000
Zinc	0.00				410.000
TEB	0.00				MS
PROP	0.00				MS
IMID	0.00				MS
Creosote (PAH)	0.08	5.474	0.131	5.61	10.64
PENTA	0.00				0.360
DDAC	0.00				MS

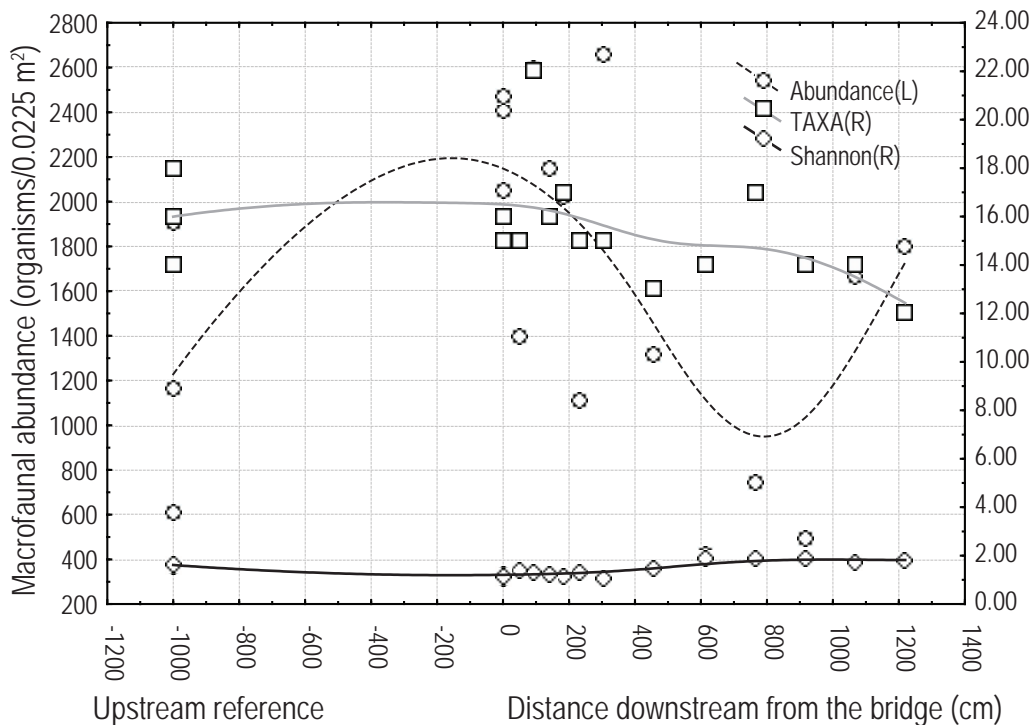


Figure 9.19 Macrofaunal abundance, species richness (TAXA) and Shannon's Index as a function of distance downstream from the Anderson Creek Bridge and at the upstream reference location. All fits are distance weighted least squares.

Table 9.38 Comparison of predicted and observed mean PAH concentrations (mg Σ PAH/kg) at the four project sites examined in this model verification assessment.

Site	Predicted (mg Σ PAH/kg)	Maximum observed (mg Σ PAH/kg)
Sooke aerobic (d 384)	25.16	18.0
Sooke anaerobic (d 3,650)	Under anaerobic conditions, the model predicts a maximum accumulation of 131.7 mg Σ PAH/kg	Accumulation over the 18 cm depth where significant PAH increases were observed = 132.6 mg Σ PAH/kg
Meadowbrook Creek	25.33	9.02
Seabeck Lagoon	2.66	Average in the box = 1.32 \pm 0.61; maximum 3.87 – one sample
Anderson Creek	5.61	<0.006

cally significant (Figure 9.19). No adverse effects associated with any attribute of the bridge were observed in the macrofaunal community. Brooks (2005a) provides a detailed discussion of the macrofaunal community at this site and the apparent effects seawater advancing on high tides has on the proportion of marine and freshwater invertebrates observed as a function of tidal height along the stream gradient.

9.10 MODEL SENSITIVITY

Several user inputs for these studies were determined by using point-in-time observations. Understanding how the

model responds to variation in user inputs can yield a better understanding of the model output's sensitivity to errors or changes in the environment.

9.10.1 Sooke Basin

Predictions for aerobic Sooke Basin sediments exceeded the observed maximum accumulation by 40% (Table 9.38). At the end of 10 y, sediments throughout the Pim Head area had become anaerobic and measurable quantities of PAH had been buried by organic loading from the epifaunal community resident on the piling. The average PAH concentration in the upper 15 cm of the cores was 17.7

Table 9.39 Sensitivity analysis showing the effects of altered user inputs on model predictions for the Meadowbrook Creek Bridge as a function of changes in user inputs.

	Maximum PAH accumulation
Best Model	25.3
Increase immersed lumber area by a factor of +2x	32.8
Increase rainwater exposed surface area by a factor of +2x	25.6
Increase annual rainfall by a factor of +2x	25.3
Increase annual water temperature by a factor of +1.5x	24.8
Increase average current speed by a factor of +2x	13.7
Decrease average current speed by a factor of +0.5x	44.2
Increase RPD to 4.0 cm	14.6
Decrease RPD to 2.0 cm	44.1

mg Σ PAH/kg in a 15-cm core. When concentrated in the top 2 cm of the core (as assumed by the model), the concentration would be 132.6 mg Σ PAH/kg, which is very close to the 131.7 mg Σ PAH/kg predicted by the model under anaerobic conditions (RPD = 0).

9.10.2 Meadowbrook Creek

Brooks (2005a) modified the user inputs by the factors provided in Table 9.39 and repeatedly ran the model to assess the effects of changes on the predictions of maximum Σ PAH accumulation at the Meadowbrook Creek Bridge. In general, the factors used to modify the user inputs were chosen to represent worse cases. The Best Model was based on field and database determinations of the User Inputs (Table 9.28). The model is sensitive to changes (or errors) in estimates of the exposed surface area of immersed wood, but less sensitive to errors in estimating the surface area of wood exposed to rain. It is sensitive to errors in determining the current speed and depth of the RPD. As a result, current speeds should be determined by using field equipment or unit hydrographs coupled with channel profiles, and this should be accomplished at the time of year when project construction is anticipated. If that is unknown, then current speeds and water depths should be conservatively estimated. In basaltic sediments, the RPD can be difficult or impossible to see. In these situations, or where the RPD is indistinct, redox potentials should be measured with a probe and the RPD entered, using Table 9.2 of this chapter as a guide.

Note that measuring redox potential with a field probe can be difficult and requires strict adherence to protocols. Where the RPD is distinctly visible, the field probe is the least expensive and most accurate measure of redox potential for use in this model.

9.10.3 Seabeck Lagoon

Long-term PAH accumulations at this lagoon were increased by rainwater runoff from the nearly 5 million cm² of wood exposed to rainfall. The major factors affecting these predictions were current speeds, water depth, and the surface area exposed to rain. It was assumed that all four surfaces of the wood received rainwater runoff. However, as noted earlier in this report, the low water solubility of most PAH influences their concentration in rainwater. Although the undersurfaces of the wood are wetted, they may contribute little to the end concentration because the water has already reached its solubility limit as it passes over the upper wood surface. In this case, halving the area assumed to be contributing to the concentration of PAH in the rainwater results in a decrease of 17% in the maximum PAH accumulation. For this exercise, the maximum tidal current speeds were measured during a minimal tidal exchange. Assuming that flow through the tide gate and culvert are proportional to the tidal head, a larger tidal exchange would likely lead to higher current speeds. Assuming that $V_{\text{model}} = 12$ cm/s, rather than 9.0 cm/s, results in the further displacement of the far-field area contaminated to 113.8 m downcurrent and a decrease in the predicted maximum PAH accumulation from 2.66 to 1.81 mg Σ PAH/kg. This discussion suggests that the model is sensitive to the user's understanding of the hydrodynamics of the receiving water body and that increased confidence in the output can be achieved by rigorous assessments of the direction, magnitude, and temporal characteristics of local current patterns, particularly in harmonically driven systems.

The Meadowbrook Creek Bridge results generally fit the model assumptions; however, the observed mean concentration in sediments collected within 15 cm of the bulkhead was 9.02 mg Σ PAH/kg, which was only about a third of the 25.33 mg/kg predicted by the model (Table 9.38). It should be noted that this bridge was well past the time at which accumulated PAH was predicted to peak.

The average observed sediment concentration within the modeled box at the Seabrook Lagoon Bridge (2.66 mg Σ PAH/kg) was nearly twice the average observed Σ PAH

(1.32 ± 1.6 mg Σ PAH/kg); however, three of the eighteen samples from the vicinity of the bridge exceeded model predictions. PAH contamination has generally been found to vary widely at a given site and it is the mean of replicates that are predicted by the model.

9.10.4 The Anderson Creek Bridge

The Anderson Creek Bridge evaluation illustrates a perhaps overly conservative assumption when applying the model in erosional environments. The model predicted a maximum accumulation of 5.61 mg Σ PAH/kg dry sediment at this bridge. However, only two PAH compounds were detected in sediments and those were both <0.006 mg/kg. The bridge is decades old, and peak sediment accumulations of creosote-derived PAH were predicted to occur about 800 d after construction. Even if all the PAH had remained in the sediments where they were first deposited, the concentrations would likely have declined over the decades. Second, Anderson Creek is a relatively swift salmon-spawning stream located in an area of heavy rainfall. It is likely that contaminants from the road and bridge have been washed into Hood Canal and diluted on an annual basis. These characteristics help explain the variations between the predicted and actual PAH levels.

9.11 SUMMARY

The model presented herein was designed to predict PAH accumulation in worst-case depositional environments with no resuspension of accumulated PAH during seasonally high flows. The purpose of the model presented in this chapter is to determine those situations where concentrations of dissolved contaminants or accumulation of contaminants in sediments may pose unacceptable environmental risks. The model-verification studies presented above and the risk assessments presented in Chapter 10 support the model's ability to make conservative but reasonable predictions.

Model sensitivity

The model-verification studies and sensitivity analyses presented in this chapter suggest that care must be exercised in providing information for the User Input section of the model. As with any model, the predictions are only as good as the inputs. Preservatives containing organic biocides must carefully evaluate factors that affect degradation rates. At Sooke Basin, changes in sediment redox potential increased the predicted and observed concentrations of PAH by factors of six and seven, respectively.

Dissolved PAH

Intermediate-weight PAH that characterize creosote have low water solubility and they should not be expected in the water column. Dissolved PAH have only been measured at Sooke Basin, where they were found to be ~ 0.020 μ g Σ PAH/L and not elevated above reference concentrations. The dissolved concentrations of PAH predicted by the model in all of these exercises was very low and in no case did the resulting Σ TU approach the biological effects benchmark of 0.186 TU.

Model performance

The four model-verification studies presented for creosote-treated structures indicate that the model reasonably predicts the maximum mean concentrations of contaminants that can be expected in proximity to treated wood structures. The model appears to alert users about projects requiring closer examination.

Modeling rigor

The model is amenable to several levels of project scrutiny. It can be used with numerous default values as a screening tool. The model can also be further refined using site-specific user inputs where results suggest that a project or its use of a particular preservative may be problematic.

REFERENCES

- American Wood Protection Association (AWPA). 2008. American Wood Protection Association 2008 Annual Book of Standards. American Wood Protection Association, Birmingham, AL.
- Baker, M.D., C.I. Mayfield and W.E. Inniss. 1980. Degradation of chlorophenols in soil, sediment and water at low temperature. *Water Res.* 14:1765–1777.
- Benner, D.B., and R.S. Tjeerdema. 1993. Toxicokinetics and biotransformation of pentachlorophenol in the topmelt (*Atherinops affinis*). *J. Biochem. Toxicol.* 8(3):111–117.
- Bauer, J.E., and D.G. Capone. 1985. Degradation and mineralization of the polycyclic aromatic hydrocarbons anthracene and naphthalene in intertidal marine sediments. *Appl. Environ. Microb.* 50(1):81–90.
- Borthwick, P.W., and J.M. Patrick. 1982. Use of aquatic toxicology and quantitative chemistry to estimate environmental deactivation of marine-grade creosote in seawater. *Environ. Toxicol. Chem.* 1(4):281–288.
- Boyle, T.P., E.F. Robinson-Wilson, J.D. Petty, and W. Weber. 1980. Degradation of pentachlorophenol in simulated lentic environment. *Bull. Environ. Contam. Toxicol.* 24(2):177–184.
- Brockway, D.L., P.D. Smith, and F.E. Stancil. 1984. Fate and effects of pentachlorophenol in hard- and soft-water microcosms. *Chemosphere* 13(12):1363–1377.
- Brooks, K.M. 1993. Literature Review and Assessment of the Environmental Risks Associated with the Use of Treated Wood Products

- in Aquatic Environments. Western Wood Preservers Association, Vancouver, WA.
- Brooks, K.M. 1995. Literature Review, Computer Model and Assessment of the Potential Environmental Risks Associated With Creosote Treated Wood Products Used in Aquatic Environments (Second Edition). Western Wood Preservers Institute, Vancouver, WA.
- Brooks, K.M. 1996. Evaluating the environmental risks associated with the use of chromated copper arsenate-treated wood products in aquatic environments. *Estuaries* 19 (2A):296–305.
- Brooks, K.M. 1997. Literature Review and Assessment of the Environmental Risks Associated with the Use of ACZA Treated Wood Products in Aquatic Environments. Second Edition. Western Wood Preservers' Institute, Vancouver, WA.
- Brooks, K.M. 1998. Literature Review and Assessment of the Environmental Risks Associated with the Use of ACQ Treated Wood Products in Aquatic Environments. Western Wood Preservers Institute, Vancouver, WA.
- Brooks, K.M. 2000. Assessment of the environmental effects associated with wooden bridges preserved with creosote, pentachlorophenol, or chromated-copper-arsenate (CCA-C). Res. Pap. FPL-RP-587. USDA Forest Service, Forest Products Laboratory, Madison, WI.
- Brooks, K.M. 2002a. Copper loss from copper naphthenate treated piling immersed in fresh water. Technical report prepared for Naphthenic Acid Technology Manager, Merichem Company Research Center, Houston, TX.
- Brooks, K.M. 2002b. Literature review, computer model and assessment of the potential environmental risks associated with copper naphthenate treated wood products used in aquatic environments. Technical report prepared for Merichem Chemicals and Refinery Services LLC, Tuscaloosa, AL.
- Brooks, K.M. 2003a. Metal loss rates from southern yellow pine treated with ACQ-C preservative amended with and without water repellents and from CCA-C treated wood. Technical report produced for Chemical Specialties Inc., Charlotte, NC.
- Brooks, K.M. 2003b. Metal loss rates as a function of rainfall from southern yellow pine treated with ACQ-C preservative amended with and without water repellents. Technical report produced for Chemical Specialties Inc., Charlotte, NC.
- Brooks, K.M. 2005a (in review). Computer model and risk assessment predicting the aquatic environmental response to bridges constructed using creosote preserved wood. Technical report prepared for the U.S. Department of Agriculture, Forest Service, Forest Products Laboratory, Madison, WI.
- Brooks, K.M. 2005b. Copper and tebuconazole loss rates from southern yellow pine treated to a retention of 0.246 pounds per cubic foot with CA-B preservative. Technical report produced for Arch Wood Protection, Smyrna, GA.
- Brooks, K.M. 2005c. Metal loss rates to rainfall falling on 2"x6" lumber treated with ammoniacal copper zinc arsenate (ACZA) preservative. Technical report produced for J.H. Baxter and Company, San Mateo, CA.
- Brooks, K.M. 2005d. Copper, zinc and arsenic loss rates from Douglas fir piling treated to a nominal retentions 1.0 and 1.5 pounds per cubic foot with ammoniacal copper zinc arsenate (ACZA) preservative and receiving four different post treatment Best Management Practices designed to minimize metal losses to fresh- and saltwater environments. Technical report prepared for J.H. Baxter and Company, San Mateo, CA.
- Brooks, K.M. 2006a. Supplemental study of dissolved nutrients and particulate organic matter in waters near the proposed mussel farm in North Totten Inlet, Washington State, USA. Technical report prepared for Taylor Resources, Shelton, WA.
- Brooks, K.M. 2006b. Literature review, computer model, and assessment of the environmental risks associated with pentachlorophenol treated wood products used in and over aquatic environments. Technical report prepared for The Pentachlorophenol Task Force, Washington, DC.
- Brooks, K.M. 2007. Concentrations of tebuconazole, imidacloprid and propiconazole in rainwater runoff from western hem-fir decking treated to a retention of 0.02 pounds per square inch with Wolman AG™ preservative. Technical report produced for Arch Treatment Technologies, Inc., Smyrna, GA.
- Brooks, K.M. 2009a. Concentrations of copper, tebuconazole and propiconazole released from μCu Azole. Report to be completed in July 2009.
- Brooks, K.M. 2009b. Concentrations of copper and tebuconazole released from Micropro™ pressure treated southern pine. Report to be completed in July 2009.
- Brooks, K.M. 2010a. Environmental fate and effects of copper, tebuconazole and propiconazole in aquatic environments associated with rainwater runoff from Wolman Dispersed CA-C™ preserved southern pine. Technical report prepared for Arch Wood Protection, Inc. Atlanta, GA.
- Brooks, K.M. 2010b. Aquatic Environmental fate and effects of copper and tebuconazole from southern pine decking treated to retentions of 0.175 pcf with Osmose MicroPro™ or 0.244 pcf with Smartsense™ preservatives for use in constructing projects over water. Technical report prepared for Osmose, Inc., Griffin, GA.
- Brooks, K.M., C. Mahnken, and C. Nash. 2002. Environmental effects associated with marine netpen waste with emphasis on salmon farming in the Pacific Northwest. In: *Responsible Marine Aquaculture*, ed. R.R. Stickney and J.P. McVey. CABI Publishing, Wallingford, UK, pp. 159–204.
- Brooks, K.M., A.R. Stierns and C. Backman. 2004. Seven year remediation study at the Carrie Bay Atlantic salmon (*Salmo salar*) farm in the Broughton Archipelago, British Columbia, Canada. *Aquaculture* 239(September):81–123.
- Brooks, K.M., D. Goyette, and S. Christie. 2006. Sooke Basin Creosote Evaluation – Results of the October 2005 Reconnaissance Survey. Creosote Evaluation Committee, Fisheries and Oceans Canada, Pacific Yukon Region, Vancouver, BC.
- Bryant, F.O., and J.E. Rogers. Dechlorination of pentachlorophenol, 2,4-dichlorophenoxyacetic acid and 2,4,5-trichlorophenoxyacetic acid in anaerobic freshwater sediments. *Ecol. Res. Ser. U.S. Environmental Protection Agency*.
- Cerniglia, C.E. 1984. Microbial metabolism of polycyclic aromatic hydrocarbons. *Adv. Appl. Microbiol.* 30:31–77.
- Cerniglia, C.E., and M.A. Heitkamp. 1989. Microbial Degradation of Polycyclic Aromatic Hydrocarbons (PAH) in the Aquatic Environment. In: *Metabolism of Polycyclic Aromatic Hydrocarbons in the Aquatic Environment*, ed. U. Varanasi. CRC Press, Boca Raton, FL., pp. 41–68.
- Colwell, R.R. 1986. Microbial Ecology Studies of Biofouling of Treated and Untreated Wood Pilings in the Marine Environment. Department of Microbiology, University of Maryland, Final Report. U.S. Office of Naval Research: U.S. Navy Contract No. N00014-75-C-0340 P0003.

- Crossland, N.O., and C.J.M. Wolff. 1985. Fate and biological effects of pentachlorophenol in outdoor ponds. *Environ. Toxicol. Chem.* 4(2):73–86.
- DeLaune, R.D., R.P. Gambrell, and K.S. Reddy. 1983. Fate of pentachlorophenol in estuarine sediment. *Environ. Pollut. B* 6(4):297–308.
- Eisler, R. 1989. Pentachlorophenol hazards to fish, wildlife, and invertebrates: A synoptic review. U.S. Fish and Wildlife Service, Biological Report 85(1.17). Contaminant Hazard Reviews Report No. 17. U.S. Fish and Wildlife Service, Patuxent Wildlife Research Center, Laurel, MD.
- EVS Consultants. 1994. Creosote Evaluation Project. Technical Report WQWM-93-13. Prepared for the Fraser River Estuary Management Program by EVS Consultants, North Vancouver, BC.
- Fisher, S.W. 1990. The pH dependent accumulation of PCP in aquatic microcosms with sediment. *Aquat. Toxicol.* 18(4):199–218.
- Gardner, W.S., R.F. Lee, K.R. Tenore, and L.W. Smith. 1979. Degradation of selected polycyclic aromatic hydrocarbons in coastal sediments: importance of microbes and polychaete worms. *Water Air Soil Poll.* 11(3):339–347.
- Gilluly, J., A.C. Waters, and A.O. Woodford. 1968. Principles of Geology – Third Edition. W.H. Freeman and Company, San Francisco, CA.
- Glickman, A.H., C.N. Statham, A. Wu, and J.J. Lech. 1977. Studies on the uptake, metabolism and disposition of pentachlorophenol and pentachloroanisole in rainbow trout. *Toxicol. Appl. Pharm.* 41:649–658.
- Gonzalez, J.F., and W.S. Hu. 1991. Effect of glutamate on the degradation of pentachlorophenol by *Flavobacterium* sp. *Appl. Microbiol. Biot.* 35(1):100–104.
- Goyette, D., and K.M. Brooks. 1998. Creosote Evaluation: Phase II. Sooke Basin Study – Baseline to 535 Days Post Construction 1995 – 1996. Environment Canada, North Vancouver, BC.
- Goyette, D., and K.M. Brooks. 2000. Addendum Report – Continuation of the Sooke Basin Creosote Evaluation Study (Goyette and Brooks, 1998). Year 4 – Days 1360 and 1540. Environment Canada, North Vancouver, BC.
- Green, T., and D.F. Houk. 1979. The mixing of rain with near-surface water. *J. Fluid Mech.* 90(3):569–588
- Guthrie, M.A., E.J. Kirsch, R.F. Wukasch, and C.P.L. Grady Jr. 1984. Pentachlorophenol Biogradation-II: Anaerobic. *Water Res.* 18(4):451–461.
- Hambrick, G.A., R.D. DeLaune, and W.H. Patrick. 1980. Effect of estuarine sediment pH and oxidation-reduction potential on microbial hydrocarbon degradation. *Appl. Environ. Microbiol.* 40:365–369.
- Herbes, S.E. 1981. Rates of microbial transformation of polycyclic aromatic hydrocarbons in water and sediments in the vicinity of a coal-coking wastewater discharge. *Appl. Environ. Microb.* 41(1):20–28.
- HydroQual. 2007. Biotic Ligand Model – Windows Interface, Version 2.2.3. HydroQual, Inc. 1200 MacArthur Blvd., Mahwah, NJ 07430. Accessed on January 27, 2009 at http://www.hydroqual.com/wr_blm_windows.html.
- Jarvinen, K.T., E.S. Melin, and J.A. Puhakka. 1994. High-rate bioremediation of chlorophenol-contaminated groundwater at low temperatures. *Environ. Sci. Technol.* 28(13):2387–2392.
- Jarvinen, K.T., and J.A. Puhakka. 1994. Bioremediation of chlorophenol contaminated ground water. *Environ. Technol.* 15(9):823–832.
- Kang, S.-M, J.J. Morrell, J. Simonsen, and S.T. Lebow. 2005. Creosote movement from treated wood immersed in fresh water. *Forest Prod. J.* 55(12):42–46.
- Kudo, A. 1989. Decomposition of pentachlorophenol by anaerobic digestion. *Water Sci. Technol.* 21(12):1685–1688.
- Larsson, P., L. Okla, and L. Tranvik. 1988. Microbial degradation of xenobiotic, aromatic pollutants in humic water. *Appl. Environ. Microbiol.* 54(7):864–1867.
- Larsson, P., and K. Lemkemeier. 1989. Microbial mineralization of chlorinated phenols and biphenyls in sediment-water Systems from humic and clear-water lakes. *Water Research WATRAG.* 23(9):1081–1085.
- LANXESS. 2004. Preventol TM Summary of Toxicity and Ecotoxicity. LanXess Deutschland GmbH, D-51369. Leverkusen, Germany.
- LANXESS. 2005. Preventol A8 and Preventol A8-F – Summary of Toxicity and Ecotoxicity. LanXess Deutschland GmbH, D-51369. Leverkusen, Germany.
- Liu, D., K. Thomson, and W.M.J. Stachen. 1981. Biodegradation of pentachlorophenol in a simulated aquatic environment. *Bull. Environ. Contam. Toxicol.* 26(1):85–90.
- MacGillivray, A.R., and M.P. Shiaris. 1993. Biotransformation of polycyclic aromatic hydrocarbons by yeasts isolated from coastal sediments. *Appl. Environ. Microb.* 59(5):1613–1618.
- Malins, D.C., M.M. Krahn, M.S. Myers, L.D. Rhodes, C.A. Wigren, D.W. Brown, C. Krone, B.B. McCain, and S.L. Chan. 1985. Toxic chemicals in sediments and biota from a creosote-polluted harbor: relationships with hepatic neoplasms and other hepatic lesions in English sole (*Parophrys vetulus*). *Carcinogenesis* 6:1463–1469.
- McAllister, K.A., H. Lee, and J.T. Trevors. 1996. Microbial degradation of pentachlorophenol. *Biodegradation* 7(1):1–40.
- Middaugh, D.P., S.M. Resnich, S.E. Lantz, C.S. Heard, and J.G. Mueller. 1993. Toxicological assessment of biodegraded pentachlorophenol: Microtox and fish embryos. *Arch. Environ. Contam. Toxicol.* 24(2):165–172.
- PSEP. 1986. Puget Sound Estuary Protocols. U.S. Environmental Protection Agency, Region 10, Seattle, WA.
- Robinson-Wilson, E.F., T.P. Boyle, and J.D. Petty. 1983. Effects of increasing levels of primary production on pentachlorophenol residues in experimental pond ecosystems. *In: Aquatic Toxicology and Hazard Assessment: Sixth Symposium, ASTM STP 802*, ed. W.E. Bishop, R.D. Cardwell, and B.B. Heidolph. American Society for Testing and Materials, Philadelphia, pp. 239–251.
- Sayler, G.S., and T.W. Sherrill. 1981. Bacterial Degradation of Coal Conversion By-Products (PAH) in Aquatic Environments. Final Report ed. Office of Water Research and Technology, U.S. Department of Interior; Contract DI-14-34-0001-9096.
- Shimizu, Y., S. Yamazaki, and Y. Terashima. 1992. Sorption of anionic pentachlorophenol (PCP) in aquatic environments: The effects of pH. *In: Hazard Assessment and Control of Environmental Contaminants in Water*, ed. S. Matusi. 25(11):41–48.
- Schlussel, P., A.V. Soloviev, and W.J. Emery. 1997. Cool and freshwater skin of the ocean during rainfall. *Boundary-Layer Meteorology* 82(3):437–472.
- Seidler, J.J., M. Landau, F.E. Dierberg, and R.H. Pierce. 1986. Persistence of pentachlorophenol in a wastewater-estuarine aquaculture system. *Bull. Environ. Contam. Toxicol.* 36(1):101–108.
- Smith, P.D., D.L. Brockway, and F.E. Stancil, Jr. 1987. Effects of hardness, alkalinity and pH on the toxicity of pentachlorophenol

- to *Selenastrum capricornutum* (Printz). *Environ. Toxicol. Chem.* 6(11):891–900.
- Smith, J.A., and J.T. Novak. 1987. Biodegradation of chlorinated phenols in subsurface soils. *Water Air Soil Pollut.* 33(1–2):29–42.
- Swartz, R.C., D.W. Schultz, R.J. Ozretich, J.O. Lambeerson, R.A. Cole, T.H. DeWitt, M.S. Redmond, and S.P. Ferro. 1995. Σ PAH: A model to predict the toxicity of field-collected marine sediment contaminated by polynuclear aromatic hydrocarbons. *Environ. Toxicol. Chem.* 14:1977–1987.
- Topp, E., R.L. Crawford, and R.S. Hanson. 1988. Influence of readily metabolizable carbon on pentachlorophenol metabolism by a pentachlorophenol-degrading *Flavobacterium* sp. *Appl. Environ. Microbiol.* 54(10):2452–2459.
- Trevors, J.T. 1982. Effect of temperature on the degradation of pentachlorophenol by *Pseudomonas* sp. *Chemosphere* 11(4):471–475.
- USDA. 1980. The biological and economic assessment of pentachlorophenol, inorganic arsenicals, creosote. Volume 1: Wood preservatives. USDA Tech. Bull. No. 1658-1, USDA, Washington, DC.
- Yu, J., and W.P. Ward. 1994. Studies on factors influencing the biodegradation of pentachlorophenol by a mixed bacterial culture. *Int. Biodeterior. Biodegrad.* 33:209–221.
- Valo, R., J. Apajalahti, and M. Salkinoja-Salonen. 1985. Studies on the physiology of microbial degradation of pentachlorophenol. *Appl. Microbial Biotechnol.* 21(5):313–319.
- Van Gestel, C.A.M., and W.C. Ma. 1988. Toxicity and bioaccumulation of chlorophenols in earthworms, in relation to bioavailability in soil. *Ecotoxicol. Environ. Saf.* 15(3):289–297.
- Wong, A.S., and D.G. Crosby. 1981. Photodecomposition of pentachlorophenol in water. *J. Agric. Food Chem.* 29(1):125–130.
- Xiao, Y., J. Simonsen, and J.J. Morrell. 2001. Laboratory simulation of leaching from creosote treated wood in aquatic exposures. Document No. IRG/WP/00-5157, International Research Group on Wood Preservation, Stockholm, Sweden.

APPENDICES

Appendix 9.1 Predicted accumulation of PAH ($\mu\text{g PAH}/1000 \text{ cm}^2$) in sediments over a 35-y period as a function of depth of the RPD, temperature, and average annual rainfall.

Appendix Table 9.1A Maximum accumulation ($\mu\text{g PAH}/1000 \text{ cm}^2$ leaching surface area), 25 cm/y rainfall.

RPD	Temperature ($^{\circ}\text{C}$)						
	5	10	15	20	25	30	35
0	712,427	616,050	550,333	500,767	461,416	429,165	401,826
0.5	602,076	485,080	413,346	363,019	324,990	295,269	270,997
1	503,510	381,232	312,364	266,704	233,688	208,555	188,650
2	379,355	265,099	207,128	170,908	146,012	127,990	113,791
3	334,904	226,906	174,304	142,376	120,527	104,973	92,440
4	328,541	221,815	169,946	138,717	117,193	101,906	89,857

Appendix Table 9.1B Maximum accumulation ($\mu\text{g PAH}/1000 \text{ cm}^2$ leaching surface area), 50 cm/y rainfall.

RPD	Temperature ($^{\circ}\text{C}$)						
	5	10	15	20	25	30	35
0	387,335	354,769	328,659	307,302	289,688	274,809	261,995
0.5	349,110	300,363	267,412	242,590	222,848	206,667	193,068
1	308,538	251,823	216,004	190,632	171,383	156,151	143,748
2	250,895	189,718	155,302	132,530	116,116	103,590	93,669
3	228,040	167,470	134,705	113,582	98,593	87,289	78,442
4	224,738	164,332	131,886	110,926	96,215	85,117	76,463

Appendix Table 9.1C Maximum accumulation ($\mu\text{g PAH}/1000 \text{ cm}^2$ leaching surface area), 100 cm/y rainfall.

RPD	Temperature ($^{\circ}\text{C}$)						
	5	10	15	20	25	30	35
0	208,809	196,292	186,364	178,093	170,955	164,684	159,060
0.5	194,280	175,316	161,464	150,502	141,464	133,769	127,133
1	178,581	154,600	138,242	125,901	116,064	107,998	101,178
2	154,184	125,437	107,529	94,858	85,234	77,627	71,450
3	143,870	114,013	96,084	83,654	74,513	67,321	61,498
4	142,358	112,351	94,484	82,154	73,051	65,938	60,150

Appendix Table 9.1D Maximum accumulation ($\mu\text{g PAH}/1000 \text{ cm}^2$ leaching surface area), 150 cm/y rainfall.

RPD	Temperature ($^{\circ}\text{C}$)						
	5	10	15	20	25	30	35
0	142,754	136,152	130,805	126,249	122,268	118,691	115,453
0.5	135,078	124,715	116,832	110,399	105,006	100,316	96,173
1	126,525	112,849	103,041	95,410	89,169	83,922	79,401
2	112,612	95,122	83,612	75,084	68,481	63,203	58,795
3	106,434	87,809	75,961	67,469	60,945	55,772	51,553
4	105,534	86,720	74,835	66,413	59,922	54,682	50,550

Note: RPD = redox potential discontinuity.

Appendix Table 9.1E Maximum accumulation ($\mu\text{g PAH}/1000 \text{ cm}^2$ leaching surface area), 200 cm/y rainfall.

RPD	Temperature ($^{\circ}\text{C}$)						
	5	10	15	20	25	30	35
0	108,500	104,446	101,022	98,061	95,431	93,063	90,902
0.5	103,698	97,044	91,828	87,535	83,885	80,730	77,860
1	98,226	89,159	82,566	77,314	72,894	69,127	65,842
2	89,062	77,113	68,907	62,722	57,805	53,757	50,356
3	84,892	71,948	63,344	57,009	52,055	48,049	44,696
4	84,250	71,178	62,532	56,178	51,240	47,227	43,914

Appendix Table 9.1F Maximum accumulation ($\mu\text{g PAH}/1000 \text{ cm}^2$ leaching surface area), 250 cm/y rainfall.

RPD	Temperature ($^{\circ}\text{C}$)						
	5	10	15	20	25	30	35
0	87,014	84,263	82,384	80,300	78,442	76,762	75,229
0.5	83,740	79,581	75,887	72,807	70,131	67,736	65,589
1	79,937	73,993	69,139	65,179	61,848	58,971	56,455
2	73,343	65,024	58,804	54,020	50,169	46,967	44,221
3	70,430	61,127	54,511	49,545	45,605	42,363	39,637
4	69,961	60,542	53,876	48,893	44,948	41,709	38,998

Note: RPD = redox potential discontinuity.

Appendix 9.2 Days of steady rain when the maximum accumulation of PAH occurs in association with runoff from creosote-treated wood exposed to rainfall.

Appendix Table 9.2A Day on which the maximum accumulation occurs, 25 cm/y rainfall.

RPD	Temperature (°C)						
	5	10	15	20	25	30	35
0	3,550	2,750	2,350	2,050	1,850	1,750	1,650
0.5	2,650	2,050	1,650	1,450	1,250	1,150	1,050
1	2,150	1,550	1,250	1,050	950	850	750
2	1,550	1,050	850	650	650	550	450
3	1,350	950	750	550	550	450	350
4	1,350	850	650	550	450	450	350

Appendix Table 9.2B Day on which the maximum accumulation occurs, 50 cm/y rainfall.

RPD	Temperature (°C)						
	5	10	15	20	25	30	35
0	1,795	1,785	1,515	1,395	1,275	1,155	1,095
0.5	1,725	1,335	1,125	1,005	915	855	765
1	1,395	1,065	885	765	705	615	585
2	1,065	765	615	525	465	435	375
3	945	675	555	465	405	375	345
4	915	675	525	435	405	345	315

Appendix Table 9.2C Day on which the maximum accumulation occurs, 100 cm/y rainfall.

RPD	Temperature (°C)						
	5	10	15	20	25	30	35
0	1,305	1,095	975	885	825	765	735
0.5	1,065	855	735	675	615	555	525
1	885	705	585	525	465	435	405
2	705	525	435	375	345	315	285
3	615	465	375	315	285	255	255
4	615	465	375	315	285	255	225

Appendix Table 9.2D Day on which the maximum accumulation occurs, 150 cm/y rainfall.

RPD	Temperature (°C)						
	5	10	15	20	25	30	35
0	975	795	705	675	615	585	555
0.5	795	645	555	525	465	435	405
1	675	525	465	405	375	345	315
2	525	405	345	315	255	255	225
3	425	375	315	255	225	225	195
4	65	345	285	255	225	225	195

Note: RPD = redox potential discontinuity.

Appendix Table 9.2E Day on which the maximum accumulation occurs, 200 cm/y rainfall.

RPD	Temperature (°C)						
	5	10	15	20	25	30	35
0	765	655	595	545	515	485	455
0.5	645	535	465	425	395	365	355
1	525	445	375	345	325	295	275
2	435	345	295	265	235	215	205
3	405	315	265	235	215	195	175
4	395	305	265	235	205	195	175

Appendix Table 9.2F Day on which the maximum accumulation occurs, 250 cm/y rainfall.

RPD	Temperature (°C)						
	5	10	15	20	25	30	35
0	630	595	495	465	435	405	385
0.5	510	445	395	355	345	325	305
1	450	375	335	305	275	255	245
2	330	305	255	235	205	195	175
3	330	275	235	205	185	175	155
4	330	265	225	205	185	165	155

Note: RPD = redox potential discontinuity.